Norwegian University
of Life Sciences

Master's Thesis 2022 60 ECTS
Faculty of Chemistry, Biotechnology, and Food Science
Morten Kjos

Exploring the role of novel biofilm-associated genes in *Staphylococcus aureus*

Rebekka Moe
Biotechnology

Acknowledgements

This master's thesis was completed as part of the Master's programme in Biotechnology at the Norwegian University of Life Sciences (NMBU). The work was conducted in the Molecular Microbiology research group at the Faculty of Chemistry, Biotechnology and Food Science (KBM) between August 2021 and May 2022.

I want to express my gratitude to my co-supervisor, Dr. Danae Morales Angeles, for her support and guidance throughout this project, both with experiments in the laboratory and during the writing process. You are incredibly knowledgeable and a great teacher. Thank you for always answering my questions and taking time out of your day to help me, however big or small the issue. I would also like to thank my main supervisor, Dr. Morten Kjos, for his invaluable advice and feedback. You have acted both inspiring and reassuring during this time. Thank you both for allowing me to contribute to such an exciting project.

I want to thank everyone at the Molecular Microbiology group for providing a great work environment, professionally and socially. I have greatly appreciated your expertise, as well as your inclusiveness. I want to give a special thanks to Zhian Salehian for his exceptional helpfulness and Marita Mårli Torrissen for conducting the bioinformatic analyses for this work. A huge thanks to my fellow master's students, Jennie Ann Allred, Tiril Mathiesen Knutsen, Ingrid Petersheim, Vilde Sandegren, and Anne Ohren Nordraak, for your great support and company.

I would like to express gratitude to my family, especially my parents, for all their love and encouragement. Thank you to my friends Johan Tryti, Guro Ronglan Aarnes, and Espen Evju, for all the laughs and good conversations, throughout my five years at NMBU. Lastly, I want to give a special thanks to my partner Thobias H. Østvedt for being especially caring and supportive during this last year.

Rebekka Moe

Ås, May 2022

Abstract

Staphylococcus aureus is a major opportunistic pathogen in humans. Its success can be attributed to its variety of virulence factors, including the formation of biofilms. Biofilms are sessile three-dimensional bacterial communities attached to a surface, embedded in an extracellular matrix consisting of extracellular DNA (eDNA), polysaccharides, and proteins. Bacteria in biofilms exhibit increased resistance to the host's immune system and antimicrobials, limiting infection treatment options. A class of enzymes known as peptidoglycan hydrolases facilitate the first stage of biofilm-formation, the attachment of cells to a surface, by releasing adhesive eDNA. However, biofilm-formation is a complex process, and many other components are involved. Understanding how these components contribute to the formation is key to discovering ways to combat *S. aureus* biofilm infections. Therefore, this thesis explored the role of novel biofilm-associated genes in the following three parts.

This work explored the function of putative peptidoglycan hydrolase SAOUHSC_00671 (hereafter 00671), previously reported to be involved in biofilm formation. By comparing features of biofilms formed by a wildtype- and a 00671-knockout strain, a different attachment phenotype was discovered. However, the results in this thesis indicate that 00671 does not majorly contribute to biofilm-formation in *S. aureus*. Interestingly, a genetic correlation between 00671 and SsaA, another putative peptidoglycan hydrolase, was found in planktonic cells and biofilms, which may have counteracted the effect of knocking out 00671. The correlation suggests that there is an intricate interplay between peptidoglycan hydrolases in *S. aureus*, where cells can sense a lack of hydrolase activity by one enzyme and upregulate other peptidoglycan hydrolases to maintain homeostasis.

Additionally, the newly discovered *S. aureus* cell morphology determinant SmdA was demonstrated to be involved in biofilm-formation in strain NCTC8325-4, and the mechanism was linked to the biofilm-associated *ica*-operon. By depleting SmdA using CRISPR interference, a decrease in biofilm mass and polysaccharide intracellular adhesins were observed. Consistent with these observations, no decrease in biofilm-formation was seen for strains SH1000 and JE2, strains associated with biofilm-formation independently of the *ica*-operon.

Finally, to screen *S. aureus* for new genes involved in attachment, the initial phase of biofilm formation, a CRISPR interference screen was performed using a genome-wide CRISPR

interference library. This revealed three novel putative attachment-related genes; two hypothetical proteins encoded by *SAOUHSC_0957* and *SAOUHSC_02888*, and *xdrA*. XdrA regulates eDNA release and the surface protein SpA, although its mechanisms is still largely unknown. The role of these genes in biofilm-formation should be studied further.

Sammendrag

Staphylococcus aureus er en opportunistisk humanpatogen bakterie med evnen til å forårsake en rekke alvorlige infeksjoner. Bakteriens suksess kan tilskrives dens mange varierte virulensfaktorer, inkludert dannelsen av biofilmer. Biofilmer er tredimensjonale bakterielle samfunn festet til en overflate, omgitt av en ekstracellulær matriks som består av ekstracellular DNA (eDNA), polysakkarider, og proteiner. Bakterier i biofilmer har en økt resistens både mot vertens immunforsvar og antimikrobielle midler. Dette begrenser behandlingsmulighetene ved en infeksjon. En gruppe enzymer kjent som peptidoglykanhydrolaser bidrar til det første stadiet i biofilmdannelsen, bestående av å feste cellene til en overflate. Biofilmdannelse er en kompleks prosess, og mange andre komponenter er involvert. Å forstå hvordan de ulike komponentene bidrar i dannelsen er nødvendig for å oppdage måter å bekjempe *S. aureus* biofilm-infeksjoner. I denne mastergradsavhandlingen ble derfor rollen til nye biofilm-assosierte gener utforsket i følgende tre deler.

Den antatte peptidoglykanhydrolasen SAOUHSC_00671 (heretter 00671) har tidligere blitt rapportert til å være involvert i biofilmdannelse. Ved å sammenligne egenskaper ved biofilmer dannet av en villtype- og en 00671-knockoutstamme, ble det oppdaget at 00671 endrer biofilm-fenotypen i det første stadiet av dannelsen. De resterende resultatene i denne oppgaven indikerer imidlertid at 00671 ikke bidrar til biofilmdannelse i *S. aureus* i særlig grad. Det ble funnet en genetisk korrelasjon mellom 00671 og SsaA, en annen antatt peptidoglykanhydrolase, i planktoniske celler og biofilmer. Korrelasjonen antyder at det er et intrikat samspill mellom peptidoglykanhydrolaser i *S. aureus*, hvor cellen kan oppfatte mangel på hydrolaseaktivitet av ett enzym og oppregulere andre peptidoglykanhydrolaser for å opprettholde homeostase.

I tillegg ble den nyoppdagede cellemorfologideterminanten i *S. aureus*, SmdA, vist å være involvert i biofilmdannelse i stammen NCTC8325-4, og mekanismen ble knyttet til det biofilmassosierte *ica*-operonet. Ved å nedregulere uttrykket av SmdA ved bruk av CRISPR-interferens, ble det observert en reduksjon i biofilmmasse og «polysaccharide intracellular adhesins». I samsvar med disse observasjonene ble det ikke sett noen reduksjon i biofilmdannelse for SH1000 og JE2, stammer assosiert med biofilmdannelse uavhengig av *ica*-operonet.

For å oppdage nye gener i *S. aureus* involvert i det første stadiet av biofilmdannelse, ble en genomomfattende screen utført ved brukt av et CRISPR-interferensbibliotek. Dette avdekket

tre nye mulige gener involvert i denne prosessen; to hypotetiske proteiner kodet av *SAOUHSC_0957* og *SAOUHSC_02888*, og *xdrA*. XdrA regulerer utslipp av eDNA og uttrykk av overflateproteinet SpA, men mekanismen er fortsatt ukjent. Rollen til disse genene i biofilmdannelse bør studeres videre.

Index

1 Introduction

1.1 *Staphylococcus aureus*

Staphylococcus aureus is a Gram-positive, coccoid bacterium belonging to the phylum Firmicutes. It is commonly found to colonise the skin and mucous membranes of about one-third of the human population (1). The discovery of the bacterium in the 1880s is credited to Scottish surgeon Alexander Ogston (1844-1929) and German surgeon Friedrich J. Rosenbach (1842-1923) (2–4). Ogston hypothesised that a germ was the cause of surgical infections and examined pus from a patient under the microscope. He observed micrococci clustered together like grapes, and in 1882 he named them "staphylococci", from the Greek staphyle, meaning a bunch of grapes (2, 3). Two years later, Rosenbach isolated *S. aureus* and named it after its golden colour from the Latin aurum, meaning gold (4). To this day, the bacterium remains a major human pathogen.

1.1.1 Clinical and economic impact

S. aureus is a versatile pathogen causing a range of different diseases such as skin infections, osteomyelitis, endocarditis, food poisoning, toxic shock syndrome, and urinary tract infections (5). It is especially prominent in nosocomial hospital-acquired infections. The European Centre for Disease Control and Prevention reports it as the most frequently isolated microorganism from nosocomial infections, second only to *E. coli* (6). *S. aureus* was isolated from 12.3% of all nosocomial infections, 15.9% of bloodstream infections, and 12.6% of lower respiratory tract infections (6). It was the most common microorganism in surgical site infections, with 17.9% containing the bacterium (6). The reports are similar in the US, where *S. aureus* was found in 12% of all nosocomial infections, making it the second most frequently isolated microorganism from surgical site infections (7).

The mortality rate of *S. aureus* infections is dependent on several factors such as type of infection, environment, host condition, and virulence factors. *S. aureus* bacteraemia (SAB) has a mortality rate of 20% and was estimated to cause almost 20,000 deaths in the US in 2017 (8, 9). The economic burden for *S. aureus* infections was estimated to be $14.5 billion in the United States in 2003 (10).

1.1.2 Antibiotic resistance

Ernest Duchesne (1874-1912) discovered penicillin in 1896, but the antibiotic was not put to use until Alexander Fleming (1881-1955) accidentally rediscovered it in 1928, and when Howard Florey and Ernst Chain (1906-1979) purified it in 1940 (11). Fleming observed that the antibiotic, produced by *Penicillin notatum,* inhibited the growth of staphylococci inoculated in a petri dish (11). However, penicillin-resistant staphylococci were identified in 1942, shortly after the first human trials (12). Bacteria can achieve antibiotic resistance in many ways, such as drug target modification, drug inactivation, and by minimising the antibiotic concentration in the cell (11). As for penicillins, a well-known mode of resistance is to acquire β-lactamase enzymes, which hydrolyse the β-lactam ring, an example of drug inactivation (11). In response to penicillin-resistant staphylococci, methicillin was introduced in 1959, only for strains of methicillin-resistant *S. aureus* (MRSA) to be found two years later (13). MRSA strains carry a staphylococcal cassette chromosome *mec* (SCC*mec*) element that contains the *mec* gene encoding an alternative penicillin-binding protein 2a (Pbp2a), making the strain resistant to virtually all β-lactam antibiotics (14, 15). In addition, SCC*mec* encodes resistance genes for other antibiotics and recombinases, allowing mobility of the cassette (15). MRSA strains can readily acquire resistance to other antibiotics by undergoing several mutational events, further limiting treatment options (15, 16). In 2010 it was reported that in Europe, MRSA strains accounted for 44% of all hospital-acquired infections requiring 41% of extra days of hospitalisation, resulting in an estimated annual cost of 380 million euros (17). To combat MRSA, the use of vancomycin significantly increased, which led to the emergence of vancomycin-intermediate *S. aureus* (VISA) and vancomycin-resistant *S. aureus* (VRSA). It is currently not as widespread as MRSA but raises concerns as vancomycin is often considered a last resort antimicrobial (16).

1.1.3 Pathogenesis

S. aureus is considered an opportunistic pathogen, meaning it can become pathogenic, but does not cause harm to the host under normal circumstances. Although the bacterium can cause various infections, including life-threatening toxin-mediated disease, asymptomatic carriage is more common than infection (18, 19). Longitudinal studies report persistent carriage in 10-35% and intermittent carriage in 20-75% of the population (18). Children have been found to have a substantially higher persistent carriage rate than adults (20). The anterior nares are the primary

colonisation site; however, other notable sites include the skin, pharynx, gastrointestinal tract, and vagina (20, 21).

Host predisposition and virulence-associated genes are major factors that determine *S. aureus*' ability to shift from a commensal coloniser to an invasive pathogen. Common skin infections caused by *S. aureus* in healthy individuals include impetigo, folliculitis, and cutaneous abscesses, requiring little to no medical treatment (22). More severe infections are caused when the bacteria enter the bloodstream, coupled with the fact that they can infect a large variety of body sites, including vital organs. The presence of intravascular medical devices remains the major risk factor for SAB, and injection drug use, underlying medical diseases, and immunodeficiencies predispose the host (23, 24). Possible complications of SAB are numerous and are associated with a more severe outcome of the infection (24). Nosocomial acquisition is also a pivotal contributor to *S. aureus* infections, especially for individuals who have undergone surgeries, are immunocompromised, or possess indwelling medical devices, the latter often resulting from the formation of biofilms (24–26). Biofilms are associated with chronic infections and are especially challenging due to their resistance to the host immune system and antimicrobial agents (25). See section 1.2 for more details on *S. aureus* biofilms. Nasal carriage has been identified as a risk factor for infections and is correlated with the colonisation of other bodily sites (27). To cause a systemic infection, *S. aureus* must breach the epithelial layer, during which evasion of the innate immune system is essential in the establishment (28). *S. aureus* is also known to infect animals, with bovine mastitis being a well-known example. Although concerns have been raised in the agricultural industry with the emergence of livestock-associated MRSA, these strains are not a significant source of human MRSA infections (28).

1.1.4 Virulence factors

The ability to shift from a commensal to a pathogen, as staphylococcal infections usually arise, is due to *S. aureus* strains possessing a large assortment of virulence factors carefully regulated by different systems (28). Both environmental signals, such as molecular oxygen, pH, and nutrient levels and detection of population density using quorum sensing, are cues that *S. aureus* utilise to form a response in the form of modulation of virulence genes (22, 29). The ability to sense the surrounding environment makes the bacterium a successful pathogen. As a response, it can evade the host's immune system, form capsules and biofilms, and tune toxin production

and metabolic pathways (22, 28). The presence of quorum sensing accessory gene regulator (Agr) system is one such system that plays a major role in virulence by gene expression and is associated with all groups of *S. aureus* virulence genes (30, 31).

Epithelial cells are joined in tight junctions creating a barrier to prevent pathogens from entering the body through the skin- and mucous layers, thereby causing infections (32). *S. aureus* can secrete several different toxins, such as hemolysin A (Hla), to circumvent this barrier, resulting in alterations of the actin cytoskeleton, ultimately leading to disruptions of the host cell-matrix adhesion by gap formation (33, 34). As described in detail by Cheng G., Bae J., and Otto M. (2021), *S. aureus* has a plethora of mechanisms to inhibit the host's innate immune response to the infection. Briefly, secreted molecules can inhibit opsonisation, complement activation, neutrophil activation- and extravasation, decrease pro-inflammatory activity, and eliminate antimicrobial peptides. Cytotoxins lyse cells, such as leukocytes, and some have been shown to trigger apoptosis. Finally, the ability to form extracellular capsules, cell aggregates, and biofilms prevents phagocytosis (28). Adhesion proteins facilitate tissue invasion, especially those belonging to the microbial surface components recognising adhesive matrix molecules (MSCRAMM) family (28, 35). These proteins, as well as peptidoglycan hydrolases (section 1.2.5), are also important in the initial stage of biofilm formation (section 1.2.2), a virulence factor associated with the maintenance of infection over long periods of time (25, 28). This can be attributed to the fact that cells growing in a biofilm attach to a surface and embed themselves in an extracellular matrix, serving as a barrier against certain immune defences and antibiotics (25). It has been suggested that the biofilm is able to "hide" from macrophages by gene down-regulation, and a study shows that neutrophils were unable to infiltrate and decrease bacterial numbers in biofilms (36, 37). In addition, biofilm cells have a 10-1000 fold increased resistance to antibiotics and accomplish this by entering a transient state of altered physiology or by the increased occurrence of horizontal gene transfer seen in biofilms (25, 38–40).

S. aureus can also cause food poisoning, by contaminating foods with staphylococcal enterotoxin, in addition to menstrual staphylococcal shock syndrome, also known as toxic shock syndrome, when toxic shock syndrome toxin-1 producing strains form biofilms on tampons (28).

1.2 *S. aureus* biofilms

As 90% of bacteria exist in and form biofilms, whereas only 10% are in a free-floating (planktonic) form, biofilms are the preferred microbial mode of life (41). A biofilm is a three-dimensional sessile bacterial community embedded in a self-produced extracellular polymeric substance, also known as an extracellular matrix (ECM), consisting of extracellular DNA (eDNA), polysaccharides, and proteins (40). Bacterial cells usually make up 5-35% of the volume (42). Biofilm formation begins with planktonic cells attaching to a biotic or an abiotic surface, such as cell tissue or indwelling medical devices, respectively (40). Maturation and dispersion follow the attachment, making up the three main stages of biofilm formation. In natural settings, including human disease, biofilms are usually polymicrobial and can form communities with other species of bacteria, yeasts, and viruses (40, 43). These interactions further complicate treatment options (40). Biofilm formation relies on various proteins and several regulatory systems that largely depend on environmental signals in their control of the regulation, thus making the formation and life cycle of biofilms complicated and sensitive to their microenvironment (40).

1.2.1 Clinical impact and antibiotic resistance

The Centre for Disease Control (CDC) and the National Institute of Health (NIH) estimate that 65-80% of human infections involve the formation of biofilms (44). *Staphylococcus epidermidis* and *S. aureus* are the most prevalent microbial species in medical device infections (45). However, as described in section 1.1.3, *S. aureus* can also cause severe systemic device-unrelated infections. Biofilm infections pose an especially challenging threat because of their evasion of the immune system and increasing resistance to antibiotics compared to planktonic cells and are associated with increased morbidity and mortality (28, 38, 46). Infected medical devices often require surgical removal (46).

The adhesive extracellular matrix acts as a barrier against antibiotic penetration, gradually decreasing the antibiotic concentration towards the biofilm's centre, resulting in non-lethal exposure across the gradient (40). This could activate antibiotic resistance mechanisms leading to collective resistance throughout the biofilm, e.g., by antibiotic inactivation (40, 47). The diffusion efficacy is poorer with large, positively charged antibiotic molecules, whereas smaller molecules, such as β-lactams, appear unaffected (47). However, through spatial organisation, antibiotic inactivating enzymes can concentrate near the biofilm surface, forming an additional

layer of protection (40, 47). Furthermore, an increased occurrence of horizontal gene transfer promoting the spread of antibiotic resistance genes is seen by *S. aureus* biofilm-residing cells, possibly due to close cell-to-cell contacts and increased stability of contact points, as suggested by Savage V. J., Chopra I., and O'Neill A. J. (39). It has also been proposed that metabolically dormant cells within the biofilm, due to low nutrient and oxygen levels, are major determinants of antibiotic resistance, as metabolically inactive cells are tolerant to drugs targeting actively growing cells (48). For instance, β-lactams target cell wall synthesis and is ineffective against non-dividing cells (48).

1.2.2 Stages of biofilm formation

Biofilm formation is generally described in three distinct stages: attachment, maturation, and dispersal, as illustrated in **Figure 1.1**. During the attachment stage, planktonic cells attach to a surface of either biotic or abiotic nature. For *S. aureus*, attachment is mediated by surface proteins, teichoic acids, and eDNA from lysed cells. (40). Peptidoglycan hydrolases, such as major autolysin AtlA in *S. aureus* and AtlE in *S. epidermidis*, hereby referred to as Atl, facilitate attachment by peptidoglycan cell wall hydrolysis of a subpopulation of the biofilm-associated cells, releasing adhesive eDNA (49–52). Teichoic acids, glycopolymers anchored either to the cell wall or the membrane, have also been shown to mediate attachment by their net negative charge (53). It has been suggested that surface proteins mainly facilitate the attachment to biotic surfaces, such as epithelial cells, whereas peptidoglycan hydrolases and teichoic acids predominantly mediate attachment to abiotic surfaces, such as glass and polystyrene (46). Of the surface proteins, those belonging to the MSCRAMM family have been well studied, and many are involved in the attachment (54). *S. aureus* encodes multiple MSCRAMMs, including ClfA, FnBPA, and SdrC, facilitating binding to fibrinogen, fibronectin, and epithelial cells, respectively (54). Cells with a mutated Atl cannot form biofilms due to their inability to attach to a surface, underlining the importance of the attachment stage (51). More knowledge about how *S. aureus* initiates the biofilm formation process could reveal possible strategies to combat biofilm infections.

The maturation stage is characterised by the production of the majority of the adhesive ECM and rapid cell division, allowing the biofilm to grow in size and produce multiple layers, resulting in a three-dimensional structure (25, 40). Currently, two pathways for ECM formation have been recognised, a polysaccharide dependent and a -independent pathway (55). The

polysaccharide-dependent pathway relies on the production of polysaccharide intracellular adhesin (PIA, also known as PNAG) biosynthesised from components encoded within the *ica*-operon (55). PIA and the *ica*-operon are described in in section 1.2.4.3. The PIA-independent pathway of biofilm maturation, more frequently observed in MRSA than in methicillin-sensitive *S. aureus* (MSSA) strains, produces a proteinaceous biofilm and is mediated by accumulation of and interactions between proteins, such as FnBPA and FnBPB (40, 56). Atl is important in the attachment stage of MRSA and for MSSA on hydrophobic surfaces (56).

After the maturation stage, the ECM may be degraded to release clusters of cells from the biofilm, allowing the re-establishment of a biofilm elsewhere, in the final phase of biofilm formation, known as the dispersal (or detachment) stage (25, 57). The composition of the ECM may vary. Thus several dispersal agents targeting different components are known, many of which are under the regulation of the Agr system, such as proteases and phenol-soluble modulins (PSM) (25, 58). Additionally, nucleases have been suggested as significant dispersal agents in biofilms with eDNA-rich ECMs (59). Dispersal can be triggered by glucose depletion, suggesting biofilms may detach in response to low nutrient levels (60).

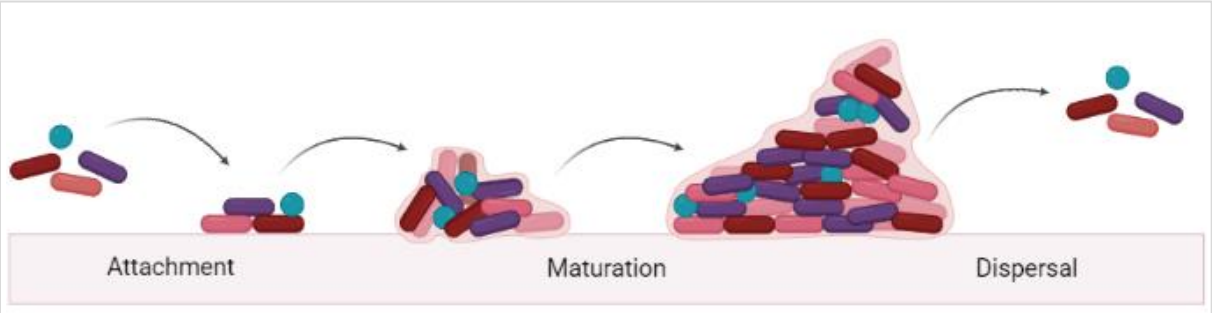

Figure 1.1. Schematic illustration of the three main stages of formation in a polymicrobial biofilm. During attachment, the initial stage of biofilm formation, planktonic cells attach to a surface in a process mediated by surface proteins, teichoic acids, and eDNA. The latter as a result of cell lysis mediated by peptidoglycan hydrolases. Cell division and production of the bulk of the ECM characterise the maturation stage. The ECM is produced either by the PIA-dependent or -independent pathway. In the final stage, dispersal, a subpopulation of cells is released from the biofilm by the degradation of the ECM. Created in BioRender.com.

Biofilm formation is sometimes referred to in five stages, in which a multiplication- and an exodus stage follow attachment (46). In the multiplication stage, cells divide to form a mat, and the ECM begins to form around them (46). Exodus is characterised by the detachment of a subpopulation of the biofilm cells, mediated by partial degradation of the ECM (46).

1.2.3 Regulation of *S. aureus* biofilm development

Biofilm formation is a complex process, evident by the extensive number of proteins and regulatory systems involved (40). Quorum sensing and an array of environmental signals, such as pH, and nutrient- and oxygen availability, are among the factors that determine the composition of the ECM and the activation of different regulatory paths (40, 58).

The well-studied Agr system is vital for regulating both the attachment- and the dispersal stage of biofilm formation by *S. aureus* (58). Briefly, the *agrABCD* genes encode components necessary for biosynthesis, export, and signal transduction of autoinducing peptide AIP, which will accumulate in the extracellular space (30, 58). At a certain threshold, AIP will signal cells to upregulate the expression of proteases and PSMs involved in the dispersion stage and block the expression of adhesive molecules involved in the attachment stage (30, 40, 58). The Agr system is itself under regulation by the staphylococcal accessory regulator SarA which can upregulate its expression and downregulate the expression of proteases (58). *S. aureus* strains with mutations in *sarA* exhibit a decreased ability to form biofilms (61). The two-component SaeRS system recognises human host factors and subsequently regulates the expression of biofilm-associated genes, such as MSRAMMs, and the nuclease Nuc, facilitating eDNA degradation (58). Interestingly, the SaeRS system has been shown to counterbalance the inability of *S. aureus* Newman strains to form biofilms due to their mutated SarA system, further underlining the complexity of biofilm formation regulation (58). Many *S. aureus* peptidoglycan hydrolases are regulated by the two-component system WalRK (62), which is described in section 1.2.5.1.

1.2.4 Components of the extracellular matrix

As mentioned above, the composition of the ECM can vary depending on the local microenvironment, and in addition, between closely related strains of *S. aureus*. The main substances involved are proteins, polysaccharides, and eDNA, possessing several functions in the biofilm (63). In addition to forming a rigid structure and adhering biofilm cells together and to the attached surface, all the ECM components may serve as a nutrient source by providing the biofilm-associated cells with composites containing carbon, nitrogen, and phosphorus (63).

The role of eDNA, proteins, and polysaccharides in the biofilm ECM will be further described in the following sections.

1.2.4.1 Extracellular DNA

Extracellular DNA (eDNA) was first recognised as an integral component of the biofilm ECM in *Pseudomonas aeruginosa* and has later proved to be central in biofilm adherence in *S. aureus* (64, 65). Staphylococcal biofilms treated with DNase I, an enzyme that degrades DNA, display a significant reduction in adherence, underlining the importance of eDNA in the attachment stage (65, 66). The charged phosphate backbone of DNA gives it a net negative charge allowing it to electrostatically attach the bacterial cells to surfaces, host factors, and each other (25, 40). eDNA, and teichoic acids, have been suggested to predominantly facilitate attachment to abiotic surfaces, as opposed to biotic surfaces, as is especially relevant in medical device-related infections (46). Lysis of the cell by degradation of the cell wall facilitated by peptidoglycan hydrolases is the majorly recognised mechanism for the release of eDNA in staphylococci (63). In addition to its role in attachment, a synergetic interaction of eDNA and both proteins and PIAs has been observed, suggesting that eDNA also maintains adhesion between cells and rigidity of the biofilm (67, 68).

1.2.4.2 Proteins

Protein-mediated biofilm formation, in contrast to PIA-dependent biofilm formation, is more frequently seen in MRSA than MSSA strains, as well as laboratory strain SH1000 (60, 69). Proteins occur in the ECM both as cell wall anchored (CWA) structural proteins and extracellular enzymes (63). *S. aureus* expresses up to 24 different CWA proteins anchored to the peptidoglycan cell wall by sortase A by recognising the LPXTG motif within a sorting signal located at the N-terminal of the CWAs (70). One such protein, *S. aureus* surface protein G (SasG), has been found to mediate ECM production and cell adhesion by forming an antiparallel twisted structure protruding from the cell wall, which can undergo spontaneous cleavage (70, 71). CWAs of the MSCRAMM family promote attachment and adhesion between cells, e.g., by FnBPs, as often seen in MRSA strains (69, 70). Extracellular proteins include ECM-modifying enzymes, such as nucleases, and virulence-associated enzymes, such as Hla (40, 63, 72).

1.2.4.3 Polysaccharide intracellular adhesin (PIA)

Polysaccharide intracellular adhesin (PIA) is the dominant molecule in the PIA-dependent (also known as *ica*-dependent) mode of biofilm formation (40, 55). PIA was named based on its function but is alternatively called poly-β-1-6-N-acetylglucoseamine (PNAG) to describe its chemical properties (55). Despite the discovery of PIA-independent biofilm phenotypes, it is still considered a major biofilm-forming agent in *S. aureus* (55, 73). The *ica* (intracellular adhesion) operon, first described in 1996, encodes four genes, *icaA, -B, -C, and -D*, all of which are necessary for PIA synthesis and are under the regulatory control of *icaR* (**Figure 1.2**) (44, 55). The *icaR* regulator is itself regulated by other regulators, in addition to environmental cues (73). Briefly, IcaAD synthesises a poly-*N*-acetylglucosamine (poly-Glc*N*Ac) from Glc*N*Ac precursors, which is subsequently exported from the cell by the membrane-protein IcaC (55). In the extracellular space, the polymer is deacetylated by IcaB, giving it the net positive charge to which its functionality is owed (55).

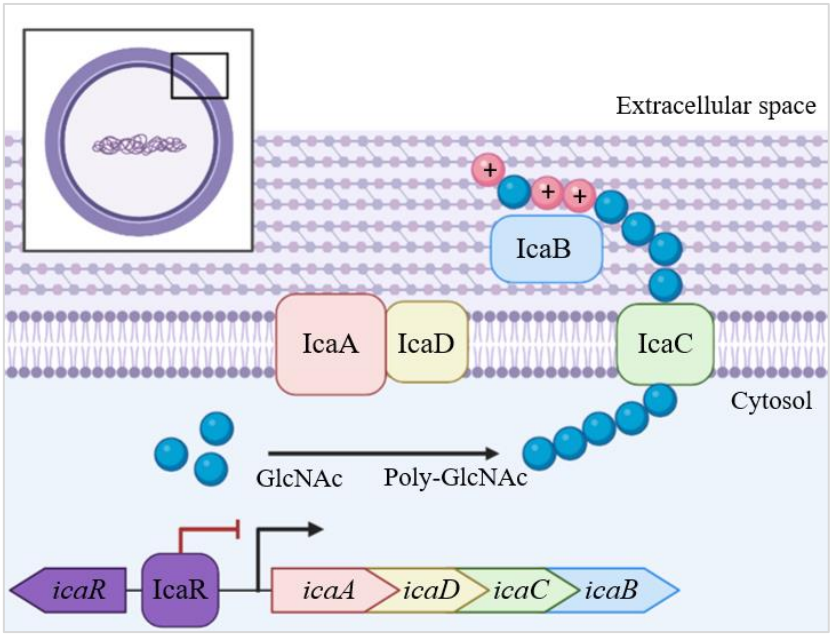

Figure 1.2. The *ica*-operon consists of the genes *icaA, -D, -C,* and *-B,* all of which are required for PIA biosynthesis. IcaR, encoded by the upstream *icaR,* regulates the operon by binding to the promoter region and inhibiting transcription (55). IcaA and IcaD produce a poly-Glc*N*Ac chain from precursor Glc*N*Acs. IcaC exports the chain, which is subsequently deacetylated by IcaB. The figure is adapted from Nguyen H. T. T., Nguyen T. H., and Otto M (2020) and created in BioRender.com

PIAs mainly function in the maturation stage of biofilm formation by forming large nets, making up the bulk of the ECM, and thus embedding cells and other substances in the biofilm (55). Additionally, PIAs interact electrostatically with the negatively charged teichoic acids (55). A study found that MRSA strains forming biofilms by the PIA-dependent pathway had an increased resistance to antibiotics, particularly vancomycin, a frequently utilised drug in MRSA infections (74).

1.2.5 Peptidoglycan hydrolases

The main component of the *S. aureus* cell wall is, like other Gram-positive bacteria, a thick layer of peptidoglycan, also referred to as murein. The peptidoglycan glycan chains are made up of alternating units of amine sugars *N*-acetylglucosamine (Glc*N*Ac) and *N*-acetylmuramic acid (Mur*N*Ac) and are connected by short peptides bound to the Mur*N*Ac residues (75, 76). The nascent stem peptides consist of L-alanine, D-*iso*glutamine, L-lysine with a penta-glycine attached, and a terminal D-alanine-D-alanine (76). About 90% of these stem peptides are cross-linked via the pentaglycine bridge, creating a strong and rigid mesh (75–77). Peptidoglycan hydrolases are enzymes capable of peptidoglycan cell wall cleavage, giving them roles in many cellular- and viral processes, such as cell separation, -growth, and -division, peptidoglycan tailoring and -recycling, and predation by bacteriophages (78). All glycosidic and amide bonds in peptidoglycan can be cleaved by different hydrolases, which are classified according to their cleavage site (**Figure 1.3)** (78, 79). Broadly, they can be characterised as either glycosidases or peptidases, making cuts in the glycan backbone or the stem peptides and cross-links, respectively (78).

As mentioned, they also serve an essential function in the attachment stage of biofilm formation by cleaving peptidoglycan, leading to cell lysis and the subsequent release of adhesive eDNA (40). In addition to its role in cell division, the predominant peptidoglycan hydrolase in staphylococci, Atl, is known to majorly contribute to biofilm formation by mediating attachment (40, 51).

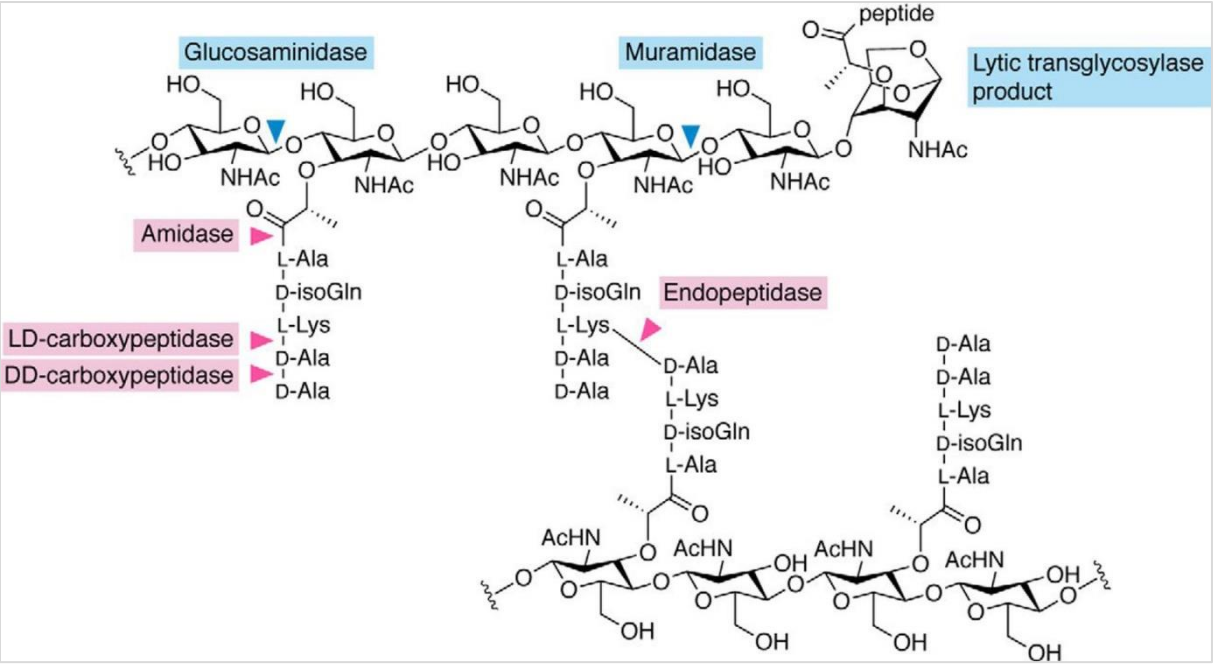

Figure 1.3. Classes of peptidoglycan hydrolases and their respective cleavage sites. The glycosidases (glucosaminidases, muramidases, and lytic transglycosylases) (in blue) cleave bonds within the glycan backbone of peptidoglycan. Peptidases (amidases, LD-carboxypeptidases, DD-carboxypeptidases, and endopeptidases) (in pink) cleave the peptide cross-links and bonds within the stem peptides. The figure is from Do T., Page J. E., and Walker S. (2020).

1.2.5.1 Regulation of peptidoglycan hydrolases

As peptidoglycan hydrolases have the ability to compromise the structural integrity of the cell wall, a fine-tuned regulatory system that allows essential functions to be carried out whilst still preventing uncontrolled cell lysis is crucial (78). In *S. aureus*, many hydrolases are under the regulation of the WalRK system. The two-component regulatory system WalRK (also known as YycG/YycF) is highly conserved and specific to low GC %, Gram-positive bacteria, including *S. aureus* (80, 81). WalK is a histidine kinase which, in response to environmental signals, auto-phosphorylates a conserved histidine residue and subsequently phosphorylates the regulatory domain of the response regulator, WalR, which in turn acts as a transcriptional regulator (82). The system is essential in *S. aureus* and is involved in cell division, biofilm formation, and virulence (82). Several peptidoglycan hydrolases are under regulation by this system, including Atl, SsaA, LytM, and Sle1, and SAOUHSC_00671 (SAOUHSC_00671 is described in section 1.2.5.2) (80, 81, 83). In a study where WalR was constitutively expressed, an increase of several peptidoglycan hydrolases and virulence genes, as well as a downregulation of negative *ica*-regulator *icaR*, was observed (83). Depletion of the system in

S. aureus leads to abnormal division septa, rougher cell surfaces, and eventually death (81, 82). Other systems may be involved in the regulation of peptidoglycan hydrolases as well, such as the *cid* and *lrg* operons which are known to be involved in biofilm formation by controlling cell lysis and thereby the release of eDNA (84).

1.2.5.2 The uncharacterised peptidoglycan hydrolase *SAOUHSC_00671*

In the master's thesis of Torrissen Mårli M. (2020), a depletion screen involving several putative peptidoglycan hydrolases, all under the regulation of the WalRK system, was conducted (85). A considerable decrease in biofilm formation of *S. aureus* was seen when depleting *SAOUHSC_00671* (85). The results were later verified by Morales Angeles, D. (unpublished). *SAOUHSC_00671* is the locus tag of a gene in strain NCTC8325-4 encoding a putative peptidoglycan hydrolase (UniProt ID Q2G0D4). The translated protein, hereby referred to as 00671, contains two Lysin Motif (LysM) domains, known to bind to peptidoglycan, as well as a cysteine, histidine-dependent amidohydrolase/peptidase (CHAP) domain, with a peptidoglycan hydrolytic activity (86, 87). The AlphaFold predicted structure of 00671 is shown in **Figure 1.4A**, and a schematic illustration of the structure is displayed in **Figure 1.4B**.

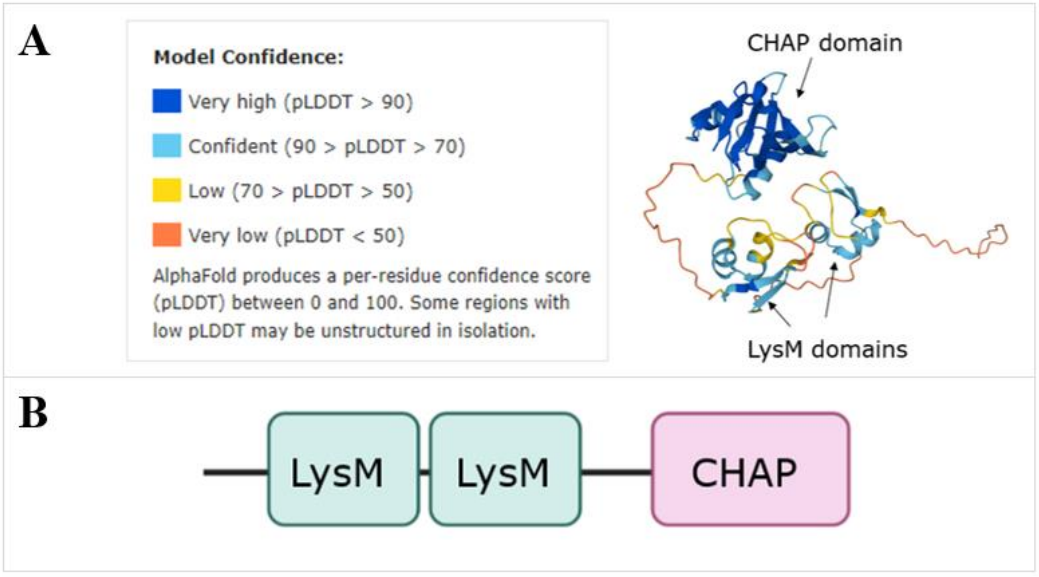

Figure 1.4. A. The predicted three-dimensional structure of 00671 (AlphaFold). 00671 contains two LysM domains and a CHAP domain known to bind to and hydrolase peptidoglycan, respectively. The structure's colour displays the model's confidence, as explained in the left panel. **B.** Schematic illustration of the 00671 predicted domains.

Studies have shown that the protein has a weak lytic activity toward *S. aureus* cells and is regulated by the WalK/WalR system (section 1.2.5.1) (referred to as SA0620 and SsaALP in references 80 and 88, respectively) (80, 88). However, the hydrolase remains largely uncharacterised. Understanding the different components in biofilm formation is vital to discover ways to tackle biofilm-associated infections, and peptidoglycan hydrolases have been demonstrated as a potential treatment option (89). In this work, the role of 00671 in biofilm formation was explored further, in addition to its genetic correlation with structurally related protein SsaA (section 1.2.5.3).

1.2.5.3 Genetic correlation between peptidoglycan hydrolases

Negative genetic correlation is a term that in this work is used to describe the correlation in expression between two genes in which one gene is being upregulated due to the downregulation of another, and vice versa. This type of correlation has been observed with WalRK-regulated peptidoglycan hydrolases ClwO and LytE in *Bacillus subtilis* (90). The authors provided evidence that the WalRK system modulated their expression in response to both increased and decreased cell cleavage activity to maintain homeostasis (90). In *S. aureus,* WalRK-regulated hydrolases have been suggested to compensate for the loss of Atl activity (91). In fact, previous results from our lab have shown such a correlation between 00671 and the structurally related putative peptidoglycan hydrolase SsaA (unpublished). The experiments were performed using expression reporter plasmids (described in 1.4.2), producing luminescent light as a measurement for expression. By using the CRISPRi system (described in section 1.4.3) for depletion and measuring the emitted luminescence during growth, it was seen that 00671 is increased when SsaA is depleted and vice versa. SsaA contains a CHAP domain and, like 00671, is regulated by the WalR/WalK two-component system (80, 81, 83). Genetical negative correlation between peptidoglycan hydrolases has not yet been elucidated in *S. aureus,* especially not in biofilms.

1.3 Novel cell morphology determinant SmdA

Staphylococcal morphology determinant A (SmdA) was recently identified as a critical protein for normal cell division in *S. aureus* (92). Depletion of SmdA, which consist of a large intracellular NERD-, a transmembrane-, and an extracellular domain, resulted in abnormal

phenotypes regarding division septa, roundness, and cell size (92). Similarly, overexpression of SmdA also led to irregularly dividing cells (92). In an RNA sequencing analysis of an SmdA-depleted strain, a downregulation of *icaA, -B,* and *-D* was observed (**Table 1.1**, Kjos M., unpublished). As described in section 1.2.4.3, the *ica*-genes are heavily associated with biofilm formation in *S. aureus*. However, it is unknown how SmdA affects the formation of biofilms.

Table 1.1. Downregulation of *icaA, -B, and -D* in an SmdA-depleted strain (Kjos M., unpublished). Change in expression is stated in $\log_2$ fold change compared with a wildtype-like strain.

Gene name	$\log_2$ fold change	Locus tag
icaA	-4.96	*SAOUHSC_03002*
icaB	-3.75	*SAOUHSC_03004*
icaD	-4.68	*SAOUHSC_03003*

1.4 *In vitro* approaches in *S. aureus* biofilm research used in this work

1.4.1 Confocal laser scanning microscopy

Confocal laser scanning microscopy (CLSM) is a microscopy technique that became commercially available in 1987 and is often considered an essential tool in biofilm research (93). The technique can provide three-dimensional live imaging, thus allowing visualisation and analysis of complex and dynamic biological structures, such as biofilms. This is acquired by local laser imaging- and layering of the focal planes (93). Biofilm CLSM is frequently coupled with fluorescent probes to analyse different cellular features, in which LIVE/DEAD staining is a well-known example. LIVE/DEAD staining is performed using SYTO9, a permeant green-fluorescent dye with a high affinity for DNA and Propidium Iodide, a DNA-binding red-fluorescent dye only permeant to dead cells. The properties of these two dyes allow assessment of the proportion of live-to-dead cells in a biofilm, which is useful, e.g., in the study of peptidoglycan hydrolases. In this work, fluorescent dyes and expression reporter plasmids expressing fluorescent proteins (section 1.4.2) were used to study biofilms.

1.4.2 Expression reporter plasmids

There are several different methods to study the expression of genes. Some methods quantify the amount of mRNA transcribed from a specific gene, such as Northern blots, RNA-sequencing, or qRT-PCR (94). Another method is the use of reporter genes, which is done by replacing the coding parts of the gene of interest with a reporter gene, encoding a protein whose expression can be measured (94). Alternatively, the reporter genes can be integrated directly downstream of the gene of interest or be fused with the promoter on a plasmid (referred to as expression reporter plasmids in this work) (95). As the promoter belongs to the original gene, the amount expressed and the timing of the expression of the reporter gene will reflect that of the gene of interest (94). Examples of reporters are fluorescence- and bioluminescence-producing proteins, with the emitted light as a measurement of expression. These proteins also allow for the visualisation of spatiotemporal expression by microscopic imaging. Reporter gene assays provide several benefits, including that analyses can be performed on living cells with repeated measurements under different conditions, and expression can be monitored in real-time (96).

Additionally, reporter genes are useful tools in the study of biofilms. Yellow fluorescent protein (YFP) fused with the constitutive *sarA* P1 promoter has been used to monitor the formation of *S. aureus* biofilms over the course of several days (97). The method has also been utilised to study the expression of specific genes and regulatory systems in biofilms, as demonstrated in reference 95. By the same principle, reporter genes can be used to study genetic correlation, as was done in our lab for the correlation between SsaA and 00671. Promoters of the hydrolases were fused with reporter genes *gfp* (Green fluorescent protein) and *luc* (luciferase) on two separate plasmids (pDMA032 for 00671 and pDMA038 for SsaA). See section 3.12 for more details about the specific plasmids. The change in expression of one hydrolase when depleting the other was measured as luminescent light and compared with a wild-type-genetic background carrying the same reporter plasmid.

1.4.3 CRISPRi/Cas9 interference and libraries

CRISPR (Clustered Regularly Interspaced Short Palindromic Repeats) is an adaptive immunity defence system against foreign nucleic acids, such as from phages, found in the genome of all bacterial genomes sequenced (98). The main features of the CRISPR sequence are shown in **Figure 1.5A**. Conserved repeated sequences of about 30 bp are separated by so-called spacer sequences of similar length (normally 20 bp). The bacterium has acquired these spacers from infecting phages (98). Upon re-infection, the entirety of the CRISPR is transcribed and processed into short strands complementary to a spacer sequence and the adjacent repeat, called crRNAs (CRISPR RNA) (98). These will, in turn, bind to conserved endonucleases, known as Cas-proteins, and target foreign nucleic acids for destruction (98). To further increase the specificity of the system, a short (2-5 bp) sequence known as a protospacer adjacent motif (PAM) is required on the phage DNA for the Cas to be functional (99). This system has proved to be a valuable tool in genetic engineering, and the most well-known is the CRISPR/Cas9 system to make knock-ins or knockouts of genes, illustrated in **Figure 1.5B** (100). CRISPR/Cas9 utilises a specifically designed single-guide RNA (sgRNA), combining the 20 bp spacer sequence complementary to target genes with a structural part responsible for interaction with the Cas9 proteins. Upon recognition of the target sequence complementary to the sgRNA and assembly of the sgRNA-Cas9 complex, the Cas9 protein makes double-stranded DNA cuts (100).

CRISPR interference (CRISPRi) is another example of how CRISPR/Cas9 can be utilised as a tool in research. First developed in *E. coli*, the system has later been utilised in several other species for transcriptional depletion, as illustrated in **Figure 1.5C** (101–103). The main difference between CRISPRi and CRISPR/Cas9 is that the CRISPRi system uses a catalytically inactive "dead" Cas9 (dCas9) with its DNA-binding function still intact (101). As such, dCas9 will bind to the target gene complementary to the designed sgRNA. This will inhibit RNA polymerase, thus resulting in a transcriptional knockdown of the gene (104). The CRISPRi system for *S. aureus* is a two-plasmid system in which the sgRNA is constitutively expressed, whereas *dcas9* is placed downstream of an IPTG-inducible promoter, thereby allowing standard transcription in the absence of IPTG (105). Other versions of the system have been constructed, such as with *dcas9* chromosomally integrated, inducible by anhydrotetracycline, and this latter version was used in the current work.

By designing unique sgRNAs with 20 bp long sequences complementary to the genes of interest and subsequent cloning, this system is utilised both in specific gene depletion and to construct large CRISPRi libraries (more info below), a useful tool, e.g., in screening assays (102). Additionally, the system allows for the study of essential genes. By low level induction of the system, essential genes can be depleted to the degree that allows survival of the cell whilst still exhibiting phenotypic changes. Compared to traditional knockout protocols, the CRISPRi system provides a fast, easy, and reversible approach to gene depletion.

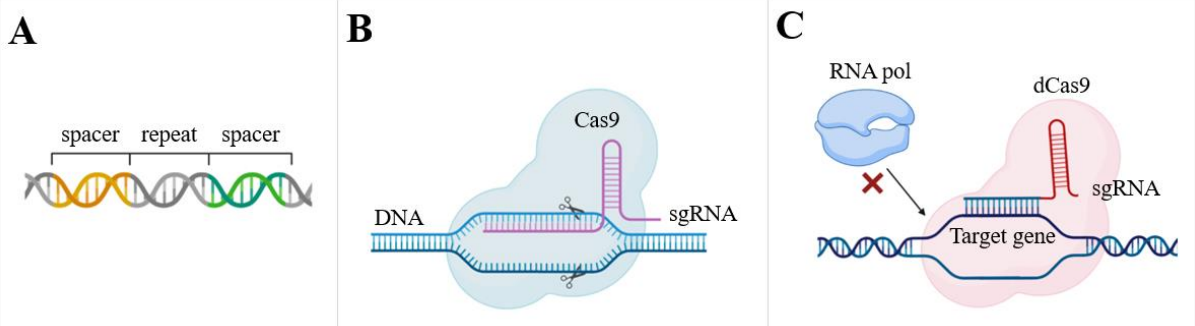

Figure 1.5. Schematic illustration of CRISPR and CRISPR interference. **A.** Structure of CRISPR in the bacterial genome. Spacer sequences acquired from infecting viruses and conserved repeating sequences, each of about 20 bp, in an alternating fashion, make up the main feature of CRISPR. **B.** The CRISPR/Cas9 system. Cas9, guided by the sgRNA to the complementary target gene, makes a double-stranded cut in the DNA. C. The CRISPRi system is used for transcriptional depletion. The catalytically inactive dCas9 binds to the target gene by complementation to the sgRNA, acting as a transcriptional roadblock and thus preventing transcription. Created in BioRender.com.

CRISPRi libraries are collections of cells harbouring sgRNAs, ideally covering all genomic features of an organism's genome. This collection is materialised as a pool of strains carrying unique plasmids containing the specific sgRNAs (106). This pooled CRISPRi library allows screening assays to assess genome-wide gene fitness in several conditions (104). When the system is induced, all genomic features present in the library are depleted across different cells. To perform a screening assay using a CRISPRi library, cells in the library can be subjected to specific treatments (e.g., different growth conditions, antibiotic treatments), resulting in changes in sgRNA abundancies resulting from enrichment or depletion of cells carrying specific gene-targeting sgRNAs (104). The bacterial cells are harvested after treatment, and the sgRNA-plasmids are isolated for sequencing of the sgRNA 20 bp sequence. Bioinformatic analyses of the sequenced sgRNAs are performed to reveal which gene depletions lead to a significant increase or decrease in sgRNA abundance, indicating which genes are costly or essential for

the condition being studied (104). **Figure 1.6** shows a schematic illustration of the principles of a screening assay. CRISPRi library screening assays has been shown to be a useful tool in biofilm studies, as demonstrated by Torrissen Mårli M., who used the method to identify novel genes involved in macrocolony biofilm formation (85).

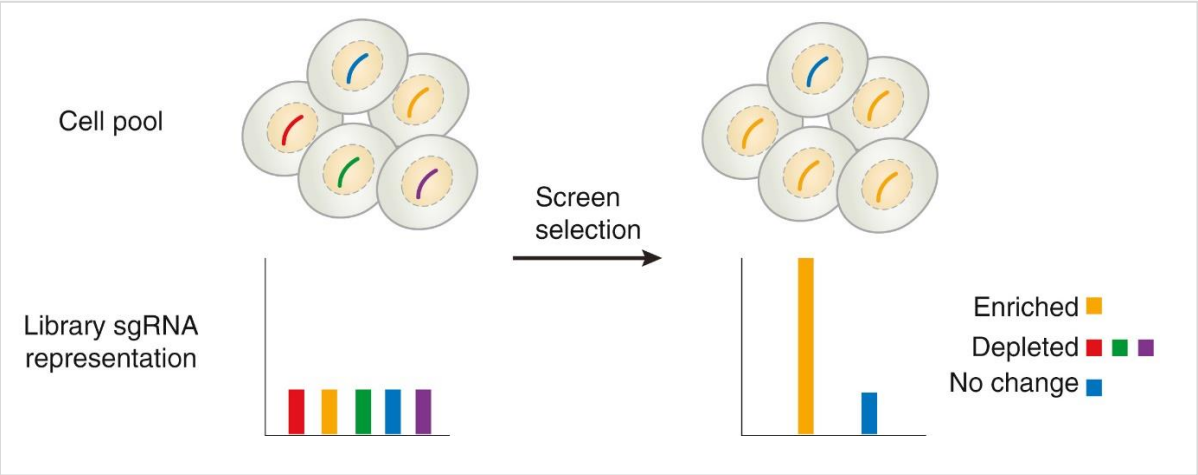

Figure 1.6. The principles of CRISPRi library screens. A library (cell pool) with all sgRNA represented is subjected to treatment. The cells selected for their target change after the treatment harbour plasmids with sgRNAs whose abundance is enriched (yellow), depleted (red, green, and purple), or not changed (blue) relative to the initial representation. Depending on the target change for selection, depletion of the genes targeted by the yellow, red, green, and purple sgRNAs alters the cell's fitness in the treatment environment. The figure is adapted from Sanjana E. N. (2017), with permission.

1.5 Aim of the study

S. aureus biofilm-associated infections are especially concerning due to their increased resistance to antimicrobials and the immune defence. An improved fundamental understanding of biofilm formation, its life cycle, and its many components is required to combat this threat. Three main topics were studied in this work. Firstly, *SAOUHSC_00671* encodes a putative peptidoglycan hydrolase, 00671, a group of enzymes associated with the attachment stage of biofilm formation. A decrease in biofilm formation was reported for a 00671-depleted strain, and therefore we wanted to explore its involvement in the process. Furthermore, we wanted to study the observed genetic correlation between 00671 and the structurally related protein SsaA, especially in biofilms. Secondly, a strain depleted of a novel cell morphology determinant (SmdA) was shown in an RNA-sequencing analysis to exhibit a downregulation of biofilm-associated *ica*-genes, which led us to explore the role of SmdA in biofilm formation. Finally, a genome-wide screen of a CRISPRi library was conducted to identify novel attachment-related genes in *S. aureus*. To summarise, this study aimed to:

1. Explore the role of the putative peptidoglycan hydrolase 00671 in biofilm formation and investigate the association between 00671 and SsaA,.
2. Explore the role of novel cell morphology determinant SmdA in biofilm formation.
3. Identify novel biofilm-associated genes by conducting a genome-wide screen of attachment-related genes in a CRISPRi library

2 Materials

2.1 Strains and plasmids

Table 2.1. List and description of plasmids used in this work.

Plasmid	Description[1]	Source or reference
pCG248	*E. coli/S. aureus* shuttle vector, *ampR*, *camR*	Helle et al. (2011)
pDMA032	pLOW with *luc* and *gfp* downstream of the 00671-promoter, *eryR*	Morales Angeles D.
pDMA038	pLOW with luc and gfp downstream of the SsaA-promoter, *eryR*	Morales Angeles D.
pDMA044	pCG248, with *cfp* downstream of the SsaA-promoter, *ampR*, *camR*	This work
pDMA045	pMAD, with a tetracycline resistance cassette flanked by sequences homologous to *ssaA*-flanking sequences, *ampR*, *tetR*	This work
pLOW	IPTG-inducible expression of proteins in *S. aureus*, *ampR*, *eryR*	Liew et al. (2011)
pMAD	X-GAL, vector for allelic replacement in Gram-positive bacteria, *ampR*, eryR	Arnaud et al. (2004)
pRN10	Shuttle plasmid for *sarA P1-mKate* expression, *ampR*, *camR*	de Jong et al. (2017)
pRN110	Temperature sensitive plasmid for chromosomal integration containing the Newman genetic region between genes 29 and 3 + *SarA_P1-mKate2-Term*	de Jong et al. (2017)

[1] ampR; ampicillin resistance gene, camR; chloramphenicol resistance gene, eryR; erythromycin resistance gene

Table 2.2. List and description of parental strains used in this work.

Species	Strain	Genotype and characteristics	Source or reference
E. coli	IM08B	DH10B, Δ*dcm*, P_{help}-*hsdMS*, P_{N25}-*hsdS* (strain expressing the *S. aureus* CC8 specific methylation genes)	Monk et al. (2015)
S. aureus	NCTC8325-4	NCTC8325 cured for φ11, φ12, and φ13	Novick (1967)
S. aureus	JE2	USA300 LAC derivative cured of plasmids p01 and p03. community-associated MRSA, SCC*mec* type IV.	Fey et al. (2013)
S. aureus	SH1000	*rsbU+* derivative strain of NCTC8325-4	Horsburgh et al. (2002)

All remaining strains used or constructed in this work are listed in **Appendix 1**.

2.2 Primers

Table 2.2. List of primers used in this work

Name	Sequence (5'-3')	Reference
Primers for pRN10 screening		
dma242	GCCGAGAAAATTTATTGTGCGTTG	Morales Angeles D.
dma243	TGACAAGGGTGATAAACTCAAATACAGC	Morales Angeles D.
Primers for overlap PCR construction of pDMA045		
dma254	CAGAGTCGACGACGACTACCATCGTATGTATTTAATGACA	Morales Angeles D.
dma255	TTAGAACTATGAGTGGCTAGTTTAAAAATATCCTCCTAAAAA TTTTAAATCTAAAATATTTTCGTT	Morales Angeles D.
dma256	TTTAGGAGGATATTTTTAAACTAGCCACTCATAGTTCTAAAC CAAAA	Morales Angeles D.
dma257	GTAAACATAGCCATCACTAATGTACATATTAATATTACTGAA CAAAAATGATATATTTAAACTATTC	Morales Angeles D.
dma258	CAGTAATATTAATATGTACATTAGTGATGGCTATGTTTACGC CA	Morales Angeles D.
dma259	CAGAGGATCCTCTGCCATTATAGTGGGGACTTT	Morales Angeles D.
Primers for overlap construction of pDMA044		
dma260	GCGTTTATAGAATTCGGTCGAGCCTTACATCCTCACATATAC AAATATATTGA	Morales Angeles D.
dma261	CCAAGATAGGTACTACACCTGTAAAAAGTTCTTCTCCCACCA TTTTAAAAATATCCTCCTAAAAATTTTAAATCTAAAATATTTT CGT	Morales Angeles D.
dma262	TTTAGGAGGATATTATGGTGTCAAAAGGAGAAGAACTTTTTA CAGGTGTAGTACCTATCTTGGT	Morales Angeles D.
dma263	GAGCTCGGTACCCGGGGATCTTATTTATAAAGTTCGTCCATA CCGTGAGTGATAC	Morales Angeles D.
Primers for sequencing of pDMA044		
rm019_cfp_fwd1	AGTTTTCACAAAGAATGCCGTAGTTATA	This work
rm020_cfp_rev1	TCAAGAAGTACCATATGGTCACGTT	This work
rm021_cfp_fwd2	TGCTATGCCAGAAGGTTATGTACAA	This work
rm022_cfp_rev2	AGTGCATACCTCTATCTCGTTTTTG	This work
rm023_pssaA_fwd1	CATCAAATAAAACGAAAGGCTCAGTC	This work
rm024_pssaA_rev1	CCCCATGTCAATGTTGTAACAAGA	This work
Primers for chromosomal *mKate* (pRN110) screening		
dma066	CCCGGGTACCTTAGGAGGATGA	Morales Angeles D.
im168	AGTACGCGTTTAACGGTGTCCCAATTTACTA	Myrbråten Storaker I.
Primers for pDMA045 sequencing		
rm013_tet_fwd1	GTTAACAAAGCACACAAGGACGC	This work
rm014_tet_rev1	TTAAAGTAATGGTACCTGGTAAATCAACAA	This work
rm015_tet_fwd2	ACTTTTTCGATAGGAACAGCAGTATATG	This work
rm016_tet_rev2	ACTTTTTCGATAGGAACAGCAGTATATG	This work
rm017_tet_fwd3	TGTTGATTTACCAGGTACCATTACTTTAAT	This work

2.3 Enzymes, chemicals, and pre-made buffers

Table 2.3. List of enzymes, chemicals, and pre-made buffers used in this work

Compounds	Product number	Supplier
1 kb DNA ladder	N0468	New England Biolabs
5x Phusion High Fidelity Buffer	B0518S	New England BioLabs
Agar powder	20767.298	VWR
Agarose	15510-027	Invitrogen
Alkaline Phosphatase, Calf Intestinal (CIP)	M0290	New England BioLabs
Ampicillin, $C_{16}H_{18}N_3O_4SNa$	A-9518	Sigma-Aldrich
Anhydrotetracycline hydrochloride, $C_{22}H_{22}N_2O_7 \cdot HCl$	13803-65-1	Sigma-Aldrich
Bacto™ Tryptic Soy Broth	211825	BD Diagnostics
Bacto™ Yeast Extract	212750	BD Diagnostics
BamHI-HF	R3136K	New England Biolabs
Brain Heart Infusion	CM1135	Oxoid
Calcium chloride dihydrate ($CaCl_2 \cdot 2\ H_2O$)	1.02381.0500	Merck
Chloramphenicol, $C_{11}H_{12}C_{l2}N_2O_5$	C0378	Sigma-Aldrich
Crystal Violet	C0775	Sigma-Aldrich
EDTA, $C_{10}H_{16}N_2Na_2O_8 \bullet 2H_2O$	20 296.360	VWR
Erythromycin, $C_{37}H_{67},NO_{13}$	E6376	Sigma-Aldrich
Gel Loading Dye Purpe (6x)	B7025S	New England BioLabs
IPTG, Isopropyl-β-D-thiogalactisidase	A1008,005	ITW Reagens
Isopropanol	L003092	Arcus
Lectin, *Triticum vulgaris* (wheat)	L3892-1MG	Sigma-Aldrich
Lysostaphin	9011-93-2	Sigma-Aldrich
Lyzosome	12650-88-3	Sigma-Aldrich
peqGreen	PEQL37-501	Saveen Werner
Phusion® High-Fidelity DNA polymerase	M0530	New England BioLabs
rCutSmart™ Buffer	B6004S	New England BioLabs
Red Taq 2X Master Mix	5200300-1250	VWR
SalI-HF	R3138S	New England Biolabs
Skim milk powder	1.15363.0500	Merck
Sodium Chloride (NaCl)	S9625	Sigma-Aldrich
Sodium hydroxide (NaOH)	1.06469.1000	Merck
Spectinomycin, $C_{14}H_{24}N_2O_7 \cdot 2HCl \cdot 5H_2O$	S9007	Sigma-Aldrich
Sucrose	84100	Sigma-Aldrich
SYTO™ 60	S11342	Invitrogen
SYTO™ 9	S34854	Invitrogen
T4 DNA ligase	M0202L	New England BioLabs
T4 ligase reaction buffer (10x)	B0202S	New England BioLabs
Tetracycline hydrochloride, $C_{22}H_{24}N_2O_8 \cdot HCl$	T3383	Sigma-Aldrich
Trizma® Base	77-86-1	Sigma-Aldrich
Tryptone	LP0042	Oxoid
Tween® 20	9005-64-5	Sigma-Aldrich
X-Gal	V394A	Promega
Yeast extract	1.04086.0250	Merck

2.4 Kits and equipment

Table 2.4. List of kits and laboratory equipment used in this work

Kit / Equipment	Model / Product number	Supplier
96-well polystyrene microtiter plates	82.1581.001	Thermo Fischer Scientific
12-well polystyrene multiwell™ plates	353043	Becton Dickinson Labware
Chambered coverglass	155411	Thermo Fischer Scientific
E.Z.N.A.® Plasmid Mini Kit I	D6943-02	Omega Bio-Tek
Gel imager	GelDoc-1000	BioRad
Laser scanning confocal microscope	LSM700	Zeiss
Microplate reader	Synergy H1 Hybrid Reader	BioTek®
NucleoSpin® Gel and PCR Clean-up	740609.250	Macherey-Nagel
PCR Thermocycler	ProFlex PCR systems	Applied Biodynamics
QIAGEN® Plasmid Midi Kit	12145	QIAGEN
Spectrophotometer	NanoDrop 2000	Thermo Fischer Scientific
Trans-Blot® Pure Nitrocellulose Membrane (0.45 µm)	162-0115	BioRad
SuperSignal™ West Pico PLUS Chemiluminescent Substrate	34580	Thermo Fischer Scientific
Imaging System	Azure c400	Azure Biosystems

2.5 Contents of prepared growth media, buffers, and solutions

1 kb DNA ladder (50 mg/mL)

50 µL 1 kb ladder, 200 µL 10x loading buffer, 750 µL dH_2O

50x TAE-buffer

424 g Tris base, 57.1 mL acetic acid, 100 mL 0.5M EDTA, pH 8.0

Adjusted to 1L with dH_2O

Lysogeny broth (LB)

10 g/L NaCl, 10 g/L tryptone, 5 g/L yeast extract, all autoclaved

Phosphate-buffered saline (PBS)

8 g NaCl, 0.2 g KCl, 1.44 g Na_2HPO_4, 0.24 g KH_2PO_4, dH_2O, pH 7.4

***Staphylococcus* lysis buffer**

40 mM NaOH, 0.2% SDS

Tris-buffered saline (TBS)

10 mM Tris-HCl (pH 7.5), 150 mM NaCl, pH adjusted with HCl

TBS with Tween® 20 (TBST)

0.1 % (v/v) Tween® 20 in TBS

3 Methods

3.1 Growth and storage of *E. coli* and *S. aureus*

All experiments were performed using the *S. aureus* strain NCTC8325-4, except in the SmdA-depletion biofilm assay (section 3.11), where JE2 and SH1000 were included. *S. aureus* was grown in liquid tryptic soy broth (TSB) or on tryptic soy agar (TSA) plates prepared with 1,5% agar (w/v). The strains used in the SmdA-depletion biofilm assay were grown in brain heart infusion broth (BHI). Media was supplemented with erythromycin (5 µg/mL), chloramphenicol (10 µg/mL), and spectinomycin (100 µg/mL) for selection and plasmid retention. Complementation was conducted with concentrations of isopropyl-β-d-thiogalactopyranoside (IPTG) ranging from 50-1000 µM. For the SmdA-depletion biofilm assay, a concentration of 300 µM IPTG was used. *E. coli* IM08B was used for cloning and was grown in lysogeny broth (LB) or on lysogeny agar (LA). Selective media was supplemented with 100 µg/mL of ampicillin. Glycerol was added to cultures at a 15-25% concentration to store *S. aureus* and *E. coli* at -80°C.

3.2 Plasmid isolation

High copy number plasmids were isolated from *E. coli* and *S. aureus* using the E.Z.N.A ® Plasmid Mini Kit I by following the manufacturer's protocol. All centrifugations were performed at 13,000 g. Cells were harvested from 1-5 mL culture by centrifugation for 1 minute, and the pellets were resuspended in 250 µL solution I, containing RNase to degrade RNA. As Gram-positive bacteria, *S. aureus* cells are more challenging to lyse. Therefore, 5 µL lysozyme (40 mg/mL) and 1 µL lysostaphin (10 mg/mL) were added to the resuspended pellet of *S. aureus* following incubation at 37°C for 30 minutes. Lysostaphin is an enzyme with hydrolytic activity against staphylococci at the pentaglycine bridge in the peptidoglycan structures of the cell wall (107). Lysozyme is an antimicrobial protein found in bodily secretions, such as tears and saliva, utilised for its peptidoglycan hydrolytic activities (108). The following steps were identical for both *S. aureus* and *E. coli*. First, 250 µL of an alkaline lysis buffer (solution II) was added, and the solution was mixed by inversion until a clear lysate was obtained. Next, 350 µL of a pH neutralising buffer was added to precipitate cellular components and genomic DNA before centrifugation for 10 minutes. The precipitated components form a pellet while the plasmid

DNA is kept in the supernatant. The supernatant was then transferred to an equilibrated HiBind® mini-column and washed with the HBC buffer. This buffer facilitates the binding of the DNA to the column by decreasing its solubility in water. Another washing step using the included wash buffer containing ethanol followed. A centrifugation of the empty column for 2 minutes was done to ensure the removal of any residual buffer. The supplied elution buffer was added (30-100 µL) to the column for release of DNA from the column. Plasmid concentration was measured using the NanoDrop™ 2000 spectrophotometer (Thermo Fischer) and the plasmids were stored at -20°C.

Low copy number plasmids, where the E.Z.N.A ® Plasmid Mini Kit I yielded insufficient concentrations, were isolated with the QIAGEN® Plasmid Midi Kit following the manufacturer's protocol. *E. coli* cells were harvested from 100 mL overnight cultures by centrifugation at 6,000 x g for 15 minutes at 4°C. The bacterial pellet was resuspended in 4 mL Buffer P1 containing RNase and 4 mL Buffer P2 (200 mM NaOH in 1% SDS (w/v) followed by 4-6 inversions and incubation at room temperature for 5 minutes. 4 mL neutralisation Buffer P3 was added and mixed as above. The lysate was incubated on ice for 15 minutes and centrifuged at 14,000-18,000 x g for 10 minutes at 4°C. The DNA-containing supernatant was applied to a QIAGEN-tip equilibrated with 100 mL Buffer QBT. 10 mL Buffer QC was used to wash the column twice before the DNA was eluted with 5 mL Buffer QF. The DNA was precipitated by adding 3.5 mL room temperature isopropanol (100% v/v) followed by centrifugation at ≥15,000 x g for 30 minutes at 4°C. A washing step with 2 mL ethanol (70% v/v) followed, and the DNA pellet was centrifuged again at ≥15,000 x g for 10 minutes. The pellet was left to air dry for 5-10 minutes before redissolving it in a suitable volume of dH_2O and measuring the concentration in the Nanodrop™ 2000 spectrophotometer (Thermo Fischer). Plasmids were stored at -20°C.

3.3 The polymerase chain reaction

The polymerase chain reaction (PCR) is a widely used method for amplifying specific fragments of DNA and is based on the principles of DNA replication naturally occurring in all dividing cells. Norwegian biochemist Kjell Kleppe (1934–1988) first described the concept in 1971, but the method was first implemented after American biochemist Kary B. Mullis (1944-2019) developed it in full by solving previous issues with the method (109). The main components of the PCR are the template DNA to be amplified, synthetic oligonucleotide

primers flanking the target sequence, a thermostable DNA polymerase, and the four deoxynucleotide triphosphates (dNTPs) dATP, dCTP, dGTP, and dTTP. Three steps of specific temperatures are repeated in 25-35 cycles: denaturation, annealing, and elongation by using a thermocycler (110). Optimally, one cycle doubles the amount of target DNA fragments (98).

In the denaturation step, the temperature is raised to 95-98°C, allowing the double-stranded DNA to separate into two single strands by breaking the hydrogen bonds holding them together (111). The temperature variation in this step is explained by the fact that different DNA polymerases vary slightly in thermostability. In the annealing step, the temperature is lowered so that the primers can bind to their complementary DNA sequence. The temperature for this step is typically 45-72°C and depends on the primer pair's melting temperature (Tm) (111). The annealing temperature should be just below the T_m, which is determined by the composition of bases and the length of the primer. The elongation step is performed at 72°C (111). In this phase, the DNA polymerases replicate the DNA strands by extending the sequence following the 3' OH end of the primers, utilising the dNTPs in the reaction mix (98). The amount of time necessary for this step varies with different DNA polymerases, their efficacy, and the length of the DNA sequence of interest. This newly synthesised strand is then used as a template in the next cycle, allowing the amount of target DNA to double for each cycle (98).

In PCRs where end-product sequences with a low mutation rate was required, such as cloning, the Phusion® High Fidelity (HF) DNA polymerase (NEB) was used. For screening, the RedTaq® DNA polymerase (Sigma-Aldrich) was used (see Colony PCR Screening). According to the producers, a *Pyrococcus*-like enzyme fused with a processivity-enhancing domain increases both the speed and the accuracy of the Phusion® High Fidelity polymerase and makes it suitable for processing long fragments.

For PCRs using the Phusion® High Fidelity polymerase, the reaction mix consisted of the DNA template, primers flanking the region of interest, dNTPs, and the 5x Phusion® HF buffer (NEB). The concentrations of the components are listed in **Table 3.1**, and all primers used in this work can be found in **Table 2.2**, section 2.2.

Table 3.1. Concentration of components in the Phusion® High Fidelity PCR reaction mix.

Component	Concentration/volume[a]
5x Phusion® HF buffer	1x
10 mM dNTPs	200 µM
10 µM forward primer	0.5 µM
10 µM reverse primer	0.5 µM
Template DNA	< 250 ng[b]
$MgCl_2$ (optional)	1 µL
Phusion® HF polymerase	1 unit
dH_2O	To a final volume of 50 µL

[a] Volumes are listed based on a total volume of 50 µL.
[b] In a 50 µL reaction, the volume of genomic DNA should be 50-250 ng, and 1 pg-10 ng for plasmid DNA.

The standard thermocycling program for PCRs using the Phusion® High Fidelity polymerase is listed in **Table 3.2**.

Table 3.2. Standard thermocycling program for Phusion® High Fidelity PCR.

Step	Temperature	Time	Cycles
Initial denaturation	98°C	30 seconds	1x
Denaturation	98°C	5-10 seconds	25-35x
Annealing	45-72°C[a]	10-30 seconds	
Elongation	72°C	15-30 seconds/kb	
Final elongation	72°C	5-10 minutes	1x
Hold	4°C	∞	

[a] Annealing temperature was adjusted per the T_m of the primers.

3.3.1 Colony PCR screening

Colony PCR is a method in which colonies or cultures of bacteria can be screened for the presence of a DNA fragment, i.e., after transformation. In this work, RedTaq® was used for colony PCR screening. The DNA of *S. aureus* cells is made available by cell lysis prior to mixing it in the reaction. Cells of *E. coli* can be added directly to the mix as they lyse during the initial denaturation step. The mix is then treated in the thermocycler with standard conditions. The fragment can be visualised on an agarose gel (section 3.4), following electrophoresis, for confirmation.

The protocol for lysing the cells differs for Gram-positive and Gram-negative bacteria due to differences in the cell wall thickness. For *E. coli*, a Gram-negative bacterium, adding 2 minutes to the initial denaturation step of the PCR program was sufficient for lysis. However, for *S. aureus*, a Gram-positive bacterium, the cells were resuspended in 30 µL of a lysis buffer (40 mM NaOH and 0.2 % SDS (w/v)) and incubated at 98°C for 5-10 minutes in the thermocycler. The cell lysate was then diluted in 170 µL dH_2O and cooled on ice before 2-4 µL was added to the PCR reaction mix.

The components of the PCR reaction mix using the RedTaq® polymerase are the template DNA, appropriate primers, and the RedTaq® ReadyMix™. The RedTaq® ReadyMix™ contains dNTPs, a buffering solution, the *Taq* polymerase, and a loading dye for gel visualisation and loading. The concentrations of the different components are listed in **Table 3.3**. The thermocycling programme used differs from the Phusion® programme only by the denaturation steps, which were carried out at 95°C, and at the elongation step, which was set to 1 minute per kb. This is due to the RedTaq® polymerase's instability at temperatures above 95°C and that its extension speed is approximately 1,000 bp per minute.

Table 3.3. Concentration of components in the RedTaq® PCR reaction mix.

Component	Concentration/Volume[a]
RedTaq® Master Mix 2x[b]	1x
10 µM forward primer	0.2 µM
10 µM reverse primer	0.2 µM
DNA template	2-4 µL diluted cell lysate
dH_2O	To a final volume of 50 µL

[a] Volumes are listed based on a total volume of 50 µL.
[b] The Taq 2x Master Mix contains dNTPs, a buffering solution, the *Taq* polymerase, and a loading dye.

3.3.2 Overlap Extension PCR

Overlap extension PCR (OE-PCR) is a PCR method in which an overhang in the sequence of the fragment or fragments is created, allowing the fusion of short DNA fragments or mutagenesis by primer design (112). In this work, OE-PCR was applied for joining fragments together to create inserts for plasmid construction. For the plasmid pDMA044, the *ssaA* promotor (P*ssaA*) was fused with *cfp*. For the plasmid pDMA045, a tetracycline resistance cassette was fused with the flanking regions of *ssaA* on each side. Schematic maps of the

constructed plasmids are found in **Appendix 2**. Both inserts were flanked by sequences containing restriction sites for SalI and BamHI, plus an additional few bases for restriction enzyme stability.

Fragments were amplified using a high-fidelity polymerase (Phusion®). For the pDMA045 plasmid, the *ssaA* flanking regions were amplified from *S. aureus* NCTC8325-4 chromosomal DNA (sequence 2232387-2233422 (upstream) and 2234227-2235267 (downstream)) using primers dma254 and dma255 for the upstream region, and primers dma258 and dma259 for the downstream region. The tetracycline resistance cassette containing *tetB* and -*D* was amplified from the plasmid pMG020 using the primers dma256 and dma257. The pDMA044 plasmid P_{ssaA} was amplified from *S. aureus* NCTC8325-4 chromosomal DNA (sequence 2232814-2233422) using the primers dma260 and dma261. *cfp* was amplified from the pLOW-ftsZ-CFP plasmid using the dma262 and dma263 primers. All the primers used had an additional sequence at the ends containing either the restriction enzyme sites or a sequence homologous to the fragment to be joined (**Figure 3.1A&B**). The PCR products were run on an agarose gel using gel electrophoresis (section 3.4) to confirm the presence of bands with the expected sizes and purified using the Nucleospin PCR clean-up kit. As the plasmid construction required a low mutation rate, the OE-PCR was conducted using the Phusion® High Fidelity polymerase. The reaction mix contained the components per **Table 3.1**, with two exceptions: the mix contained no primers, and the fragments were added in a 1:1(:1) molar ratio with 50 ng of the longest fragment. The program was run for 15 cycles, joining the fragments together by using the overlapping sequences as primers (**Figure 3.1C&D**). Primers binding to the ends of the insert, with restriction site sequences, were added for the remaining cycles resulting in amplification of the joined insert. For the pDMA045 plasmid, these primers were dma54 and dma259, and for pDMA044, they were dma260 and dma263.

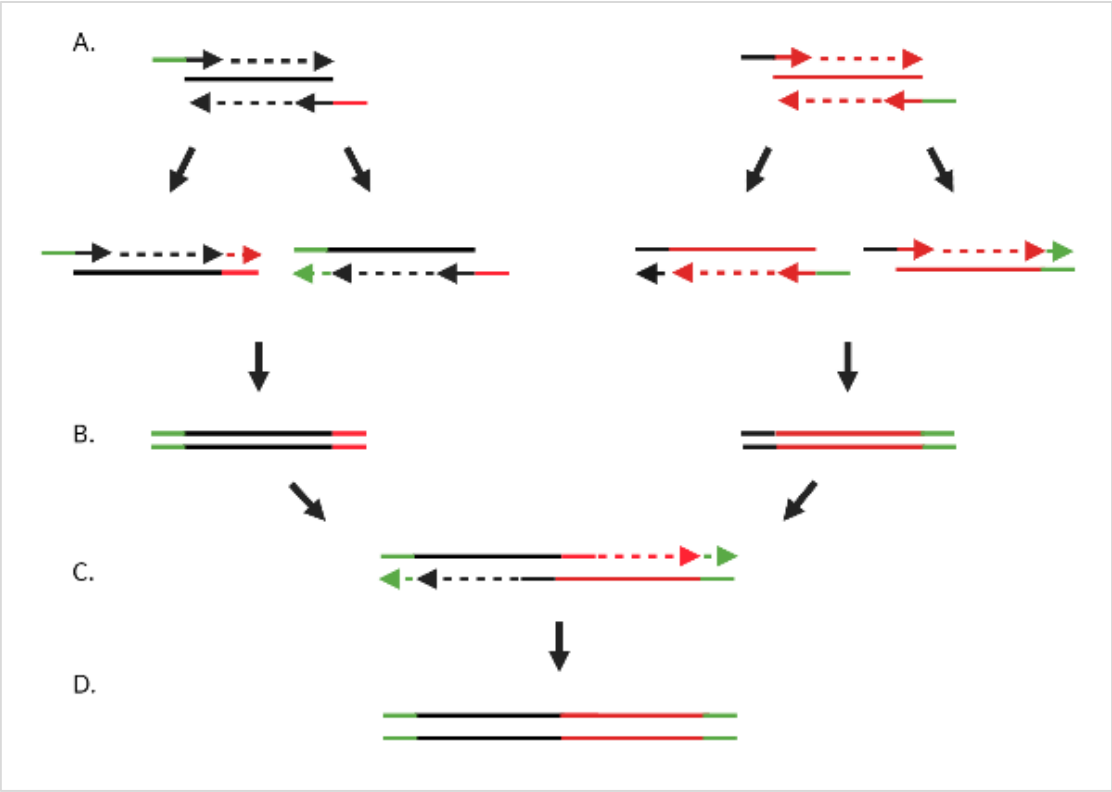

Figure 3.1. Schematic diagram of splicing two DNA fragments using OE-PCR.
A. Primers (arrows) are designed with an overhang complementary to the fragment to be joined (red/black) or enzyme restriction sites (green). The dashed lines represent polymerase extension. Using the original fragment as a template, the polymerase joins the fragment and the overhanging sequence of the primers. **B.** This results in both overhanging sequences being added to both fragments. **C.** The complementary overlapping sequences in both fragments anneal and act in place of primers in the PCR. The sequence is extended, joining the two fragments together (**D**).

3.4 Agarose gel electrophoresis

Agarose gel electrophoresis is a method for DNA visualisation and separation of fragments by length. Agarose consists of repeating L- and D-galactose units, forming polymers during gelation (113). Pores in the gel allow the negatively charged DNA to move through the gel towards the anode when a current is applied (113). DNA molecules have a uniform mass to charge ratio and will subsequently be separated by size, as smaller fragments move faster through the gel than larger ones (113). DNA localisation can be visualised by adding a DNA-binding dye that fluoresces under UV light to the gel. A mix of DNA fragments of known sizes, known as a ladder, is applied to the gel for comparison to determine the size of the DNA samples.

In this work, the method was applied both to separate and subsequently purify a fragment and to determine the size and thereby the presence of a fragment. To create a 1% (w/v) agarose gel, 0.5 g agarose was boiled in 50 mL TAE (40 mM Tris-Acetate, 1 mM EDTA) buffer. Following the addition of 1 µL of the fluorescent dye peqGREEN (Saveen-Werner), the gel was poured into a cast. Combs were put in the cast to create wells, and the gel was left at room temperature to set for approximately 20 minutes. The gel was then transferred to a gel electrophoresis chamber. Samples were mixed with a 6x gel loading dye (NEB) to a concentration of 1x and applied to the wells. The loading dye contains glycerol and bromophenol blue, which eases the loading of samples. After that, 5 µL of a ladder of an appropriate size interval was added to a well. The current was set to 100 V, and the electrophoresis was run for approximately 25-35 minutes for sufficient separation of the fragments. The fragments were visualised by UV light in a GelDoc-1000 (BioRad).

3.4.1 Purification of DNA from agarose gels

For further use, DNA fragments were excised from the agarose gel using a sterile scalpel, followed by purification using the Nucleospin® Gel and PCR Clean-up Kit (Macherey-Nagel). The agarose gel containing the DNA fragment was dissolved in NTI buffer (200 µL/100 mg agarose gel) at 55°C for 5-10 minutes, vortexing the tube briefly every 2-3 minutes. The solution was added to a Nucleospin® Gel and PCR Clean-up column and centrifuged at 11,000 x g for 30 seconds. The NTI buffer contains chaotropic salts, facilitating DNA binding to the column. Next, the column was washed with the NT3 buffer. Residual ethanol was removed by centrifuging the empty column for 1 minute. The DNA was eluted by adding 15-30 µL NE buffer and incubating at room temperature for 1 minute before centrifugation. The purified DNA was stored at -20°C.

3.5 Restriction digestion and ligation

Restriction enzymes are endonucleases produced by bacteria to protect themselves against foreign DNA, such as bacteriophages. They recognise specific sequences of DNA known as recognition sites and make double-stranded cuts either within or outside the recognition site. Restriction enzymes are divided into three main groups depending on where they cleave compared to the recognition site (114). These enzymes are utilised in cloning to make accurate

and predictable cuts to fragments of DNA. In this work, restriction enzymes were used in plasmid construction. All digestions were performed using two different enzymes (double digest), and restriction digestion reactions were made following manufacturer protocol (NEB) as described in **Table 3.4**.

Table 3.4. Components in a standard restriction digestion reaction

Component	Final concentration/Volume
DNA	1 µg
10x supplied reaction buffer	1x/5 µL
Restriction enzyme 1	1 µL
Restriction enzyme 2	1 µL
dH_2O	To a final volume of 50 µL

Incubation temperature and time vary for different enzymes. For all enzymes in this work, incubation at 37°C for 5-15 minutes was optimal. Reactions with digested vectors were supplied with 1 µL CIP (Alkaline Phosphatase, Calf Intestinal) when about one-third of the incubation period remained. CIP catalyses the dephosphorylation of 5' and 3' ends of DNA, thereby inhibiting the re-ligation of the digested ends of the vector. In cases where the restriction produces more than one fragment, as in the case of some vector plasmids, the digestion was verified using agarose gel electrophoresis (section 3.4) and purified as described in section 3.4.1. Otherwise, fragments were purified directly using the NucleoSpin® Gel and PCR Clean-up Kit (Macherey-Nagel).

The two plasmids (pDMA045 and pDMA044) were constructed by inserting a fragment between SalI and BamHI restriction sites. SalI and BamHI are type II restriction enzymes, meaning they cut within their recognition sequence. BamHI binds to the DNA at the recognition sequence 5'-GGATCC-3' and cuts the strand after the 5'-guanine. SalI binds to the sequence 5'-GTCGAC-'3 and, like BamHI, cuts the strand after the 5'-guanine. Recognition and restriction sites of the enzymes are visualised in **Figure 3.2**. Both enzymes leave so-called sticky ends, an overhang of 4 and 5 bases, respectively. Cutting both insert and vector with the same enzymes results in complementary overhangs, making ligation possible.

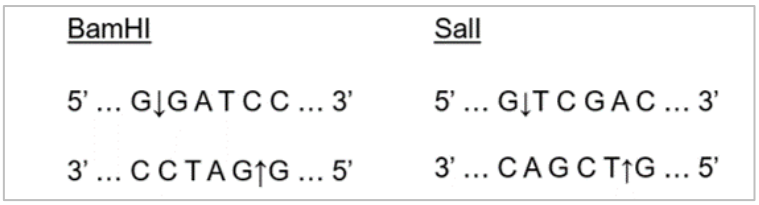

Figure 3.2. Recognition and restriction sites of BamHI and SalI. Arrows indicate restriction sites.

Ligation of the insert and the vector were catalysed by T4 ligase, forming phosphodiester bonds between the 5'-phosphate and 3'-hydroxy termini. The ligation reaction included 50 ng of the vector and an insert amount approximal to a 5:1-7:1 insert/vector ratio. A high insert/vector ratio seeks to satiate the vector with insert, making empty vector re-ligation less probable. The ligation reaction also consisted of 2 µL of the supplied 10x buffer, 1 µL T4 ligase and dH_2O to a final volume of 20 µL and was incubated at 16°C ON. The mix was transformed directly into *E. coli* IM08B, or otherwise stored at -20°C.

3.5.1 Restriction analysis

Restriction analyses were conducted to verify the presence of the correct insert after plasmid construction. Plasmids were restricted with the same restriction enzymes BamHI and SalI (section 3.5) used in the construction plasmid, excising the insert from the vector. The analysis was verified using agarose gel electrophoresis (section 3.4), by the presence of a band corresponding to the size of the insert.

3.6 Targeted gene sequencing

3.6.1 Sanger sequencing

After transformation and purification from *E. coli*, plasmids were sent to GATC, Eurofins genomics to be sequenced using Sanger sequencing. The sequencing was done to ensure that the insert did not contain mutations. The solution sent contained 300-400 ng of plasmid DNA, 2 µL of the sequencing primer at a concentration of 10 µM, and dH_2O to a final volume of 10 µL. Sanger sequencing produces a read of approximately 1000 bp, with a decreased quality of the first and last ~100 bp. Therefore, sequencing primers were designed so each would cover no more than 800 bp.

3.6.2 Illumina sequencing of CRISPRi plasmids

To quantify the distribution of strains in the samples, the sgRNAs of the plasmids harvested after the attachment assay described in section 3.16 were sequenced by Illumina amplicon sequencing. After isolating the plasmids, the specific regions containing the sgRNAs were amplified by PCR using primers with barcodes specific for each sample. The PCR products were pooled and ligated with adapter sequences on both ends. These adapter sequences are complementary to oligonucleotides on the flow cell used in Illumina sequencing, and the amplicons are in this way anchored to the flow cell. The amplicon library was then sequenced on a paired-end flow cell by Illumina sequencing, generating reads of about 250 bp. Bioinformatic analysis were performed by Torrissen Mårli M. (section 3.16), and sample preparations and sequencing by Novogene (UK) Company Limited.

3.7 Genetic modification of *S. aureus*

3.7.1 Transformation in *E. coli*

Transformation is the process of uptake of exogenous DNA by competent cells. In order to protect itself from foreign DNA, *S. aureus* recognises and degrades DNA that does not match its specific methylation profile (115). This ability has previously been a significant hindrance in *S. aureus* transformation (115). The IMXXB strain series of *E. coli* constructed by Monk and his colleagues mimic these methylation patterns, streamlining the transformation process of *S. aureus.* Therefore, plasmids not previously methylated to match *S. aureus* profiles were first transformed in *E. coli IM08B* before subsequent transformation in *S. aureus.*

The $CaCl_2$ heat-shock induced transformation was used to introduce plasmids into cells of *E. coli*. Treating the cells with divalent cations, such as Ca^{2+}, is thought to neutralise the negative charges of the membrane and DNA and thereby lessening the charge repulsion (116). The change in temperature by the heat shock facilitates transformation and is suggested to enlarge membrane pores and decrease their fluidity (116, 117).

The $CaCl_2$ method, to make the cells chemically competent, was performed as follows. *E. coli* IM08B cells were inoculated in 5 mL of LB medium and incubated at 37°C with shaking overnight. The culture was then diluted 1/100 in 100 mL LB and incubated at 37°C with shaking till they reached an OD_{600} of about 0.3-0.4. Cells were centrifuged for 10 minutes at 3,000 g at

4°C. The pellet was resuspended in 12.5 mL ice-cold 100 mM $CaCl_2$ and stored for 30 minutes on ice. Another identical centrifugation followed before the pellet was resuspended in 2.5 mL 100 mM $CaCl_2$ with 20% (v/v) glycerol. The competent cells were used in transformation directly or otherwise aliquoted in Eppendorf tubes and stored at -80°C.

Transformation in *E. coli* ensued as follows. First, 50 µL competent cells were thawed on ice and supplied with the plasmid (1-2 µL) or ligation mix to be incorporated. The cells were then stored on ice for 30 minutes before being heat-shocked in a water bath at 42°C for 30 seconds. After that, 400 µL of LB medium was added to the cells, and they were incubated at 37°C with shaking for 1 hour with the Eppendorf tubes turned horizontally. The horizontal positioning allows for better aerobic conditions. Following incubation, 150 µL of the transformed cells were plated on LB plates with ampicillin (100 µg/mL) for transformation selection. The plates were incubated at 37°C overnight before colonies were picked and verified by colony PCR (section 3.3.1).

3.7.2 Transformation in *S. aureus*

Electroporation is the preferred method for transformation in S. aureus, as a Gram-positive, non-naturally competent bacteria. The transmembrane potential is altered when applying an electric pulse, making the membrane permeable to the plasmid DNA (118). Competent cells are prepared by growing them to the exponential phase to ensure fresh and active cells before a series of washing steps with water or non-ionic solutions to remove salts and stabilise the cells. An excessive concentration of salts during electroporation may result in arcing, which can be fatal to the cells. The following steps were performed to prepare competent *S. aureus* cells. The cells were inoculated in 5 mL TSB medium and grown overnight at 37°C with shaking. After that, the culture was diluted 1/100 in 100 mL TSB medium and incubated at 37°C with shaking until the cells had an OD_{600} of 0.4-0.6. The cells were then stored on ice for 10 minutes before centrifugation at 4,000 rfc for 10 minutes at 4°C. All subsequent centrifugation steps between washing steps were performed at 4°C at 4000 rfc for 5 minutes. The cells were washed with 25 mL ice-cold dH_2O twice and washed with 25 mL ice-cold 10% (v/v) glycerol three times. Depending on the size of the final pellet, it was resuspended in 1.5-3 mL ice-cold 10% (v/v) glycerol with 0.5 M sucrose. Aliquots were made in 1.5 mL tubes, and the cells were either directly transformed or stored at -80°C.

The electroporation was performed as follows. Electrocompetent cells (40-50 µL) were thawed on ice and mixed with 750-1000 ng plasmid DNA before being transferred to a 1 mm electroporation cuvette and electroporated at 2.1 volts, 100 Ω, and 25 µF. 950 µL of TSB with 0.5M sucrose were quickly added after electroporation, and the cells were incubated for 2 hours at 37°C with shaking or 3 hours at 28-30°C for temperature-sensitive plasmids. This incubation period allowed for recovery and for growth to begin before the cells were plated on TSB agar plates with the appropriate selective antibiotic(s).

3.7.3 Chromosomal integration of *mKate* in *S. aureus*

Chromosomal integration of genes results in greater genetic stability, thereby a more consistent expression than plasmid transformation. In addition, it eliminates the required use of antibiotics for plasmid retention in host cells. In this work, the red fluorescence protein mKate was used to outline the entirety of the biofilms examined in the studies of 00671 and SsaA expression patterns (section 3.11). Expression of mKate was attempted directly from the plasmid pRN10. However, varying signal intensity led to the decision to integrate the gene chromosomally between *SAOUHSC_00037* and *SAOUHSC_00038* by homologous recombination using the pRN110 plasmid from de Jong et al. (119). In the pRN110 plasmid, mKate-expression is controlled by the constitutive promoter *SarA_P1*, ensuring continuous expression in all cells.

The protocol described by Jong and her colleagues was followed precisely, with the exception of using TSB medium in place of Todd Hewitt medium. pRN110 was introduced into *S. aureus* by electroporation, and the cells were subsequently incubated at 30°C for 3 hours, as pRN110 is a temperature-sensitive plasmid. Following incubation, the cells were plated on TSB agar plates containing chloramphenicol (10 µg/mL) and incubated overnight at 30°C. The next day, colonies were verified by colony PCR (section 3.3.1) using primers dma066 and im168. Positive transformants were streaked on a fresh TSB agar plate and incubated overnight at 45°C. This temperature exceeds what is replication-permissive for pRN110, making it non-functional and facilitating plasmid loss from the cells. In this way, the previous step allows for the selection of chromosomal integration of the plasmid. Large colonies, thought to be single recombinants, were re-streaked on TSB agar plates containing chloramphenicol (10 µg/mL) and incubated overnight at 45°C. Growth at this stage required the section of the plasmid containing the chloramphenicol-resistance gene to be integrated chromosomally, and single-recombinants would have integrated the plasmid as a whole. Single colonies were picked to TSB medium and

incubated at 30°C with shaking ON, followed by 5-7 dilution cycles of 1/1000 with ~7 and ~16 hours apart to allow double cross over events to occur. The final culture was then plated on TSB agar plates containing anhydrotetracycline (100 ng/mL) and incubated overnight at 37°C. Anhydrotetracycline induces the expression of the Pxyl/tetO promoter, which results in the expression of antisense RNA targeting the essential gene *secY* (120). As a result, *secY* is depleted, ultimately inhibiting the growth of *S. aureus*, causing partial plasmid excision and loss. In this manner, the antisense *secY* RNA, induced by anhydrotetracycline, serves as a counter-selectable marker. The next day, single colonies were plated on TSB agar plates with and without chloramphenicol (10 µg/mL) and incubated overnight at 37°C. Finally, colonies unable to grow on the antibiotic plate were verified by colony PCR (section 3.3.1) with *SarA_P1-mKate*-specific primers.

3.7.4 Construction of an *S. aureus ssaA* knockout mutant

For constructing an *ssaA* knockout mutant, the temperature-sensitive pMAD vector was used to construct an allelic replacement plasmid pDMA045 (121). When transformed into the host, one of the homologous regions will cause the plasmid to be integrated into the chromosomal DNA before the excess parts of the plasmid, together with the gene to be knocked out, will be excised. A schematic illustration of the allelic replacement is illustrated and described in **Figure 3.3**. The vector, constructed by Arnaud M., Chastanet A. and Débarbouillé M., discriminates between plasmid-carrying bacteria by the colour of colonies when grown on 5-bromo-4-chloro-3-indolyl-β-D-galactopyranoside (X-gal) plates (121).

The pDMA045 plasmid was constructed using OE-PCR (for details, see section 3.3.2), restriction, and ligation (section 3.5). Agarose gel electrophoresis (section 3.4) was used to separate the fragments before they were excised and purified using the Nucleospin® kit (section 3.4.1). An OE-PCR (section 3.3.2) was conducted to combine the three fragments, and the OE-PCR product was purified as described above. The fragment and the vector (pMAD) were cut using restriction enzymes SalI and BamHI, creating complementary overhangs to facilitate ligation using the T4 ligase (section 3.5). The ligation mix was transformed into *E. coli* IM08B (section 3.7.1) and transformants were verified by Colony PCR screening (section 3.3.1). A restriction analysis (section 3.5.1) and Sanger sequencing of the plasmid (section 3.6.1) was conducted to verify proper plasmid construction. The plasmid was then transformed into *S. aureus* (section 3.7.2). This OE-PCR of the construction was challenging, and in all attempts,

the plasmid contained severe deletion mutations. The allelic replacement protocol was attempted regardless. However, it failed to give successful transformants before completion and was aborted about halfway through. Nevertheless, the protocol is written in full below as an attempt in our lab using a knockout plasmid containing a spectinomycin cassette has recently proved successful (Morales Angeles D.).

Transformants were plated on X-gal TSB agar plates containing erythromycin (5 µg/mL), which were made by plating 50 µL 40 mg/mL X-gal on top of the agar before plating the cells. The *lacZ* gene, present on the pMAD vector, encodes the β-galactosidase enzyme catalysing the cleavage of the β-glycosidic bond in D-lactose (122). X-gal, a lactose analogue first synthesised by Jerome P. Horwitz, is initially colourless but when cleaved by β-galactosidase forms a bright blue product (122, 123). Therefore, cells carrying the pMAD plasmid will form blue colonies in the presence of X-gal, whereas those not carrying it will form white colonies. The plates were incubated at 30°C for 1-2 days or until blue colonies appeared. Blue colony transformants were verified using colony PCR (section 3.3.1) and re-streaked on a TSB agar plate with erythromycin (5 µg/mL) and X-gal, which was incubated at 30°C for 1-2 days. One blue colony was picked and inoculated in TSB medium, incubated at 30°C for 2 hours and then at 42-44°C for 6 hours, followed by a 1/1000 dilution and continued incubation overnight. This is a non-permissible temperature for the pMAD replicon, and the plasmid will thus be dispossessed by the cells at this temperature. The following day dilutions of 10^{-1}, 10^{-2} as well as the undiluted culture were plated on TSB agar plates containing tetracycline (5 µg/mL) and X-gal, and the plates were incubated at 42-44°C for 1-2 days. At this stage, blue colonies are likely single integrants, whereas white colonies may have had a double-crossover event removing the *ssaA*-gene. Therefore, white colonies were spotted on TSB agar plates, one with tetracycline (5 µg/mL) and one with erythromycin (5 µg/mL). Successful *ssaA*-knockout mutants should be erythromycin-sensitive and tetracycline-resistant. Hence, such colonies were picked and verified using colony PCR (section 3.3.1).

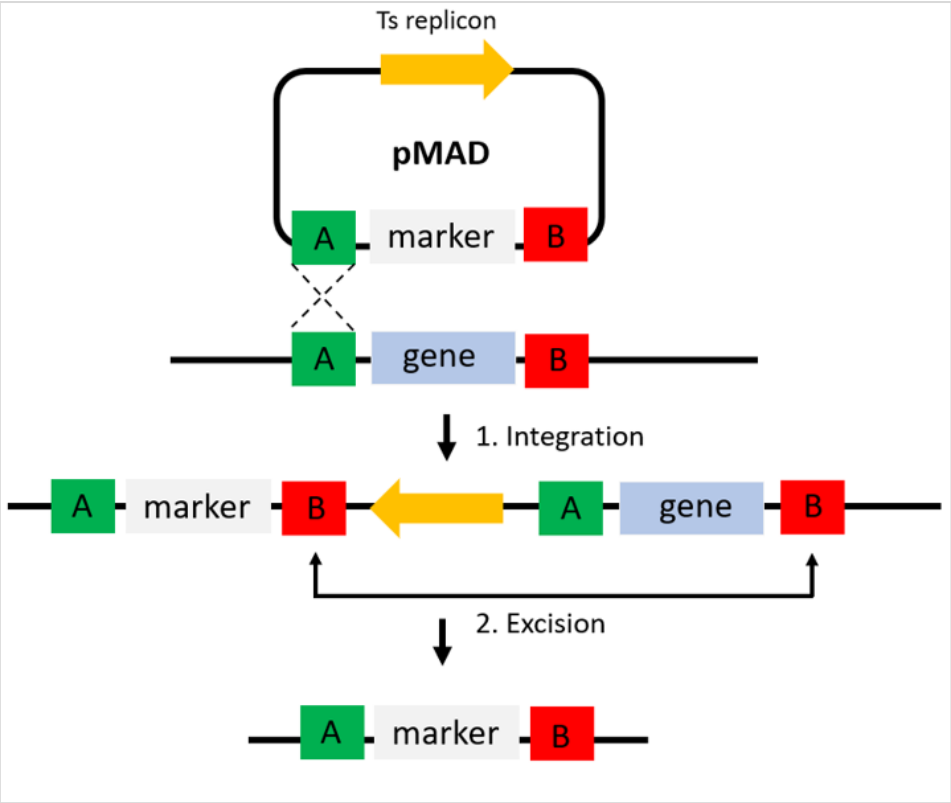

Figure 3.3. Schematic illustration of allelic replacement of a target gene using the pMAD vector. The boxes labelled A and B represent flanking regions of the gene to be knocked out, and the dotted lines represent crossover events. A single crossover event in A results in the integration of the plasmid to the chromosome. For the target gene to be excised, a second recombination event must occur in box B, which excises the gene and the remains of the pMAD backbone, ultimately resulting in an exchange of the target gene for a marker. Modified from Arnaud M., Chastanet A., and Débarbouillé (2004) and Angeles D. (2020, unpublished).

3.7.5 Construction of the fluorescence reporter plasmid pDMA044 for the expression of *ssaA*

Previous results from planktonic cell expression assays from our lab showed that SsaA and 00671 were genetically negatively correlated. These experiments were conducted using expression reporter plasmids containing fusions of the hydrolase promoter regions and the reporters *gfp* and *luc* (section 3.11). In this work, these plasmids were used with the GFP reporter to study the genetic correlation further. However, to study the expression of the two hydrolases simultaneously, an expression reporter plasmid with a differently coloured reporter was needed. Therefore the plasmid pDMA044, containing a fusion of the SsaA promoter region and a Cyan fluorescent protein gene (*cfp),* was constructed. In cells carrying both the SsaA-

reporter plasmid pDMA044 and the 00671-reporter plasmid pDMA032, the expression of both hydrolases could be visualised and distinguished by fluorescent light emission of different wavelengths. The pDMA044 plasmid was constructed using OE-PCR (for details, see section 3.3.2), restriction, and ligation (section 3.5). The fragments were separated using agarose gel electrophoresis (section 3.4), excised, and purified using the NucleoSpin® Gel and PCR Clean-up kit (section 3.4.1). OE-PCR was used again to join the fragments, and the joined insert was purified as described above. Restriction of both the insert and the vector (pCG248) was conducted using enzymes SalI and BamHI, and the ligation was catalysed using the T4 ligase (section 3.5). The ligation mix was transformed into *E. coli* IM08B for methylation consistent with *S. aureus* pattern (section 3.7.1). Transformants were verified using colony PCR (section 3.3.1), and the plasmid was isolated after replication in *E. coli*. After proper construction was ensured by restriction analysis (section 3.5.1) and Sanger sequencing (section 3.6.1), the plasmid was transformed into *S. aureus* (3.7.2).

3.8 The crystal violet microtiter plate biofilm assay

Crystal violet (CV) staining is a method to quantify biofilm formation. By staining the biofilm with CV and measuring the amount of dye bound to cells by reading the optical density at 600 nm. This method was utilised to study the roles of 00671 and cell-morphology determinant SmdA in biofilm formation by complementing 00671 in one assay and depleting SmdA in another. The 00671-complementation assay was performed as follows. Strains were inoculated in 5 mL TSB with the appropriate antibiotics and IPTG and incubated at 37°C with shaking overnight. The complementation strain used has a plasmid that allows for IPTG-inducible expression of 00671. As a control, a Δ00671 strain with the "empty" pLOW-plasmid was used to ensure that the plasmid itself was not changing the phenotype. IPTG was added in concentrations ranging from 50-1000 µM to induce expression. The overnight cultures were diluted 1/100 in TSB to a total volume of 5 mL and incubated until they reached an OD_{600} of 0.05. 100 µL of the cultures were added to microtiter plate wells, eight for each condition, and TSB medium was used as a negative control. The plate was incubated statically at 37°C for 24 hours. After incubation, planktonic cells were carefully removed from the wells, and the biofilms were washed with 100 µL saline (0.9% (w/v) NaCl) and left to dry for 5 minutes. To stain the cells, 100 µL of a solution of 0.02% CV in ethanol was added. After an incubation of 15 minutes, the CV solution was removed, and the stained biofilms were washed twice with saline to remove any excess dye. The biofilm-bound CV was solubilised with 200 µL of ethanol

during incubation of 10 minutes and transferred to a fresh microtiter plate. The quantification was done by reading the OD_{600} of the ethanol-solubilised CV in a microplate reader (BioTek®), using ethanol as a blank.

For the SmdA-depletion assay, the strains were inoculated in 5 mL of BHI with the appropriate antibiotics and IPTG (300 µM) to induce the CRISPR interference (CRISPRi) system (for details, see section 1.4.3). The CRISPRi strains contain an IPTG-inducible plasmid encoding dCas9 and a constitutively expressed sgRNA complementary to the gene of interest (101). Upon induction, the sgRNA guides the dCas9 to the complementary gene and binds to it, thereby inhibiting the RNA polymerase from transcribing it. This ultimately results in a transcriptional depletion of the gene. The cultures were incubated at 37°C with shaking overnight and then diluted 1/250 in BHI to a total volume of 5 mL. When the cultures reached an OD_{600} of approximately 0.4, they were diluted to an OD_{600} of 0.05 in TSB, and 100 µL was added to microtiter plate wells, eight for each condition. The plate was incubated statically at 37°C for 20 hours, with fresh IPTG was re-supplied midway. As per observations in our lab, the efficiency of the CRISPRi system decreases after approximately 10 hours, hence the additional supplementation of IPTG. The subsequent washing, staining, and quantification steps were identical to those described above.

3.9 Role of 00671 in the attachment stage

3.9.1 Primary attachment assay

The primary attachment assay based on the one conducted in reference 124 was conducted to explore the role of 00671 in the primary attachment stage (124). Overnight cultures of *S. aureus* were diluted 1/1,000,000 by serial dilution in TSB to a total volume of 1 mL, and 100 µL were added to 96-well plates followed by an incubation of 1 hr. The supernatant was removed, and the wells were washed twice with saline (0.9% (w/v) NaCl) to remove unattached cells. Liquid medium was added to the wells and repeatedly pipetted up and down to dissolve the attached cells before plating them out on TBS agar plates. The culture from the 1/1,000,000 dilution was also plated on TSB agar plates, and all were incubated overnight. The percentage of attached cells was calculated by dividing the number of colonies from the attached cells by the number of colonies from the initial 1/1,000,000 dilution.

3.9.2 Studying primary attachment using fluorescence microscopy

Another method to study the primary attachment role of 00671 was utilised. The method was adapted from the biofilm assay demonstrated in reference 51, and utilised a fluorescent dye to stain cells attached to borosilicate chamber wells, which were subsequently examined by microscopy (51). Bacterial cultures were grown in TSB overnight and diluted to an OD_{600} of 0.2. After that, 300 µL culture was applied to borosilicate chamber wells and incubated at 37°C for 1 hr. Planktonic cells were removed with the medium, and 300 µL of SYTO 9™ staining solution (10 µM SYTO 9™ in PBS) was added to the wells, followed by an incubation of 5 minutes. The staining solution was removed, and the wells were washed with PBS before adding 300 µL fresh PBS. The borosilicate chamber wells containing attached cells were imaged using CLSM (section 3.13.2).

3.10 Quantification of extracellular matrix components

The extracellular matrix (ECM) of biofilms consists mainly of proteins, polysaccharides and eDNA (65, 73, 125). Biofilm phenotype is largely affected by the composition and quantity of these components and can differ between species and strains within a species of bacteria (126). Two different methods were used to quantify these components: one for eDNA and proteins and one for PIAs.

3.10.1 eDNA and proteins

To quantify eDNA and proteins in the extracellular matrix (ECM), a method adapted from reference 126 was utilised, where extraction of the ECM using a high concentration (1.5 M) of NaCl was the key element (126). A high concentration of Na^+ and Cl^- is thought to coat and disrupt ionic attractive forces between the bacterial cell surfaces and the ECM components, both of which are charged, leading to the separation of the ECM from the bacterial cells (126). Biofilms were grown in 96-well plates with TSB by static incubation at 37°C for approximately 24 hours. Planktonic cells were removed with the medium, and the biofilm was washed with 100 µL of saline (0.9% (w/v) NaCl). The biofilm was resuspended in 1.5 M NaCl to separate the ECM from the bacterial cells, and all samples were normalised to an OD_{600} of 1. The samples were centrifuged at 10,000 g for 5 minutes, resulting in the separation of the pellet, which comprised the cells, and the ECM in the supernatant. DNA and protein concentrations

of the ECM were measured using the Nanodrop™ 2000 spectrophotometer (Thermo Fischer) and outliers were removed from the dataset using the package {outliers} in R studio (127, 128).

3.10.2 Polysaccharide intracellular adhesins (PIAs)

An approximate quantification of PIAs was conducted using a method adapted from Chopra S., Harjai K., and Chhibber S. (74). The strains were grown overnight in TSB with the appropriate antibiotics, and the CRISPRi strains were supplied with IPTG (300 µM). After normalising the cultures to an OD_{600} of 0.5, they were added to 12-well plates and incubated statically at 37°C for 20 hours. The CRISPRi strains were re-supplied with IPTG after 10 hours. The supernatant containing planktonic cells was removed, and the biofilms were washed with PBS before the cells were dispersed by vigorous pipetting. After that, the dissolved biofilms were adjusted to an OD_{600} of 1.5 in PBS and centrifuged at max speed for 5 minutes. EDTA (50 µL) was used to resuspend the pellet, and the samples were incubated at 100°C for 5 minutes and then on ice for 5 minutes. Both incubation steps were repeated, followed by another centrifugation at max speed for 5 minutes. The supernatants were incubated with proteinase K (2 mg/mL) for 1 hour at 60°C and subsequently at 80°C to inactivate the proteinase. Two-fold dilutions of the extracts were made in Tris-buffered saline (TBS), and 3 µL of each dilution was spotted on a nitrocellulose membrane. The membrane was left to air-dry before it was moistened with TBS and subsequently blocked using 2% skim milk in TBS with Tween® 20 (TBST) for 1 hour. Skim milk (1%) containing 130 ng/mL lectin from *Triticum vulgaris* (wheat) was added to the membrane, which was left to incubate for 30 minutes. The membrane was washed 3 times with TBST, each with incubation of 5 minutes. Finally, the blot was revealed using the SuperSignal™ West Pico PLUS Chemiluminescent Substrate (Thermo Fischer) and the Azure c400 Imaging System (Azure Biosystems).

3.11 Expression of 00671 and SsaA in planktonic cells

To further explore the individual and interactive temporal expression patterns of 00671 and SsaA in planktonic cells, two experiments were conducted in the wildtype strain and Δ00671 using expression reporter plasmids. These plasmids contain a fusion of a promoter for the respective hydrolases and a reporter gene. This way, cells carrying such plasmids will express the reporter gene upon induction of the specific hydrolase-gene, allowing its expression to be

measured. The plasmids used in this work contains reporter genes *luc* and *gfp*, causing the production of quantifiable luminescent and fluorescent light, respectively. However, only the fluorescent light emission by GFP was quantified in the following experiments. In the presence of ATP Luciferase decarboxylates luciferin, producing light with a peak emission at 560 nm (129, 130). Green fluorescent protein (GFP) is a protein that emits fluorescent green light when excited with light in the blue to ultraviolet range (131) . The GFP encoded by these plasmids has a peak emission at around 480 nm, although several other versions of the protein exist. A separate plasmid was used for each hydrolase, containing the reporter genes downstream of their respective promoter, as illustrated in **Figure 3.4**. In strains that contain the plasmid with a promoter for *SAOUHSC_00671* upstream of *luc* and *gfp* (pDMA032) *ssaA* could be depleted and the change in expression of *SAOUHSC_00671* could be measured, and vice versa (pDMA038).

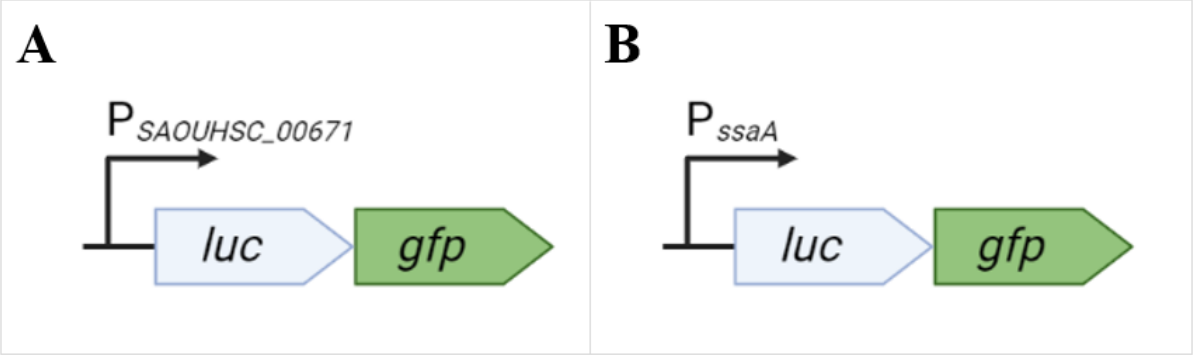

Figure 3.4. Schematic illustration of transcription reporter plasmids pDMA032 (A) and pDMA038 (B). The plasmids contain a *gfp* and a *luc* gene downstream of a region containing promoters for *SAOUHSC_00671* (A) and *ssaA* (B). Cells carrying these plasmids will produce a signal in the form of luminescent light (*luc)* and green, fluorescent light (*gfp)* when expressing the respective peptidoglycan hydrolase.

Firstly, planktonic cells harbouring the expression reporter plasmids for the hydrolases were imaged in the microscope at different stages of growth. The plasmids contain *gfp* downstream of the hydrolase gene promoters, producing a green, fluorescent signal when transcribing the hydrolases. Secondly, the same procedure was followed; only before imaging, the wildtype was stained with 1 µL of the blue-fluorescent, DNA-binding dye DAPI (5 mg/mL) to compare the fluorescent intensity of the two strains simultaneously. The cells were washed by centrifugation with PBS three times after adding DAPI.

Overnight cultures were diluted to an OD_{600} of 0.05 and incubated at 37°C until they reached the desired growth stage, which was determined by measurements of OD_{600}. For the cells imaged individually, the growth stages of imaging were the exponential phase, the transition between exponential and stationary, and the stationary phase. These stages were estimated to correspond to an OD_{600} of 0.3-0.4, 0.8-0.9, and above 1, respectively. The strains imaged simultaneously were examined at the exponential and the stationary stage. At the desired stage, 2 µL of culture was taken out, put on a 1% (w/v in PBS) agarose-covered microscopy slide, and imaged with the microscope. Incubation of the remaining culture continued until the final growth stage was reached. For the DAPI staining, 1 mL of culture was taken out, and 1 µL of DAPI (concentration) was added. The excess dye was removed by centrifugation and washing with PBS in three cycles before the final pellet was resuspended in PBS, and the cells of the two strains were mixed together and imaged by microscopy (section 3.13.1).

3.12 Expression of 00671 and SsaA in biofilms

To explore the spatial and interactive expression of 00671 and SsaA in biofilms, strains carrying the expression reporter plasmids pDMA032 and pDMA038 (**Figure 3.4**) were utilised. Overnight cultures were diluted to an OD_{600} of 0.05 and incubated at 37°C until the cultures were in the exponential growth phase (OD_{600} 0.3-0.4). The cultures were again diluted to an OD_{600} of 0.05, and 300 µL of the dilution was applied to borosilicate microscopy chamber wells and incubated statically at 37°C for 24 hours. Planktonic cells were removed along with the medium, and 300 µL of the SYTO™ 60 (Thermo Fischer) staining solution (10 µM SYTO™ 60 in PBS) was added. The cells were left to incubate with the dye for 5 minutes at room temperature before removal. After that, the biofilms were washed with PBS, and 300 µL of fresh PBS was added to prevent the biofilms from drying out during microscopy imaging. Images were acquired using CLSM (section 3.13.2).

3.13 Microscopy

3.13.1 Fluorescence microscopy of planktonic cells

Analyses of microscopy images were performed to quantify the expression of 00671 and SsaA. The utilised strains harboured expression reporter plasmids (pDMA038 and pDMA032, **Figure 3.4**). To prepare microscopy slides, approximately 700 µL of 1% agarose-PBS was added to a

microscopy slide with wells, and a glass slide was placed on top. The agarose was left to set for ~ 2 minutes before the top glass slide was removed, and 0.5 µL of bacterial culture was added to the wells. Glass slides were used as cover. Microscopy images were acquired using the Zeiss LSM700 microscope with the ZenBlue software. The microscope was coupled with a 100x phase contrast objective, an Orca-Flash 4.0 V2 digital complementary metal-oxide-semiconductor (CMOS) camera (Hamamatsu Photonics), and an HXP 120 Illuminator (Zeiss) fluorescent light source. Lasers of 480 nm and 353 nm were used for excitation of GFP and DAPI, respectively. The super-GFP- and DAPI- filters were selected to detect the fluorescent signals. Images were analysed using the MicrobeJ plug-in for ImageJ (132, 133).

3.13.2 Confocal Laser Scanning Microscopy

Confocal laser scanning microscopy (CLSM) was used for imaging *S. aureus* fluorescent biofilms with the Zeiss LSM700 microscope and ZenBlack software. The other components of the microscope are described above in section 3.13.1. Biofilms were grown in chambered cover glasses (Thermo Fischer) and were supplied with PBS prior to microscopy to prevent the biofilms from drying out. Lasers of 555 nm and 480 nm were used for the excitation of red (mKate, SYTO^{TM} 60) and green (GFP) fluorescent compounds, respectively. A TexasRed filter was used for red fluorescence detection and a EGFP-filter for green. Images were acquired using the Zeiss ZenBlack software.

3.14 Growth curves

Growth curves were made to ensure similarity in growth between strains used comparably, for instance, between a strain and its corresponding control. This was done for the strains carrying the pRN10 (mKate) plasmid and the CRISPRi strains used in the SmdA-depletion assays, and the protocol between them varied slightly. In the first step, overnight cultures of the pRN10-strains were diluted to an OD_{600} of 0.05 in TSB with antibiotics, and the CRISPRi strains were diluted 1/250 in BHI with antibiotics and IPTG. The CRISPRi system is a two-plasmid system, one encoding the sgRNA and another encoding the IPTG-inducible dCas9. The remaining steps of the protocol were similar for all the strains. After dilution, the cultures were incubated at 37°C until they reached an OD600 of 0.3-0.4 and subsequently diluted to an OD_{600} of 0.005. This dilution was added to 96-well microtiter plates in 300 µL per well and three replicates per

strain. The plates were incubated in a Synergy H1 Reader (BioTek®) at 37°C, where the plates were shaken, and the OD_{600} was measured every 5 minutes. For the CRISPRi strains, the cells were re-supplied with IPTG after 10 hours.

3.15 Testing the haemolytic activity of Δ00671

The haemolytic activity of Δ00671 was tested by spotting approximately 2 µL of overnight cell cultures of the wildtype and Δ00671 on sheep's blood agar plates. After letting the spots dry at room temperature, the plates were incubated at 37°C overnight. The next day, the haemolytic zones were visually inspected and imaged.

3.16 Screening for attachment-related genes in a pooled CRISPRi library

An attachment assay was performed using a pooled CRISPRi library to screen for attachment-related genes in *S. aureus*. The CRISPRi library used was constructed in previous works (Liu X., Heggenhougen M., Torrissen Mårli M., Kjos M.), and consists of one sgRNA per *S. aureus* NCTC8325-4 transcriptional unit, as defined in reference 134, resulting in a pool of 1928 unique sgRNAs covering 2766 genomic features (134).

Induction of the CRISPRi system using anhydrotetracycline results in transcriptional down-regulation of the genes targeted by the sgRNAs. The library was inoculated by adding 100 µL to 100 mL TSB containing chloramphenicol (10 µg/mL) and anhydrotetracycline (30 ng/mL) and incubated at 37°C for 6 hours, followed by an additional 1/1000 dilution and incubation of another 6 hours. The above steps were also conducted in another parallel without induction for comparison. After diluting the cultures to an OD_{600} of 0.2, 2 mL were added to four wells each in a 12-well plate, resulting in a total of 8 wells. The plate was incubated statically at 37°C for 1 hour before the contents of the wells were transferred to new wells. This step was repeated for a total of four incubations. After the last incubation, the plasmids of the still unattached cells were isolated (section 3.2). To determine the sgRNA counts in the different samples, the sequence encompassing the sgRNA was sequenced by amplicon Illumina sequencing (Novogene (UK) Company Limited) (section 3.6.2). **Figure 3.5** shows a simplified illustration of the experimental method. As a control condition, samples were harvested from cultures not subjected to the attachment assay, with and without induction, and the sgRNA plasmids were purified and sgRNAs were sequenced in the same manner.

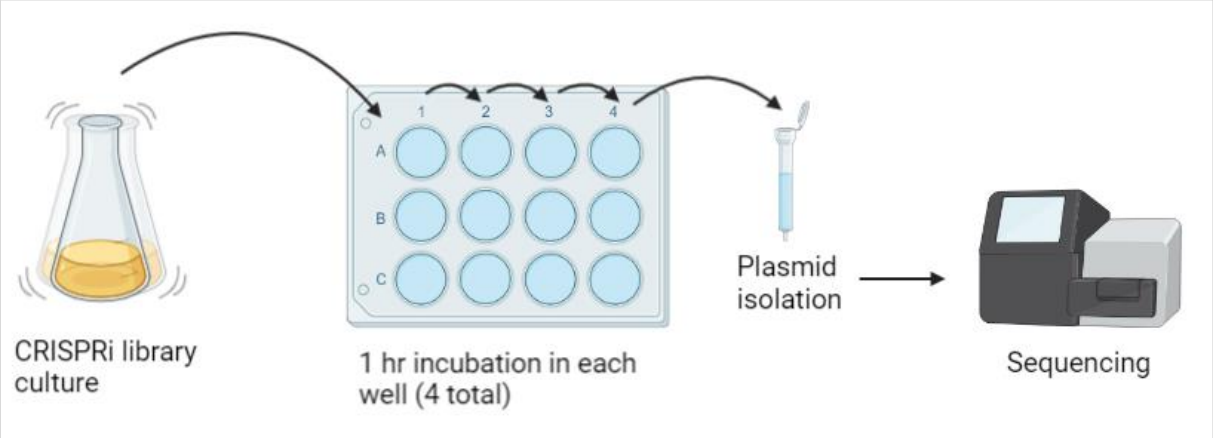

Figure 3.5. Simplified workflow illustration of experiment screening the CRISPRi library for attachment-related genes. The library culture was transferred to a well in a 12-well plate and was incubated statically for 1 hour at 37°C. Non-attached cells were then transferred with the medium to the next well and incubated again. This transfer-incubation cycle continued until the fourth and final well was reached. The remaining planktonic cells were taken out for plasmid isolation, and the plasmids were subsequently sequenced.

The bioinformatic analyses for this experiment were performed by Torrissen Mårli M. as follows. The absolute abundance of each sgRNA per condition was determined using the 2FAST2Q tool (135). This tool trims the reads to contain only the 20-bps corresponding to the sgRNA positions in the reads and performs quality filtering before aligning the reads to a list of all the sgRNA sequences. This gives a .csv file with an absolute read count for each sgRNA for each sample. The absolute read count .csv file was input in a differential enrichment analysis using the R package DESeq2 (136). For each sgRNA, the enrichment or depletion was assessed in the induced samples compared to the uninduced samples in terms of a $\log_2$ fold change ($\log_2$FC). Significance was evaluated using the false discovery rate (FDR)-adjusted p-values. Enrichment or depletion gives us information about the significant differences in abundance of the gene targets corresponding to the sgRNAs.

4 Results

In this work, three topics related to *S. aureus* biofilm formation were explored. The main topics was the role of the putative peptidoglycan hydrolase 00671 in biofilm formation (section 4.1) and its negative genetic correlation with another putative peptidoglycan hydrolase SsaA (section 4.2). As the second topic, the role of a novel cell morphology determinant SmdA in biofilm formation was studied (section 4.4). Lastly, a CRISPR interference (CRISPRi) library was screened for genes involved in the attachment stage of biofilm formation (section 4.5).

4.1 Exploring the role of 00671 in biofilm formation in *S. aureus*

The first topic explored in this work was the role of 00671, a largely uncharacterised putative peptidoglycan hydrolase suggested to play a role in biofilm formation (85). Biofilm formation in a strain in which 00671 was depleted using CRISPRi was found to be comparable to Atl- and Sle1-depletion, two peptidoglycan hydrolases previously known to facilitate cell adherence and biofilm formation (49–52, 85). In addition, a reduction in biofilm formation by Δ00671 was reported by Torrissen Mårli M. (2020) and confirmed by Morales Angeles, D. (unpublished). These results indicate a role for the peptidoglycan hydrolase in the biofilm formation in *S. aureus*. The experiments described in section 4.1 were conducted to explore this topic further.

4.1.1 Complementation of Δ00671 does not consistently alter biofilm-formation

As the absence of 00671 in *S. aureus* decreased the amount of biofilm formed, a crystal violet (CV) microtiter assay was conducted to examine if complementation of 00671 caused an increase in biofilm formation. A complement strain with a pLOW-00671 plasmid was used. This plasmid allows control of the expression of 00671 by the addition of IPTG. To ensure that the plasmid backbone caused no phenotypic effects, Δ00671 carrying pLOW-lacA-m(gfp) was used as a control. Bacterial cultures of the strains were normalised and incubated statically in a microtiter plate for 24 hours, with different concentrations of IPTG. Eight replicates for each condition were subsequently stained with CV, which was quantified in a plate reader. The mean OD_{600} for each IPTG concentration was calculated and is presented in **Figure 4.1**.

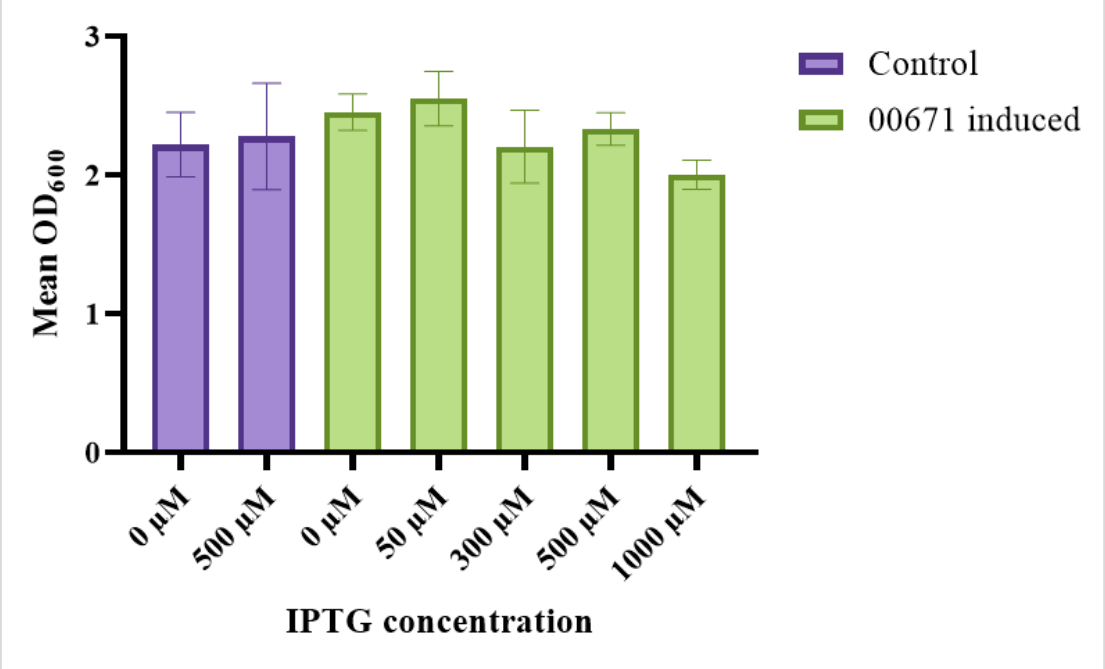

Figure 4.1. Biofilm formation by *S. aureus* Δ00671 pLOW-00671 with IPTG. Biofilms were grown in microtiter plates for 24 hours, and the amount formed was quantified by crystal violet staining. 00671 induced: Δ00671 with plasmid pLOW-00671 expressing 00671 when induced by IPTG. Control (DMA064): Δ00671 pLOW-lacA-m(gfp). IPTG was added in concentrations of 0 µM to 1000 µM for induction.

For the control strain, the two concentrations of IPTG led to similar amounts of biofilm formed, indicating that the plasmid backbone did not affect biofilm formation. If complementation of 00671 led to increased biofilm formation, the expected result would be an increased OD_{600} with increasing concentrations of IPTG. However, no such trend was observed. The two conditions with the highest amount of biofilm formed were seen with the two lowest concentrations of IPTG (0 µM, 50 µM), and the biofilm formation with 1000 µM and 300 µM IPTG were both lower than with 500 µM IPTG. The eight biofilms varied significantly within the conditions, as seen by the large standard deviation bars. In addition, the standard deviation bars overlap between almost all conditions, decreasing the likelihood of there being a significant difference between them. With repetitions of the assay, the results were inconsistent. Therefore, complementation of 00671 does not seem to cause an increase in biofilm formation in *S. aureus*.

4.1.2 Quantifying the extracellular matrix components of the Δ00671 biofilm

The three main components constituting the extracellular matrix (ECM) of a biofilm are proteins, eDNA, and polysaccharides (65, 73, 125). By cleaving the peptidoglycan cell wall, hydrolases are known to facilitate the release of eDNA, an adhesin important in the attachment of the initial biofilm-forming cells to a surface. Other proteins, such as surface proteins and nucleases, are involved in all the stages of the biofilm life cycle by interactions with surfaces or neighbouring cells or by degrading eDNA. Polysaccharide intracellular adhesin (PIA, also known as PNAG) is the dominant molecule of the *S. aureus* biofilm and was previously the only known substance responsible for biofilm formation by the bacterium (55, 74). These components play a crucial part in the biofilm life cycle, and understanding their different roles and compositions is essential in biofilm studies. Therefore, the ECMs were quantified to see if the deletion of 00671 would alter the composition of eDNA, proteins, or PIAs.

4.1.2.1 The ECM of the 00671 knockout may have lower concentrations of both eDNA and proteins

To quantify the concentrations of proteins and eDNA in the ECMs of biofilms of Δ00671 and the wildtype strain, biofilms were grown in microtiter plates for 24 hours before the ECM was separated from the cells using a high concentration of NaCl (1.5 M). The samples were normalised, and the cells were removed from the ECM by centrifugation. DNA- and protein concentrations were measured with a spectrophotometer, measuring each sample three times to exclude any inaccurate measurements. **Figure 4.2** displays the mean concentration of eDNA (**A**) and proteins (**B**) for eight biofilms by each strain, each graph from a different repetition of the experiment. The statistical significance of the means was calculated using the Student's t-test ($\alpha = 0.05$). In two of the three repetitions, the mean DNA concentration in the ECM was significantly lower in Δ00671 than in the wildtype. However, in the third, the difference was not statistically significant (**Figure 4.2A**). The mean protein concentration was also lower in the Δ00671 in all repetitions, but the difference was only statistically significant on one (**Figure 4.2B**). Although the differences are not significant in all repetitions, there was a trend of both eDNA and protein concentrations being lower when depleting 00671.

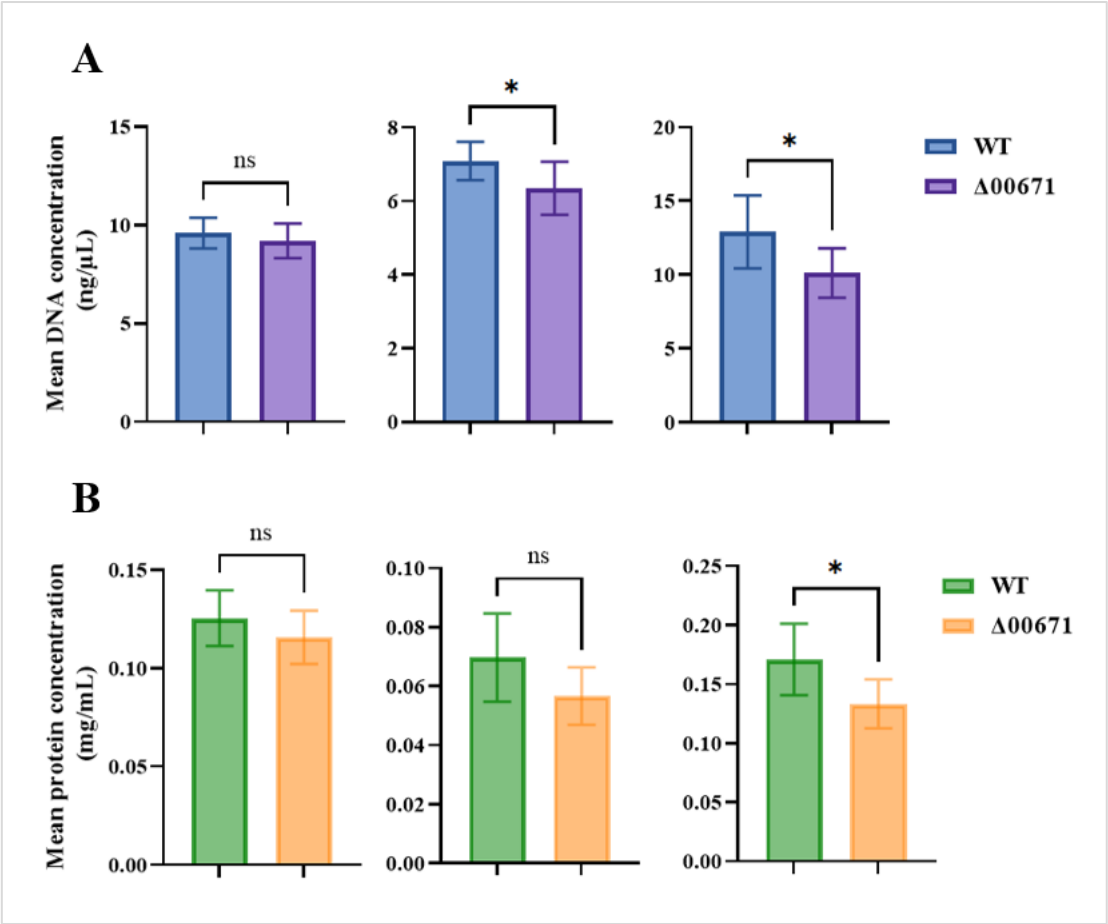

Figure 4.2. Protein and eDNA concentrations in extracellular matrices (ECM) of biofilms of *S. aureus* wildtype (WT) and Δ00671. Panel A shows the mean DNA concentrations (ng/µL), and panel B shows the mean protein concentration (mg/mL) of three replicates of the experiment. The DNA concentration was significantly lower in Δ00671 in two of the three replicates. The protein concentration was significantly lower in one of three replicates.
ns, p > .05. *, p < .05.

4.1.2.2 The Δ00671 extracellular matrix contains fewer PIAs than the wildtype

Quantities of polysaccharide intracellular adhesin (PIA) molecules in ECMs of the *S. aureus* wildtype and Δ00671 were compared by dot blot analysis. The PIAs were extracted and spotted on a nitrocellulose membrane. An *ica* knockout mutant strain (*qp i cwa*s)used as a negative control. An image of the chemiluminescent blot was taken and is displayed in **Figure 4.3**. As expected, no signal was seen from the *ica* knockout strain. The Δ00671 ECM had fewer PIA molecules than the wildtype, most apparent in the undiluted spot (N). As this experiment has only been conducted once, these results are preliminary, and the experiment should be repeated for confirmation.

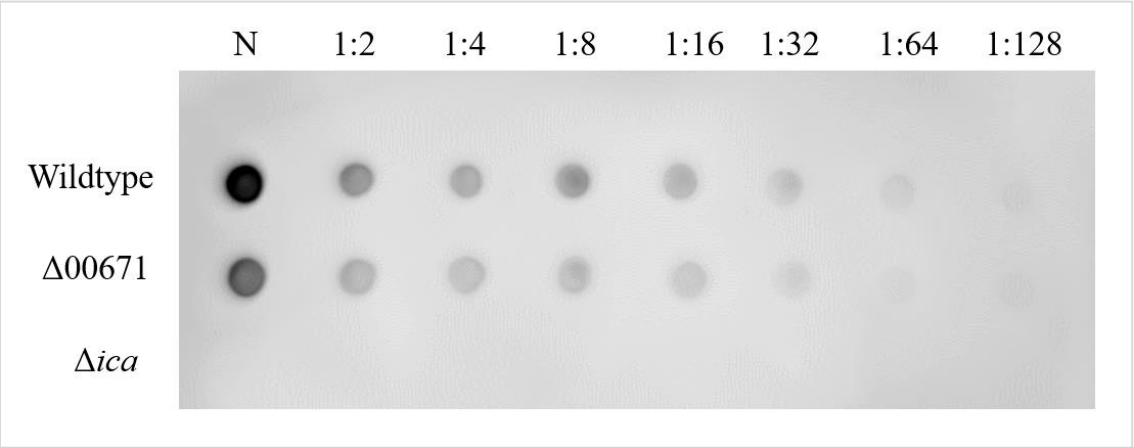

Figure 4.3. Semi-quantitative PIA estimations in biofilms formed by *S. aureus* wildtype (WT), Δ00671, and *ica* knockout (Δ*ica*) after 24 hours. PIA detection was conducted using chemiluminescence of *T. vulgaris* (wheat) lectin on a nitrocellulose membrane. The top row displays the dilution levels of the samples. N = neat (undiluted).

4.1.3 Involvement of 00671 in the primary attachment phase of biofilm formation

The most studied peptidoglycan hydrolases of *S. aureus*, Atl and Sle1, have been found to affect biofilm formation by causing adherence of cells in the attachment phase (51, 52). The hydrolysis of peptidoglycan in the cell wall causes lysis, releasing eDNA and facilitating adhesion. 00671 is believed to be a peptidoglycan hydrolase, and a trend of less eDNA in the Δ00671 was observed. Therefore, a role of 00671 in the attachment stage was hypothesised. Two different methods were tested to explore the attachment ability of 00671. Firstly, the number of cells attached to plastic surfaces after 1 hour of static incubation was compared between the wildtype and Δ00671. Secondly, cells attached to borosilicate chambers after 1 hour were fluorescently dyed and examined microscopically. In the latter experiment, cells of Δ00671 were compared with the wildtype as a positive control and an *atl* knockout mutant (Δ*atl*) as a negative control.

4.1.3.1 00671 does not consistently alter the number of attached cells in a primary attached assay

A primary attachment assay was conducted using *S. aureus* NCTC8325-4 wildtype and Δ00671 to study the attachment ability of 00671. Bacterial cultures were diluted and added to a microtiter plate for 1 hour of static incubation. A portion of the cultures was plated directly on agar plates, which was used to calculate the total number of cells before attachment. The cells attached to the microtiter plate after 1 hour were resuspend and plated on agar plates. The colonies from the attached cells were divided by the estimated total number to calculate the percentage of attached cells. The results are displayed in **Figure 4.4**, with **A** and **B** representing two different repetitions of the experiment. This experiment was repeated three times, with inconsistent results in each repetition. In the first repetition, Δ00671 had a larger percentage of attached cells (49%) compared to the wildtype (41%), whereas in the second repetition, the opposite was observed (8% and 21%, respectively). As no consistent results could be detected with this method, a second method was used to further explore if 00671 plays a role in the primary attachment stage of biofilm formation.

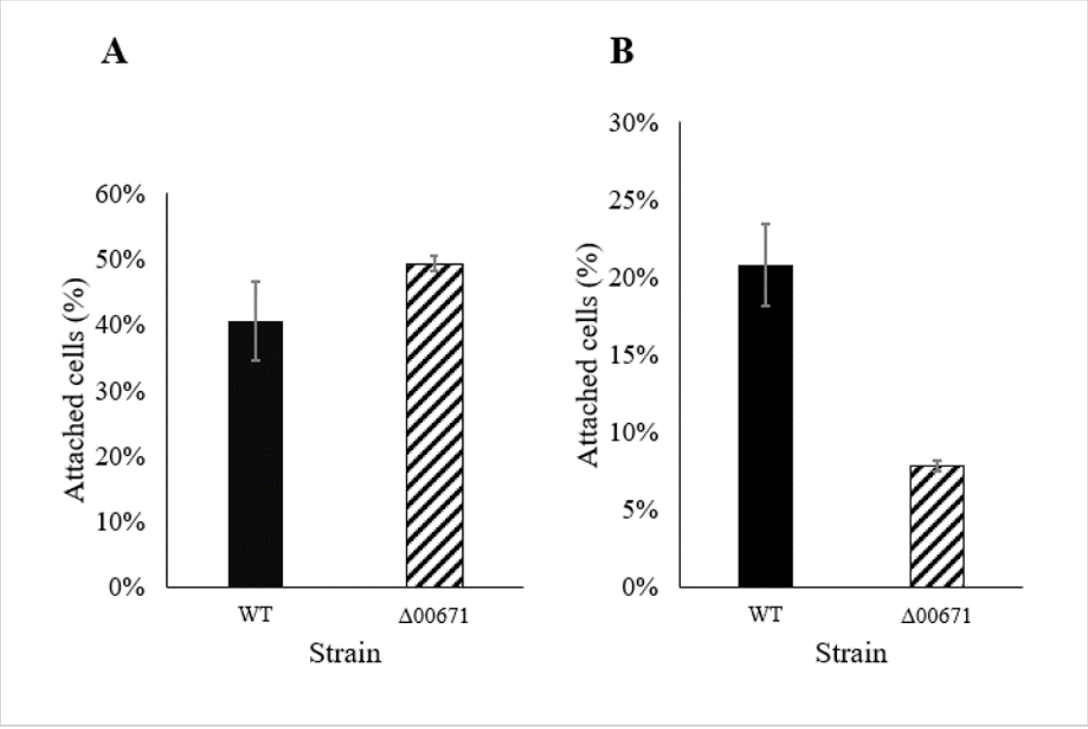

Figure 4.4. Percentages of attached cells in a primary attachment assay of *S. aureus* wildtype (WT) and Δ00671. The cells were incubated statically in 96 microtiter plates for 1 hour, and the attached cells were plated on agar plates which were incubated for 24 hours. Colonies were counted and used to calculate the percentages. A and B represent two different repetitions of the assay.

4.1.3.2 Confocal laser scanning microscopy reveals a different attachment phenotype for Δ00671

A second method was used to further explore the attachment role of 00671 in biofilm formation. As major autolysin Atl is involved in this stage, *cpa* was used as a positive control. The wildtype strain was used as the negative control. Bacterial cultures were normalised to an OD_{600} of 0.2 and incubated statically in borosilicate wells for 1 hour. Planktonic cells were removed, and the remaining attached cells were stained with SYTO™ 9, a DNA-binding green-fluorescent dye, to be able to examine the biofilms using confocal laser scanning microscopy. Images of the top view (**A**) and side view (**B**) of the cells were taken and are displayed in **Figure 4.5**.

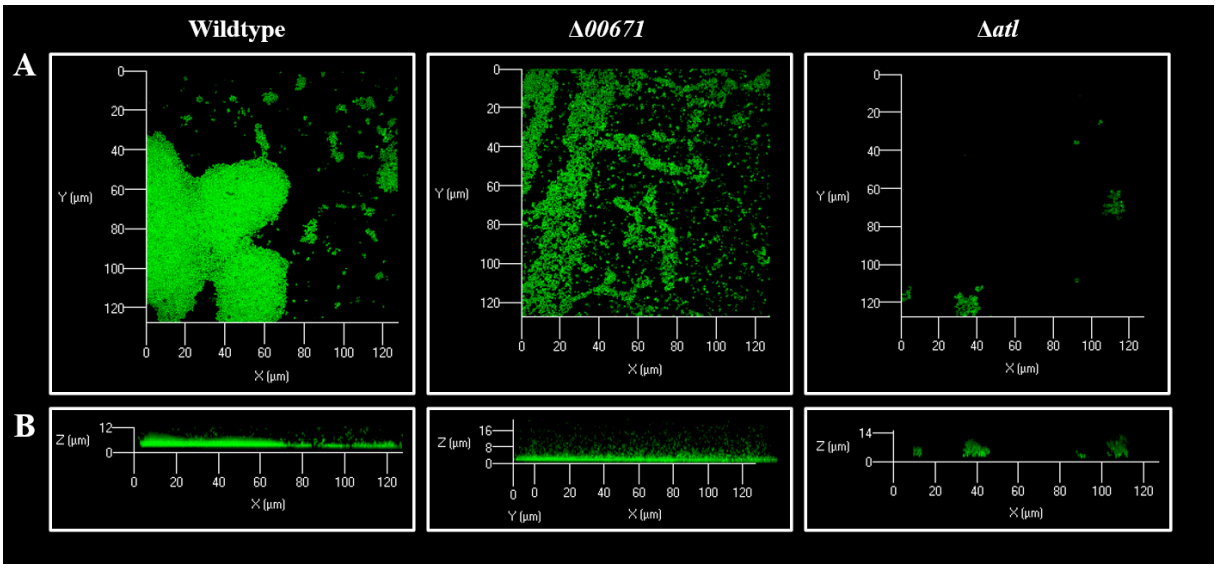

Figure 4.5. Confocal laser scanning microscopy images of attached cells of *S. aureus* strains after a 1-hour incubation in borosilicate wells. The cells were stained with SYTO™ 9. A shows the top view, and B shows the side view of the cells. The wildtype was used as a negative control and an Δ*atl* as a positive control.

The wildtype cells were clumped together in large aggregates throughout the well, unlike cells of Δ00671, which seemed more dispersed. As expected, very little attachment was observed in Δ*atl*. In the side view of the biofilm, the Δ00671 cells also appeared more loosely bound to one another, as single planktonic cells were observed from the bottom (0 µm) up to 16 µm on the Z-axis, which is not seen to the same extent in the other two strains. There were fewer attached cells in Δ*atl* compared to the two others, indicating that the role of 00671 in attachment is different, or not as strong, as that of Atl. These results suggest that 00671 indeed does affect

the early stages of biofilm formation. However, the experiment was conducted only once and should be repeated for confirmation.

4.2 The two putative hydrolases 00671 and SsaA are genetically negatively correlated

The second main topic of this work was the previously reported genetic negative correlation between 00671 and SsaA. Using luciferase as a reporter for the expression of 00671, it was found that the expression of 00671 increased when SsaA, another putative peptidoglycan hydrolase, was downregulated and vice versa. To verify these results in planktonic cells and to see if the same correlation was present in biofilm-associated cells, several experiments were performed both in planktonic cells and biofilms. The experiments were conducted using strains harbouring the expression reporter plasmids (described in section 3.11), allowing measurements of expression by fluorescent light emission. The GFP reporter was confirmed to be functional in TSB, as seen in **Figure 4.6**.

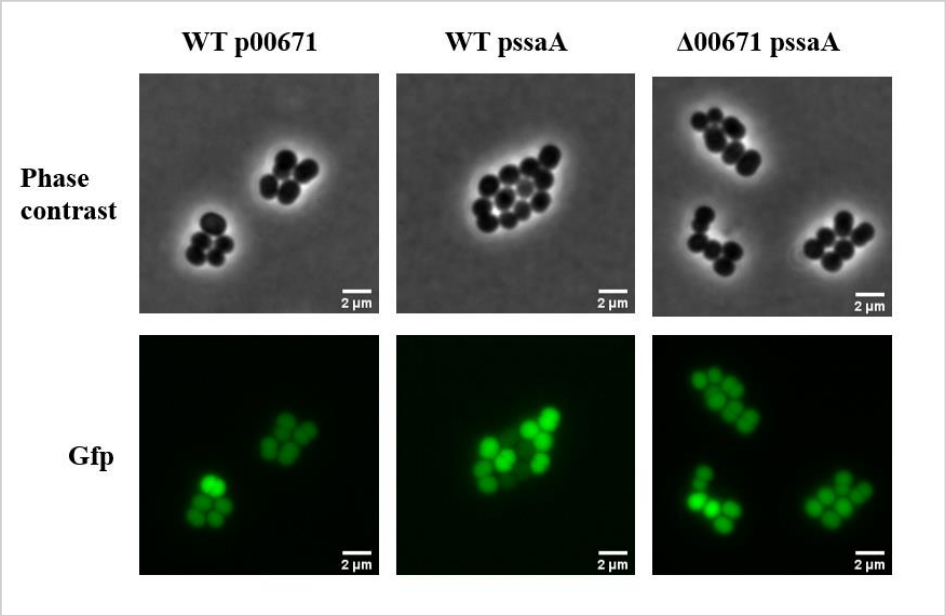

Figure 4.6. Phase contrast and fluorescence images of the strains used in the 00671 and SsaA expression experiments, confirming the functionality of the GFP reporter in TSB.

The following three experiments were initially intended to include a *ssaA*-knockout mutant strain and a *ssaA-SAOUHSC_00671* double knockout mutant strain. Construction of a *ssaA* allelic replacement plasmid was attempted several times, both by Golden Gate assembly (not

described) and OE-PCR, but was unsuccessful. The latter method resulted in a plasmid containing severe deletion mutations in regions essential for the knockout, and the plasmid could not be utilised successfully. Therefore, the experiments were only performed on wildtype and Δ00671.

4.2.1 Fluorescently labelling biofilms with SYTO^{TM} 60 is the preferred method over genetically expressed mKate

To study this interaction in biofilms using CLSM, a method for labelling all the biofilm-associated cells by fluorescence was necessary. The fluorescent labelling outlines the totality of the biofilm, dictating the starting- and stopping layers during CLSM imaging. Additionally, this would allow comparisons of the fraction of cells expressing the hydrolases and reveal possible spatial differences. As the reporter plasmids use GFP as a reporter, it was necessary to use a colour with a different fluorescent spectre, and it was decided to use red fluorescence. The fluorescent labelling was first attempted using mKate expressed from a plasmid (pRN10). However, the fluorescent signal intensity was inconsistent and non-uniform in the biofilms, as apparent in **Figure 4.7A**. Additionally, unexpected differences in biofilm-forming abilities was observed between the strains carrying the pRN10 plasmid. The wildtype-like strain (RM2) carrying the pRN10 plasmid and the SsaA-reporter plasmid was forming a biofilm that visually seemed significantly smaller in mass compared to the other strains carrying other reporter plasmids (**Figure 4.7B**). Growth curves were made to see if a difference in growth between the strains could explain their biofilm-forming abilities (**Figure 4.7C**). Surprisingly, the strain that formed less biofilm was growing faster and to a higher OD_{600} than the others. The other wildtype-like strain, carrying the 00671-reporter plasmid, was growing slower and to a lower OD_{600} than the two others. This observation was unexpected, as the strains had been shown to grow similarly prior to introducing the pRN10 plasmid (Morales Angeles D., personal communication). Thus, due to the phenotypic defects observed upon introduction of pRN10, the method could not be used to label cells.

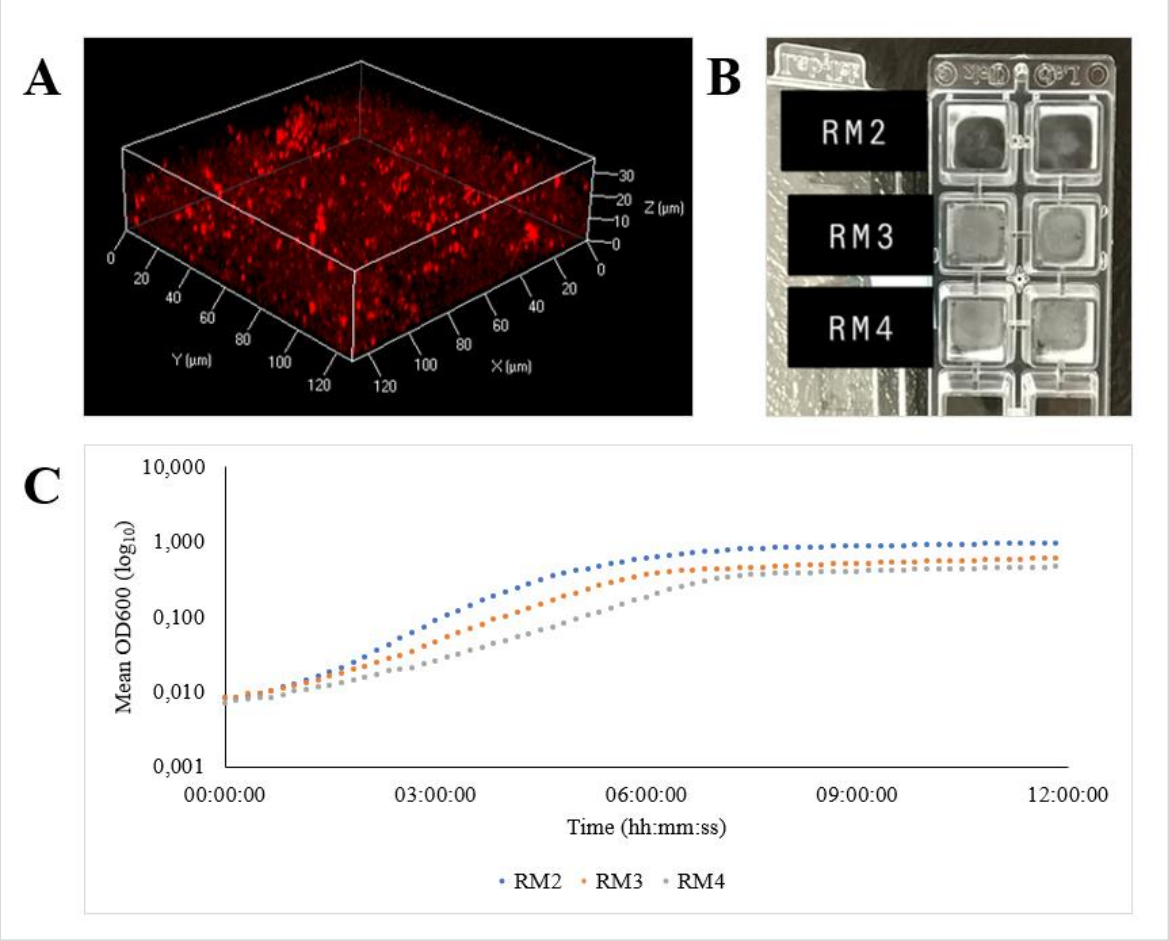

Figure 4.7. Different properties of strains labelled with pRN10. **A.** CLSM image of a biofilm formed over 24 hours by cells (of the strain RM4) fluorescently labelled with pRN10. The signal intensity was significantly inconsistent between the cells. This was the case for RM2 and RM3 as well. **B.** Biofilms of RM2, RM3, and RM4 formed over 24 hours in borosilicate chambers. **C.** Growth curves of the strains carrying pRN10. RM2: wildtype carrying plasmids for mKate-expression (pRN10) and SsaA-expression reporting (pRMA038). RM3: Δ00671 carrying plasmids for mKate-expression (pRN10) and SsaA-expression reporting (pDMA038). RM4: wildtype carrying plasmids for mKate-expression (pRN10) and 00671-expression reporting (pDMA032).

mKate was instead integrated chromosomally to overcome these issues. Chromosomal integration is considered a more stable option as this ensures that only one copy of the gene is present in the cell. Plasmids can occur in multiple copies, and it was believed that this may have been the cause of the signal inconsistency. However, the chromosomal integration did not improve consistency. In addition, the intensity of the signal was insufficient to the point that the localisation of the cells using CLSM was challenging (data not shown). An image of planktonic cells, comparing the signal intensity between cells expressing mKate from a plasmid with cells harboring a chromosomally integrated mKate (**Figure 4.8)**, clearly demonstrates the low intensity fluorescence of the latter strain.

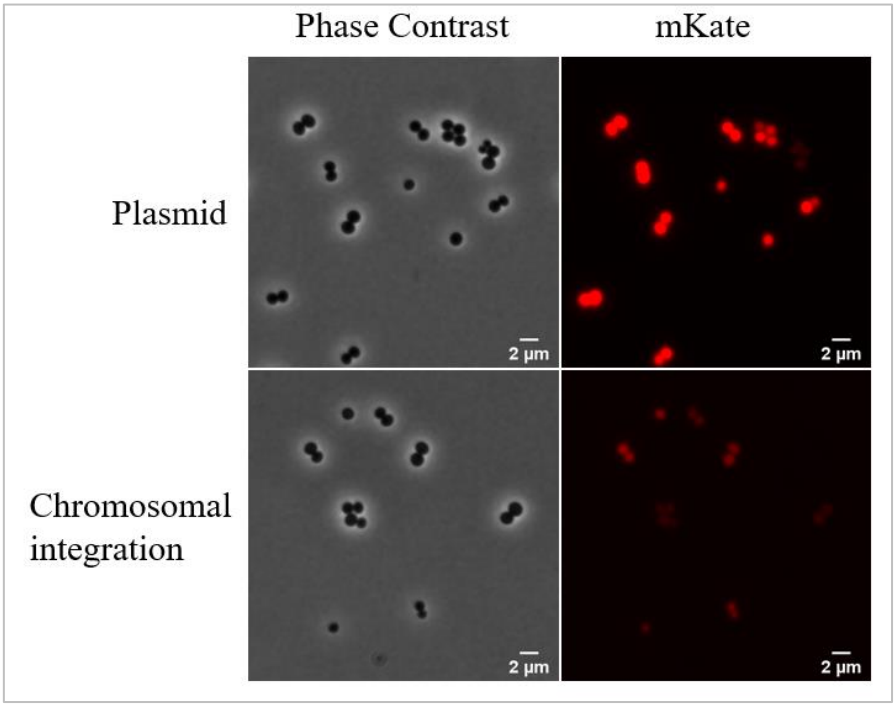

Figure 4.8. Planktonic cells imaged using phase-contrast microscopy. The top panels show cells with mKate expressed from a plasmid (pRN10), and the bottom panel shows cells with mKate chromosomally integrated.

A third method for fluorescent labelling was attempted, using the red-fluorescent nucleic acid dye SYTO^{TM} 60. This dye yielded successful results both in terms of signal intensity and consistency (**Figure 4.12**, section 4.2.5) and was used further.

4.2.2 Construction of an PssaA-cfp reporter plasmid

To allow simultaneous analysis of expression of from the SsaA-promoter and the 00671-promtoer, an expression reporter plasmid for PssaA (pDMA044) was constructed using Cyan fluorescent protein (*cfp)* gene its reporter. This reporter was meant to be used together with the 00671-gfp-reporter plasmid (pDMA032). The plasmid was successfully constructed, and the cells carrying it were displaying production of CFP, as seen in **Figure 4.9**. However, due to the lack of sufficient filters in the microscope used in this work, the fluorescent signals from GFP and CFP could not be successfully distinguished, and the plasmid was therefore not used as intended in this work.

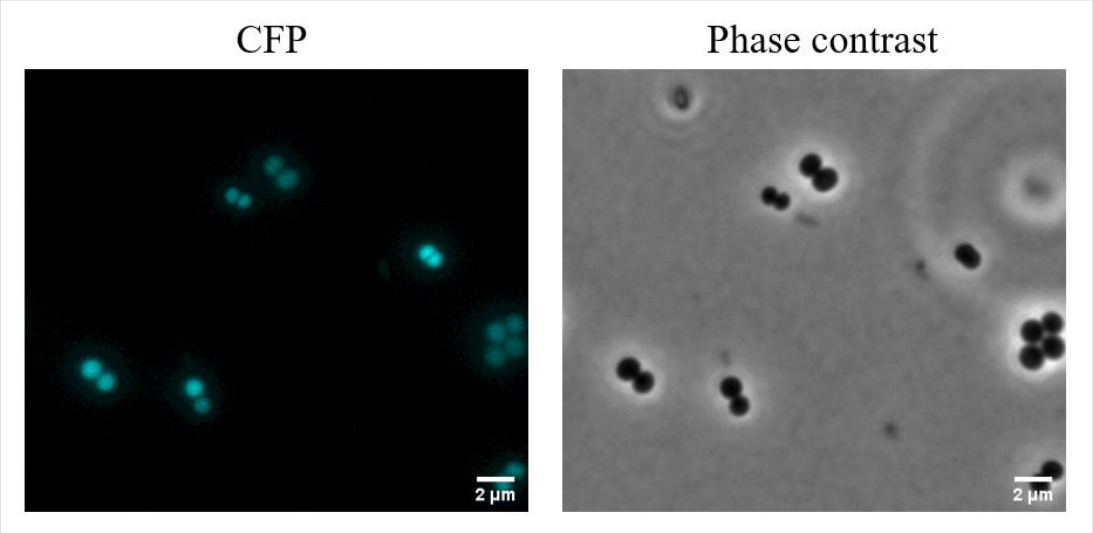

Figure 4.9. Phase contrast microscopy images of cells carrying the *ssaA*-reporter plasmid (pDMA044), using CFP as the reporter.

4.2.3 Expression of 00671 is highest during the stationary phase, whereas SsaA expression is highest during the exponential phase

To study the individual expression of the two peptidoglycan hydrolases 00671 and SsaA, bacterial cultures carrying the expression reporter plasmids for the two hydrolases were incubated in liquid medium and examined in the microscope in the exponential, the transitional, and the stationary growth phase. The term transitional growth stage is used here to describe the stage in which the cells transition from the exponential to the stationary growth phase and was estimated at an OD_{600} of 0.8-0.9. In a wild-type genetic background, 00671-expression was highest during the stationary growth phase and lowest in the exponential phase (**Figure 4.10**). In contrast, the expression of SsaA displayed the opposite pattern, with the highest expression in the exponential phase and the lowest in the stationary phase. Notably, in Δ00671, expression of SsaA increased in all stages of growth, and no significant difference between the exponential- and the transitional stage was found.

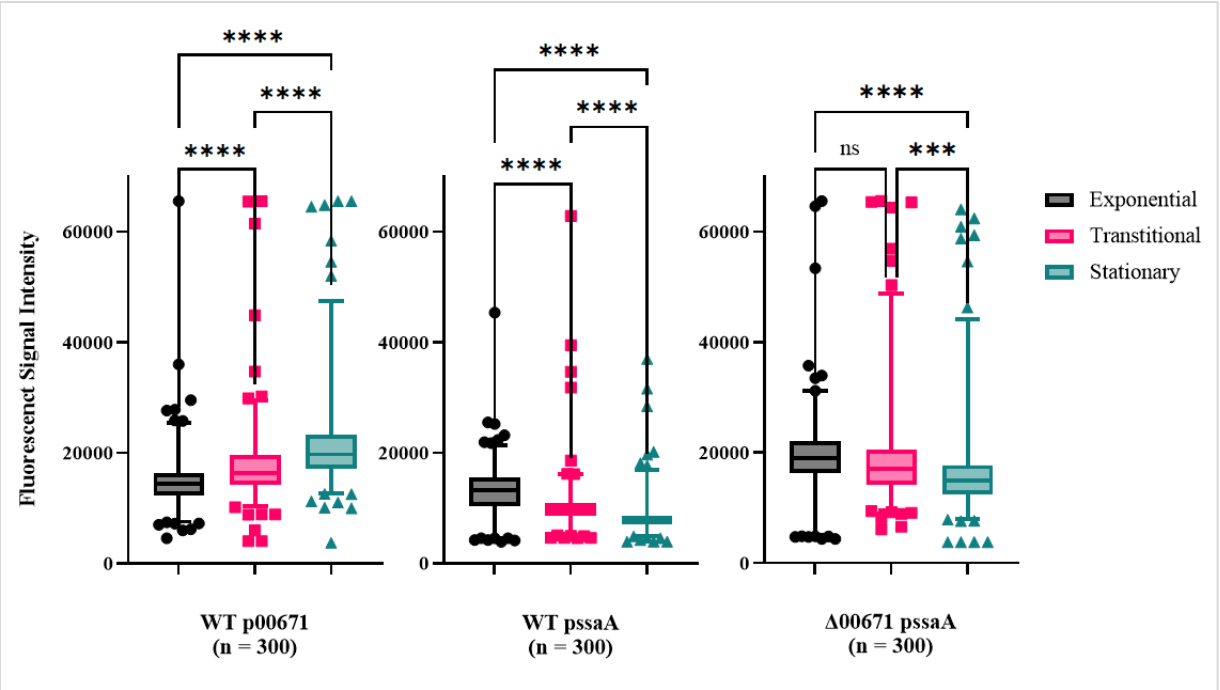

Figure 4.10. Box plot of fluorescent signal intensity as a measurement for estimation of 00671 and SsaA-expression during three stages of growth. Fluorescent signal intensity was measured using the microbeJ package in ImageJ (n = 300) (132, 133). The boxes map 97,5% of cells, and the remaining 2,5% are mapped as individual points. Statistical significance was determined using the one-way ANOVA test, followed by the posthoc Tukey test (data in A3). Median values are shown as lines within the boxes, and significance is visualised with asterixis. ns, $p > .05$; ***, $p < .001$; ****, $p < .0001$

4.2.4 SsaA expression is upregulated in Δ00671 planktonic cells

The observation above suggests that the absence of 00671 resulted in elevated expression of SsaA. Another experiment was therefore performed to compare the expression of SsaA more directly in the wildtype and Δ00671. Cultures of cells were incubated with shaking and examined in the microscope at the exponential and the stationary growth phase. Wildtype cells were stained with DAPI to distinguish these cells from the Δ00671 cells, and the cultures were mixed to view the expression in the two strains simultaneously. Indeed, the expression of SsaA was found to be significantly higher in Δ00671 than in the wildtype. This was valid both in the exponential- and stationary growth stages ($\alpha = 0.05$) (**Figure 4.11**).

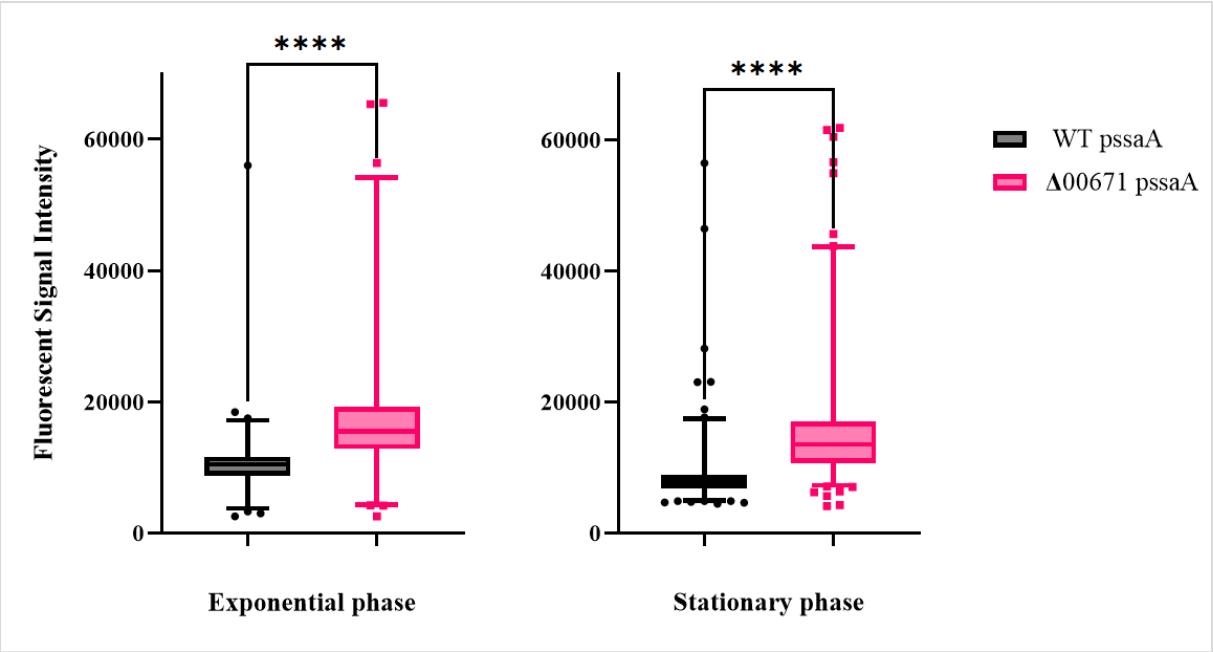

Figure 4.11. Box plot of fluorescent signal intensity as a measurement for estimating *ssaA*-expression during exponential and stationary stages of growth in the *S. aureus* wildtype and Δ00671 (n = 140). Fluorescent signal intensity was measured using the microbeJ package in ImageJ (20, 21). The boxes map 97,5% of the cells, with the remaining 2,5% plotted as individual points. Median values are shown as lines within the boxes, and significance is visualised with asterixis. Statistical significance was calculated using the Student's t-test.
****, $p < .0001$.

4.2.5 SsaA expression is upregulated in Δ00671 biofilms

As many peptidoglycan hydrolases are known to function in biofilm formation, the expression of the two putative peptidoglycan hydrolases 00671 and SsaA was also examined in biofilms of the fluorescent reporter strains. Biofilms were grown for 24 hours, washed, and dyed with SYTO^{TM} 60 to visualise the biofilm. Images acquired using confocal laser scanning microscopy are displayed in **Figure 4.12**. Comparing the expression of SsaA and 00671 in the wildtype strains, 00671 seemed to be expressed in a much larger quantity and throughout a larger fraction of the cells in the biofilm at this stage. Also, consistent with previous results, Δ00671 exhibits a higher level of SsaA-expression compared to the wildtype. Together, the results in section 4.2 demonstrate that the absence of 00671 causes an upregulated expression of SsaA, both in biofilms and planktonic cells.

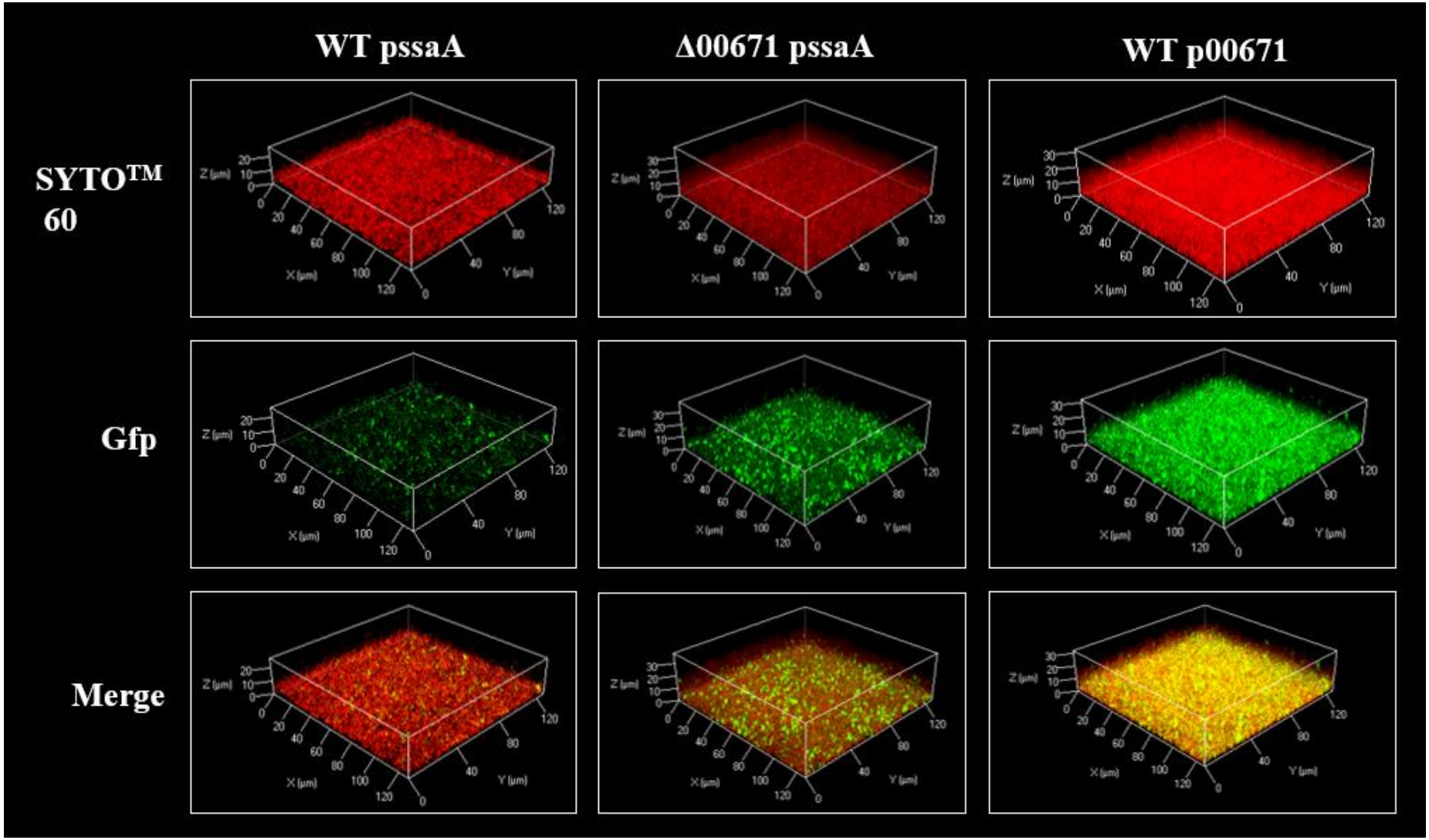

Figure 4.12. Confocal laser scanning microscopy images of *S. aureus* GFP expression reporter strain biofilms, formed in borosilicate chambers by static incubation for 24 hours. GFP expression is used as a measurement of expression of 00671 (p00671) and SsaA (pssaA). The top panel displays the totality of cells constituting the biofilm stained with a red fluorescent dye (SYTO™ 60), the middle panel displays expression of gfp in place of the peptidoglycan hydrolases, and the bottom panel shows a merge between the above images.

4.3 The downregulation of α-hemolytic protein Hla in Δ00671 causes no visible difference in hemolysis

To further understand the role of 00671, an RNA-sequencing analysis comparing transcription of Δ00671 with wild-type in exponential phase (**Appendix 4**) was conducted by Morales Angeles D. (unpublished). While no major transcriptional remodelling was observed, the results revealed downregulation of the α-haemolytic protein Hla. Haemolysin A (Hla) is considered a major virulence factor for *S. aureus* and has been found to facilitate human airway infections by disrupting host cell-matrix adhesions (34). As downregulation of Hla expression was seen in Δ00671, its haemolytic activity was assessed by spotting bacterial cultures of the knockout on sheep's blood agar plates with the wildtype strain used as a control. The plate was incubated for approximately 24 hours and subsequently photographed (**Figure 4.13**). Comparing the wildtype and knockout strain, the radius of the haemolytic zones surrounding the colonies were similar, suggesting that 00671 do not alter the haemolytic activity of this strain.

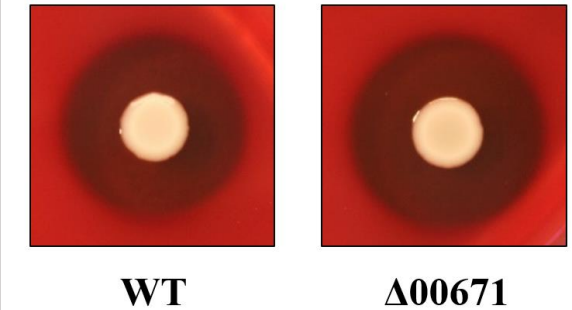

Figure 4.13. Bacterial cultures of the wildtype (WT) and Δ00671 spotted on sheep's blood agar plates. Haemolytic activity is seen in the clear zones surrounding the colonies, where the red blood cells have been lysed.

4.4 The contribution of the cell morphology determinant SmdA on *S. aureus* biofilm formation

As the third topic for this work, *Staphylococcus* cell morphology determinant A (SmdA) was recently identified as crucial for proper septum formation and cell splitting during the cell division process (92). RNA-sequencing of an SmdA-depleted strain revealed downregulation

of biofilm-associated genes, such as the *ica*-operon (**Table 1.1**, section 1.3), which called for an exploration of the effect of SmdA on biofilm formation.

4.4.1 SmdA affects biofilm formation in *S. aureus* NCTC8325-4, with a possible link to the *ica*-operon

To determine if SmdA affects biofilm formation, a CV microtiter assay using the CRISPRi system to downregulate the expression of SmdA was conducted on NCTC8325-4 strains. A strain with sgRNA targeting the *ica*-operon and a strain harbouring sgRNA with no target (none) was used as a control. The results are shown in **Figure 4.14A**. The depletion of SmdA resulted in a significant decrease in biofilm formation compared to the wildtype under these conditions. However, the reduction in biofilm formation was not as detrimental as that of the *ica* control strain.

As the RNA-sequencing showed downregulation of *ica*-genes, a dot blot to estimate PIA-quantities was performed. PIAs are the dominant molecules of the PIA-dependent *S. aureus* biofilm phenotype. The dot blot PIA quantification was conducted in the same manner as that described in section 4.1.2.2, and an image of the blot is displayed in **Figure 4.14B**. As expected, no chemiluminescent signal was detected for the *ica* control. The SmdA-depleted strain had a lower quantity of PIAs than the non-targeting control, most apparent in the 1:4 and the 1:16 dilutions.

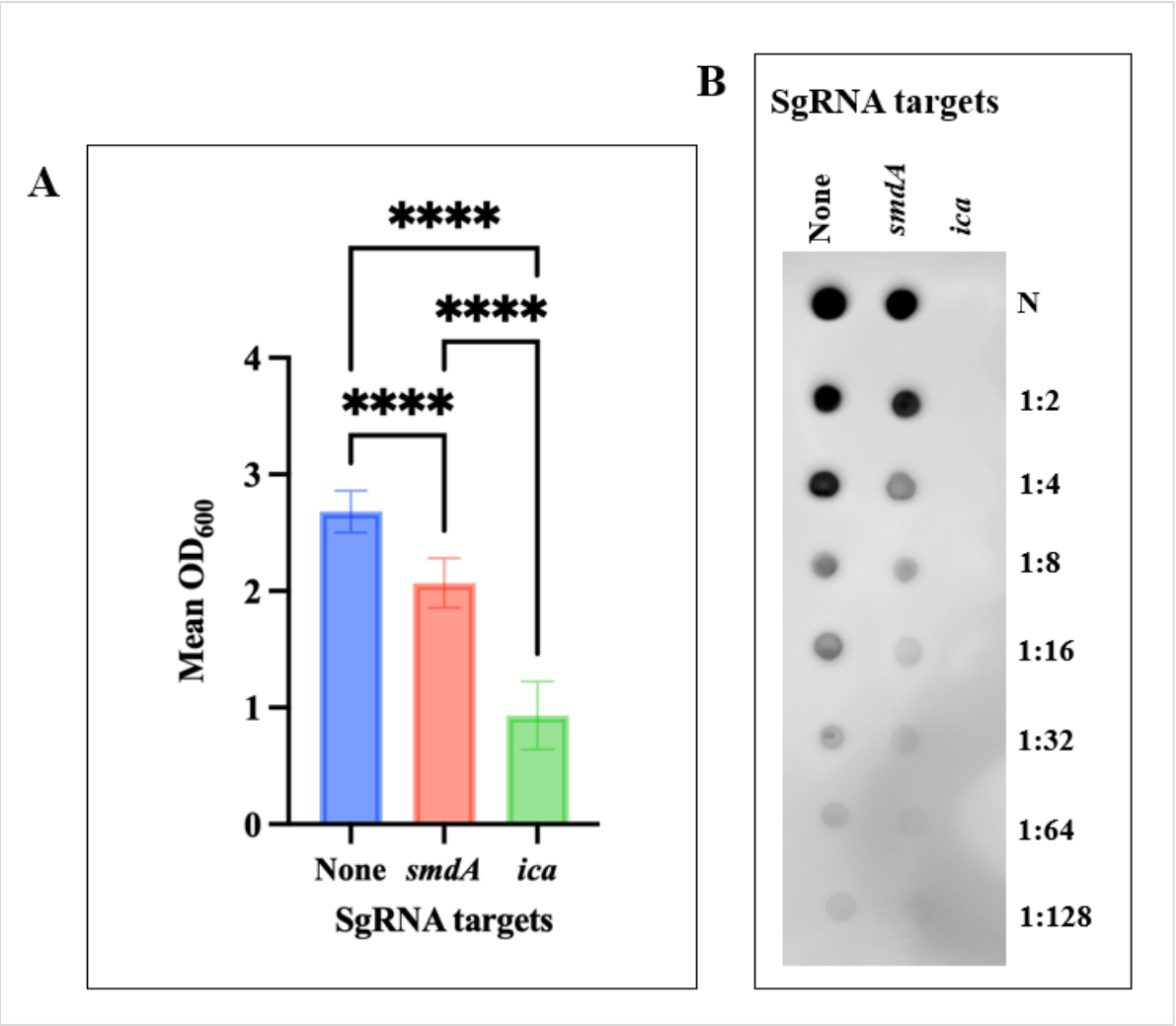

Figure 4.14. A. Mean biofilm formation quantification of CRISPRi *smdA* and *ica* depleted strains using the crystal violet microtiter assay. None = strain harbouring sgRNA with no target. B. Nitrocellulose dot blot estimate quantifications of PIAs in biofilms of the same three strains. Dilutions are seen on the right side of the blot. N = neat (undiluted). Statistical significance was calculated using the one-way ANOVA test, followed by the post hoc Tukey test, and a summary can be found in **Appendix 3**.

****, $p < .0001$.

4.4.2 The role of SmdA in biofilm-formation is not conserved across staphylococcal strains.

As SmdA was shown to affect biofilm formation in *S. aureus* NCTC8325-4, we were interested to determine whether this phenotype was conserved across staphylococcal strains. Therefore, the same biofilm quantification experiment was conducted in two additional strains of *S. aureus* (JE2 and SH1000). The results can be seen in **Figure 4.15**. For the MRSA strain JE2, no reduction in biofilm formation could be detected in the CRISPRi SmdA-depleted strain

compared to that with a sgRNA with no viable target. Furthermore, also for the SH1000 SmdA-depleted strain, no such difference was observed. However, it should be noted that neither the *ica* control strain exhibited any significant decrease in biofilm formation compared to the non-target sgRNA strain in SH1000, suggesting that a reduction in *ica* expression does not strongly affect biofilm formation in this strain.

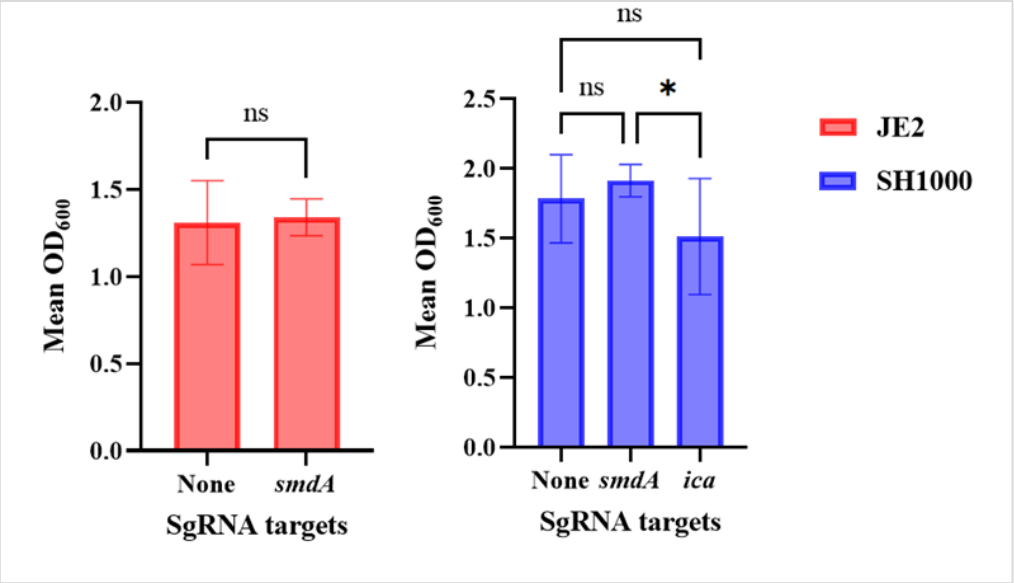

Figure 4.15. Mean biofilm formation measured as OD_{600} using a crystal violet assay with CRISPRi strains of JE2 and SH1000 targeting smdA, the *ica*-operon, or nothing (none).
*, $p < .05$. ns, $p > .05$

Growth curves were made for all *S. aureus* CRISPRi strains used in these experiments to ensure that decreased fitness, as a result of SmdA- and *ica*-depletion, were not causing the decreased biofilm formation seen in the CV assays. The growth curves are shown in **Figure 4.16**, displaying that the growth of all the strains where comparable to their respective controls. For NCTC8325-4, the SmdA- and *ica*-depleted strains have a somewhat higher OD_{600} than the NCTC8325-4 with a non-targeting sgRNA, evidently showing that the depletion did not affect the growth. The JE2 strain displayed a slight decrease in growth with SmdA-depletion, but for SH1000, the growth of all the strains was almost identical.

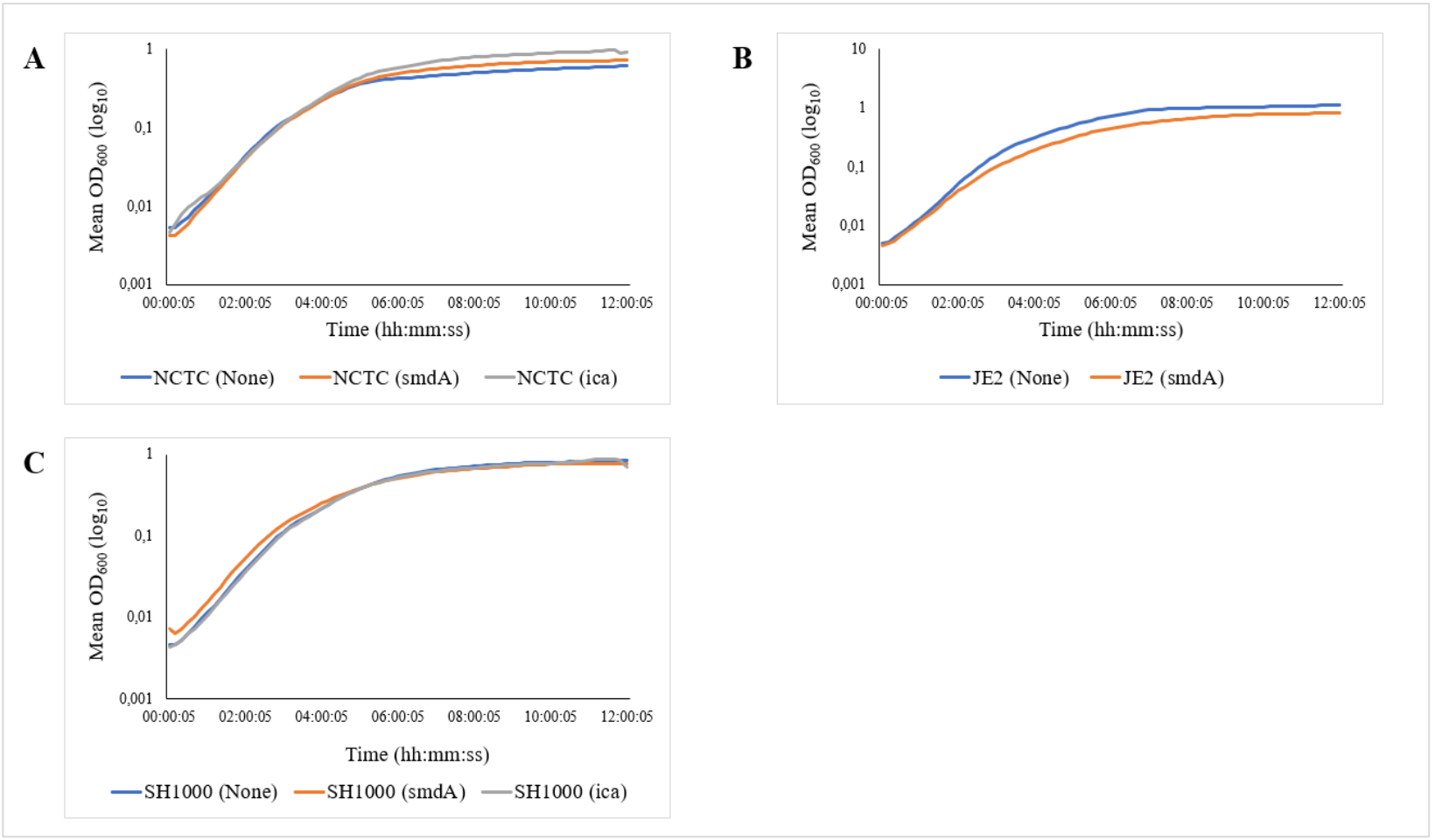

Figure 4.16. Growth curves of the *S. aureus* CRISPRi strains. The cells were incubated in 96-well plates and the OD_{600} was measured every 10 minutes. NCTC = NCTC8325-4. Respective SgRNA targets are written in parentheses. A: NCTC8325-4 strains. B. JE2 strains. C: SH1000 strains.

4.5 Screening a CRISPRi library for attachment related genes

A CRISPRi library covering 1928 genomic features was screened in an attachment assay to identify novel genes involved in the attachment stage of biofilm formation. The attachment assay was conducted by incubating the induced library in multiwell plates for 1 hour before the cells were transferred to the next well, allowing attachment to occur for a total of 4 hours. After incubation, the unattached cells were harvested and their sgRNA plasmids were isolated and sequenced by Illumina sequencing. Bioinformatic analyses were conducted by comparing the abundance of the different sgRNAs of the induced and the uninduced cells. The sgRNA target genes that are more abundant in the induced condition after the assay may be important for attachment, as their depletion leads to more unattached cells. A principal component analysis (PCA) was conducted, and the plot revealed that the induced and the uninduced samples were more-so correlated within the group than between the groups (**Figure 4.17**). This means that the CRISPRi depletion did cause a difference in the sgRNAs abundance and is explained by the fact that sgRNAs targeting essential genes will be reduced with induction. The difference between the sgRNA abundance of the cells after the attachment assay and their respective culture controls suggests some of the variance can be explained by the attachment assay treatment. The PCA plot did, however, not show that this variance is similar in the induced an uninduced conditions.

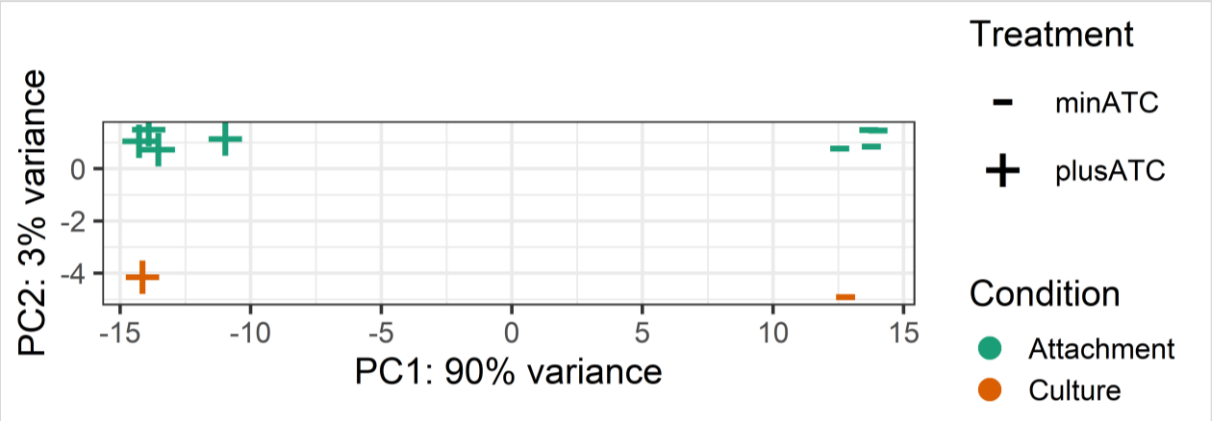

Figure 4.17. Principal component analysis (PCA) of the sgRNA abundance variance of the CRISPRi library after the attachment assay (attachment), including controls (culture). The plot shows that the majority of the variance is explained by the gene-depletion, but that there are variations as a result of the attachment assay. minATC: uninduced. plusATC: induced. The figure was created by Torrissen Mårli M.

In order to identify non-essential genes contributing to the attachment phase, sgRNA abundances in the induced and uninduced attachment samples were compared. By this analysis, only three sgRNA targets, with an abundance log2 fold change of more than 1 and with a p-value of less than 0.05 were revealed, namely *SAOUHSC_00957*, *SAOUHSC_02888*, and *xdrA* (*SAOUHSC_01979*) (**Table 4.1**). The two former of these genes encode hypothetical proteins, although predictions about their functions can be made by their amino acid sequences and by comparison to similar, or homologous, proteins. *SAOUHSC_00957* is a predicted membrane protein with 7 transmembrane helices (AureoWiki). It has been recognised as homologous to a TerC family protein in *B. subtilis*, YkoY, involved in manganese efflux (137, 138). Additionally, a protein BLAST search identified it as more than 99% identical to *S. aureus* TerC family proteins. *SAOUHSC_00957* is listed as essential on the database of essential genes (DEG), however our results suggest that it is not essential under these specific conditions, but that it contributes to attachment. *SAOUHSC_02888* is also predicted to be a transmembrane protein, with 10 transmembrane helices (AureoWiki). It shares a 99% identity in amino acid sequence with the *S. aureus* phosphotransferase system (PTS) subunit IIC, as revealed by protein BLAST. XRE (xenobiotic response regulator)-like DNA-binding regulator XdrA is a helix-turn-helix transcriptional regulator, encoded by *xdrA* (139). It was first recognised by its ability to bind to the *mecA* promoter region (139). *mecA* encodes the alternative penicillin-binding protein PBP2a, which is the major mechanism for methicillin-resistance in MRSA. Although deletion of XdrA causes an increased resistance to oxacillin, the mechanism has not been revealed, as it does not affect *mecA* transcription (139). Additionally, XdrA has been recognised as a repressor of capsule production, and a major activator for *spa*, encoding the virulence factor Protein A (140, 141). Interestingly, it has been reported that a *xdrA* knockout mutant displayed a significant decrease of eDNA in the ECM, suggesting it is involved in biofilm regulation (142).

Table 4.1. sgRNA-target genes recognized as significantly more abundant after the attachment assay.

Gene name	Log2 Fold Change	p-value	Locus tag
SAOUHSC_00957	1.649068049	0.004322093	*SAOUHSC_00957*
SAOUHSC_02888	1.559251557	8.33732E-05	*SAOUHSC_02888*
xdrA	1.272913981	0.001799628	*SAOUHSC_01979*

The remaining 31 genes with a log2 fold change of more than 1, but with p-value above 0.05, are listed in **Appendix 5**. This list includes, among others, *icaA* and *agrB.* sgRNAs targeting *SAOUHSC_00671* and *atl* were not found in an increased abundance after the attachment assay.

5 Discussion

5.1 The role of *SAOUHSC_00671* in *S. aureus* biofilm formation

SAOUHSC_00671 encodes a protein, referred to as 00671, predicted to contain two peptidoglycan-binding LysM domains and a CHAP-domain with peptidoglycan hydrolytic activities (86, 87). This structure suggests that 00671 is a peptidoglycan hydrolase, a group of enzymes with the ability to cleave peptidoglycan in the cell wall. With this ability, peptidoglycan hydrolases can be involved in several cellular processes, including biofilm formation (40, 78). Indeed, a decreased ability to form biofilms has been seen in Δ00671 in the works of Torrissen Mårli M. (2020) and Morales Angeles D. (unpublished). Therefore, exploring the role of *SAOUHSC_00671* in *S. aureus* formation was one of the main topics of this work.

5.1.1 Complementation of 00671 does not increase biofilm formation

The absence of 00671, either by depletion (Torrissen Mårli M., 2020) or knockout (Morales Angeles D., unpublished), in *S. aureus* was found to decrease its biofilm-forming abilities. A complementation assay was performed to determine the effect of gradually increased induction of 00671 on biofilm formation. Cells of a complement strain allowing for the titratable expression of 00671 by addition of IPTG were incubated to form biofilms, and the biofilm mass was quantified by CV-staining. If 00671 is a major contributor to *S. aureus* biofilm formation, an increase in biofilm mass should be seen in accordance with increased induction. The results of the complementation assay revealed no such correlation (**Figure 4.1**), indicating that the amount of 00671 does not majorly determine the overall biofilm formation abilities of *S. aureus* under these conditions.

A similar complementation experiment using the same strain has been conducted by Torrissen Mårli M. (2020) to determine if increasing induction of 00671 would recover the biofilm-forming abilities of the knockout to the wildtype phenotype. Contrary to the results in this work, the results indicate an increasing trend of biofilm formation with increased induction of 00671. Additionally, it was reported that the uninduced expression of 00671 led to a decrease in biofilm formation and that the wildtype phenotype was recovered at 500 µM. However, these experiments were conducted with the addition of glucose and NaCl and may not be directly

comparable. Osipovitich D.C., Therrien S., and Griswold K. E. observed a lack of lytic activity by 00671 (referred to as SsaALP), which they suggested was a result of proteolytic degradation of the CHAP-domain (88). A lack of lytic activity would explain why increasing induction does not affect the phenotype (88). However, LIVE/DEAD stains of a 00671-depleted (Torrissen Mårlig M., 2020) and a -knockout strain biofilm (Morales Angeles D., unpublished) did show a reduction in lysed cells compared to the wildtype, suggesting that 00671 does in fact exhibit lytic activity (85).

Limitations of the method could have contributed to the contradiction between these- and previously reported results. The crystal violet microtiter assay is considered a model method for standardized biofilm quantification with many benefits, such as the ability to study multiple strains or treatment conditions simultaneously. However, it often requires multiple washing steps that may disturb the biofilm, leading to differential removal of biofilm-associated cells. This effect was reported to result in significant variations of remaining biomass in *P. aeruginosa*, depending on the methods used to remove the supernatant prior to staining (143). Furthermore, CV binds to negatively charged molecules and can stain other biofilm components, thereby muddling the results (144). When studying the effect of peptidoglycan hydrolases on biofilm formation, this issue becomes especially apparent as their contribution to the formation is the release of negatively charged eDNA through cell lysis. However, the latter does not explain the results seen in the complementation assay in this work. If a lytic activity of 00671 is presumed, an increased induction would result in more eDNA in the biofilm matrix, thus binding more CV. In order to understand the lack of effect seen by inducing expression of 00671, some of the core premises, such as lytic activity, need to be assessed and verified, preferably by employing alternative, more accurate, and reproducible methods. Amador C. I. and colleagues recommend fluorescent labelling coupled with plate readers and microscopy as an alternative to the CV assay for high-throughput biofilm screenings (144). In addition to not presenting many of the issues associated with the CV assay, the method offers added benefits in terms of information recorded, such as cell viability and biofilm morphology (144). However, the authors reported decreased sensitivity for strains producing low amounts of biofilms as a possible limitation of this technique (144).

5.1.2 00671 may be involved in determining the composition of eDNA and PIAs in the ECM, but alternative methods are required for verification

Peptidoglycan hydrolases mainly contribute to biofilm formation by cell wall cleavage, leading to cell lysis and the release of adhesive eDNA (40). Additionally, the peptidoglycan hydrolase Atl has been found to act directly as an adhesin and is involved in both the PIA-dependent and -independent pathways of ECM production (40, 56). To further understand how 00671 might affect biofilm formation, the concentration of DNA, proteins, and PIAs was measured in the ECM of a 00671-knockout biofilm. The results were compared to a wildtype ECM. A trend of lower DNA- and protein concentrations was found in the 00671 knockout ECM. However, the difference was not statistically significant in every repetition of the experiment (**Figure 4.2**). PIAs were approximately quantified by dot blot analysis, revealing lower concentrations in the 00671 knockout ECM than in the wildtype (**Figure 4.3**). These results suggest that 00671 may contribute to compositional changes in the ECM, but not majorly so.

A lower concentration of DNA in the knockout biofilms is consistent with 00671 having peptidoglycan hydrolytic activities. Lysis of cells results in the release of adhesive eDNA to the ECM. Sle1 is a peptidoglycan hydrolase structurally similar to 00671, the only difference being that Sle1 contains an additional LysM domain. It has been reported that increased expression of Sle1 leads to increased levels of eDNA in a cell culture supernatant (52). Although these results were obtained from planktonic cells, the authors of this study claim them to apply to biofilms (52). For 00671 to function much in the same manner would be supported by their similarity in structure. However, the results from this work do not fit with the hypothesis that 00671 majorly facilitates biofilm formation by eDNA release. The differences between the 00671 knockout and the wildtype ECM were minor and, in one repetition, insignificant. Alternative methods should be utilized to further elucidate the function of 00671 as a possible contributor to eDNA release in biofilm ECMs. eDNA release mediated by peptidoglycan hydrolases is involved in the attachment stage of biofilm formation; therefore, eDNA concentrations should be compared in younger biofilms where the effect might be more prominent.

The ECM of a Δ00671 biofilm was found to have fewer PIAs in a nitrocellulose dot blot (**Figure 4.3**). Produced by components encoded in the *ica*-operon, PIAs are the dominant molecules in the polysaccharide-dependent pathway for ECM production (55). These results indicate that this strain (NCTC8325-4) exhibits the PIA-dependent mode of biofilm formation and that 00671 is somehow involved in this. Recently, a model in which eDNA and PIA synergistically

interact in *S. aureus* biofilm formation due to their electrostatic charges has been proposed, and a certain correlation between eDNA and PIA has been found in biofilms of *S. epidermidis* (68, 145). In this model, PIA is suggested to interact with eDNA under regulation by CodY (68). The eDNA subsequently associates with membrane lipoproteins functioning as anchor points between the ECM and the cell surface (68). Additionally, constitutive expression of WalR leads to increased expression of negative *ica*-regulator IcaR, and peptidoglycan hydrolases, including 00671 and SsaA (83). A global regulator of eDNA release, by regulation of peptidoglycan hydrolases and the *ica*-operon, would explain the decrease of PIAs seen in Δ00671, and this possible correlation should be investigated further. However, this hypothesis assumes a role of 00671 as a contributor to eDNA release, which, as discussed above, remains unclear. It should be noted that these are preliminary results as the approximate PIA quantification was conducted only once. A limitation of this method is the inability to provide specific concentrations. Therefore, additional experiments should be performed to make more accurate measurements. This would provide insights regarding the significance of 00671's contribution to PIA composition in the ECM.

Differences in protein concentrations between the 00671 knockout- and the wildtype ECM were insignificant in two out of three replicates (**Figure 4.2**). Strains that utilize the PIA-independent pathway for biofilm formation form proteinaceous biofilms (56). Therefore, if 00671 was involved in this pathway, one could expect a decrease in protein concentration in the knockout ECM. However, as this was not observed, these results are in line with the hypothesis mentioned above that strain NCTC8325-4 exhibits the PIA-dependent pathway for biofilm formation and that this involves 00671.

5.1.3 00671 may be involved in the attachment stage of biofilm formation

Peptidoglycan hydrolases facilitate the attachment stage of biofilm formation by lysing cells and releasing eDNA or directly serving as adhesins (40). Therefore, the attachment abilities of 00671 were examined in a primary attachment assay. The attachment was performed by calculating the fraction of cells attached to polystyrene surfaces after one hour of incubation. This short window of time gives the cells time to attach but does not allow the biofilm to increase in mass by cell division. No consistent change in terms of attachment ability between the wildtype and Δ00671 was observed (**Figure 4.4**). Limitations of the method likely caused these results as the assay had several possible issues as discussed below.

When making multiple serial dilutions using bacterial cultures, the probability of retaining the dilution ratio to the original culture decreases with every dilution. To retain the dilution ratio would require the cells to exhibit little to no clumping and be homogeneously dispersed in the culture during all steps. Both of these requirements are unlikely when working with *S. aureus*, which tends to sink to the bottom of the liquid media and sediment. Furthermore, from microscopical examination of cell cultures in this work, it became apparent that most *S. aureus* cells, when actively dividing, clumped together in pairs or clusters even after vigorous vortexing. This issue can be bypassed by sonicating the cells prior to plating. Dilutions of the cell cultures were necessary to obtain a countable number of colonies; however, they should not have been performed in series. Additionally, due to the high dilution of the culture, an assessment of the amount of pipetting required to detach the cells was challenging. Therefore, the number of cells counted as attached may be inaccurate. Lastly, performing several washing steps involve a risk of disturbing and thereby dispersing the cells. Some or all of these issues may have contributed to the apparent inaccuracy of this method.

Using a second method, different attachment phenotypes were observed between the wildtype, Δ00671, and an *atl* knockout mutant (Δ*atl*) (**Figure 4.5**). After one hour of incubation, cells attached to borosilicate chambers were fluorescently stained and examined using CLSM. In line with previous reports, few attached cells were seen in Δ*atl* (51). This strain was used as a negative control, as a knockout of Atl has been shown to significantly impact the attachment ability of *S. aureus* cells in a similar experiment (51). Compared to the wildtype, the cells of Δ00671 were more dispersed both vertically and horizontally. Some level of vertical dispersion was observed in the wildtype as well, but less so than in Δ00671. These differences suggest a role of 00671 in the attachment stage of biofilm formation consistent with that of peptidoglycan hydrolases. A less adhesive ECM resulting from less eDNA release could lead to cell dispersion, as seen in Δ00671. Using this method, washing steps with a risk of attachment disturbance were performed. However, with similar phenotypes, the same level of dispersion would be expected. These results contrast CLSM images of a 00671-depleted (by CRISPRi) biofilm, where the cells exhibited a higher degree of clumping than the wildtype (85). However, the 00671-depleted biofilm contained fewer lysed cells, as seen by propidium iodide staining, supporting the role of 00671 as an autolysin (85). Due to time restraints, this experiment was only conducted once. Further repetitions of this experiment and investigations into the role of 00671 in the primary attachment stage should be performed. Additionally, a LIVE/DEAD

staining version of this experiment to assess the viability of the biofilm-associated cells at this stage could further enlighten the role of 00671 as an autolysin.

5.2 Using constitutively expressed red-fluorescent protein mKate to visualize biofilms in CLSM

Experiments in this work required fluorescent labelling of all biofilm-associated cells to outline the biofilm. This was first attempted by using a plasmid-encoded version of red-fluorescent protein mKate downstream of a constitutive promoter in combination with the expression reporter plasmids described in section 3.11. When examining the biofilms using CLSM, the red fluorescence signal intensity was inconsistent and unable to visualize the biofilm as a whole (**Figure 4.7A**). This could be a consequence of a portion of the cells carrying multiple copies of the plasmid and therefore producing a stronger signal than those carrying a single copy. Consequently, to prevent this effect, mKate was integrated chromosomally, but surprisingly planktonic cells examined with light microscopy revealed that the chromosomal integration did not decrease the inconsistency. Additionally, the signal intensity weakened, resulting in little to no cell detection when using CLSM to image biofilms. This suggests that several and a similar number of copies of the plasmid were required to produce a fluorescent signal sufficient for detection, at least with the given microscope. A red-fluorescent dye (SYTO^{TM} 60) was utilized successfully to overcome these issues, producing a sufficiently strong and consistent signal. This dye has also proved successful in biofilms of other species, including *S. epidermidis, P. aeruginosa,* and *E. coli* (146, 147). As such, using the red-fluorescent dye SYTO^{TM} 60 to visualize biofilms is the preferred method over genetically expressed red fluorescent protein mKate in terms of signal quality, and additionally is a significantly less labor-intensive method.

5.3 SsaA and 00671 are genetically negatively correlated both in planktonic cells and in biofilms

Previous studies from our lab (unpublished data) found a negative genetic correlation between SsaA and 00671. When depleting 00671, the expression of SsaA was upregulated, and vice versa. In this work, this correlation was verified in planktonic cells by comparing the expression of SsaA in Δ00671 and wildtype (**Figure 4.11**). GFP was used as an expression reporter, as described in section 3.11. Additionally, the temporal expression of the two hydrolases in

planktonic cells was measured. Their temporal expression was distinct, as SsaA-expression was highest during the exponential phase and 00671-expression during the stationary phase. (**Figure 4.10**). For SsaA-expression, this was valid both in wildtype and Δ00671. As no successful *ssaA*-knockout mutant could be constructed, the expression of 00671 was only examined in the wildtype strain. Furthermore, as 00671 is thought to be involved in biofilm formation, we were interested in seeing if the genetic correlation was valid for biofilms. Indeed, an upregulated expression of SsaA was observed in a Δ00671 biofilm compared to a wildtype biofilm (**Figure 4.12**).

Similar results of correlation have been reported for the two WalRK-regulated peptidoglycan hydrolases LytE and CwlO in *B. subtilis* (90). This study attributed this correlation to WalRK downregulation in response to high endopeptidase activity, maintaining homeostasis in the cell (90). In staphylococci, the loss of Atl activity has been suggested to become partially counterbalanced by other hydrolases with amidase or glucosamidase activity (91). The negative genetic correlation between 00671 and SsaA observed in this work indicates that also these hydrolases are regulatory linked. This means that the absence of one hydrolase is somehow sensed by the cell, resulting in upregulation of the other to compensate for the decrease of activity, suggesting similar functions of the two hydrolases. In the studies on genetic correlation between hydrolases in *B. subtilis*, it was proposed that WalK can sense the accumulation of cell wall cleavage products and inhibits the WalRK system in response (90). Furthermore, it was demonstrated that the WalRK accessory membrane proteins YycH and YycI, previously found to control WalRK negatively, were not involved in this signalling pathway (90, 148). In contrast, *S. aureus* YycH and YycI have been reported to activate the WalRK system, as mutations of the proteins lead to downregulation of genes in the WalRK regulon (149). These include several peptidoglycan hydrolases, most notably SsaA and 00671, which were significantly downregulated from disruption of either YycH or YycI, possibly revealing their common regulatory mechanism (149). Another study presented direct evidence that YycH and YycI interact with WalK to increase phosphorylation of WalR and thus activate the WalRK system in *S. aureus* (150). However, the interaction was not found to be responsible for its essential nature (150). Although highly speculative, should this be the main regulatory mechanism of 00671 and SsaA, this would be consistent with observations of their genes as non-essential. Conflicting notes about the essentiality of *ssaA* are presented on AureoWiki, but depletion experiments from our lab demonstrate that no growth defects are seen in the absence of the gene. Furthermore, no cell wall cleavage products were found to affect WalRK regulation

in *S. aureus*, as is hypothesized for *B. subtilis*; therefore, the signal molecule remains elusive (150). Altogether, this indicates a certain overlapping in functionality between the two putative hydrolases and a regulatory link by WalRK accessory proteins YycH and YycI. The negative genetic correlation was present in planktonic cells, in addition to biofilms, suggesting that 00671 and SsaA may be involved in additional cellular processes in addition to biofilm formation, as is the case for peptidoglycan hydrolases Atl and Sle1 (40). Such processes may include peptidoglycan cleavage facilitating cell division. This is in line with the hypothesis of YycH and YycI as regulators, as YycH is located in the septal region during the exponential growth phase (151). Peptidoglycan hydrolases are essential components of the cell division machinery, and contribute by cleaving peptidoglycan to split the septum, thereby generating two daughter cells (152). The hypothesis of 00671 and SsaA facilitating cell division should be further explored by examining the cellular location of both SsaA and 00671. Despite the many similarities, the temporally distinct expression patterns suggest that the hydrolases also possess some unique functionality, possibly related to the different stages of growth. The WalRK system regulates several additional uncharacterized peptidoglycan hydrolases which could be subjects of genetic correlation. These hydrolases, the link to the accessory proteins YycH and YycI, and the signal responsible for their interaction with the WalRK system should be investigated further.

The observation of a genetic correlation between 00671 and SsaA was made both in planktonic cells and in biofilms, implying that the mechanism of maintaining homeostasis is valid in biofilms as well. As this is the first observation of a correlation between the two hydrolases in biofilms, hypotheses regarding the responsible mechanisms or biofilm-associated functions are speculative. Two different mechanisms may regulate the correlation between the two hydrolases in planktonic cells and biofilms. However, the notion that the same regulatory mechanisms regulate this correlation in biofilms as in planktonic cells is plausible. As mentioned earlier, *S. aureus* biofilms are sensitive to their surrounding environment and modulate regulatory paths in response to external signals (40, 58). Although the same central regulatory system may be at play, there might be differences in the exact components and induction signals between planktonic cells and biofilms. This should be considered in further studies of the genetic correlation between 00671 and SsaA.

To further study the correction in expression between 00671 and SsaA, a construction of additional reporter strains were attempted in this work. Unsuccessful attempts were made to construct an *ssaA*-knockout mutant using an allelic replacement plasmid (pDMA045). This

mutant could have further enlightened the genetic correlation by allowing measurements of *SAOUHSC_00671* expression in planktonic cells and biofilms of the *ssaA*-knockout mutant. Additionally, the plasmid was planned to be used to construct a double knockout mutant of both *SAOUHSC_00671* and *ssaA*. The construction of the plasmid was challenging, likely due to frequent and long mononucleotide repeats, predominantly consisting of thymine and adenine, in the sequence of the tetracycline resistance genes *tetB* and -*D* genes used for the insert. A tetracycline resistance cassette was chosen here to allow combination with other strains as plasmids used in this work already contained genes or cassettes for spectinomycin-, erythromycin-, and chloramphenicol-resistance. Major sequence changes (large deletions) were seen in the AT dinucleotide-rich *tet*-genes when sequencing the construct. Sequences rich in mono- or dinucleotide repeats are associated with a high error rate in PCR due to polymerase "slippage" or incomplete repeat fragments annealing to form mismatches, resulting in faulty repeat lengths and downstream issues (153). Recently, a *ssaA*-knockout was successfully constructed in our lab (Morales Angeles D.) using a spectinomycin-cassette. Studies using this knockout will hopefully elucidate the genetic correlation further.

Furthermore, a reporter plasmid for *ssaA* (pDMA044) using CFP as the fluorescent signal was constructed to visualize and measure *ssaA*- and *SAOUHSC_00671*-expression simultaneously in biofilms. The plasmid was supposed to be used in conjunction with the previously described GFP-reporter plasmid for 00671. This reporter plasmid would allow for further investigation into the spatiotemporal expression of the hydrolases by measuring the expression in a time-lapse, possibly revealing additional differences or similarities. Unfortunately, the microscope was unable to differentiate the signals produced by GFP and CFP, which meant that the distinct expression of the two hydrolases could not be measured. Another combination of fluorescent protein reporters with fluorescence spectra further apart should be utilized to perform these experiments.

5.4 Haemolytic activities in *S. aureus* are unaffected by knockout of 00671

RNA-sequencing results of Δ00671 showed a downregulated transcription of α-haemolysin Hla. However, no visible difference in haemolysis in blood agar plates was seen (**Figure 4.13**). These results indicate that the observed downregulation was insufficient to alter the overall haemolytic activities. Additionally, it suggests that 00671 and Hla do not exhibit interacting functions. This method could only approximately assess differences in overall haemolytic

activities. As such, it is beyond the scope of this study to make any concluding remarks about Hla in biofilms. Further experiments could include studying the expression of Hla specifically by utilizing reporter plasmids in Δ00671.

5.5 Novel cell morphology determinant SmdA is involved in biofilm formation in strain NCTC8325-4, but the role is not conserved across staphylococcal strains

RNA-sequencing results of an SmdA-depleted strain revealed that *ica* genes *A, B,* and *D* were downregulated. As the *ica*-operon is heavily associated with biofilm formation in *S. aureus*, the effect of SmdA depletion on biofilm formation was assessed. Depletion of SmdA was found to decrease biofilm formation in strain NCTC8325-4, suggesting a role of SmdA in this process (**Figure 4.14A**). Furthermore, the PIA contents of the SmdA-depleted biofilm were approximately quantified, and a lower concentration was found, consistent with the downregulation of *ica*-genes as seen in RNA-sequencing (**Figure 4.14B**). SmdA was recently discovered to be essential for cell division in *S. aureus*, but its role in biofilm formation has not been investigated (92). The predicted structure of the protein is an N-terminal transmembrane helix and a C-terminal cytoplasmic part with a region homologous to a nuclease-related domain (NERD) of unknown function (92). Cells depleted of SmdA showed abnormalities in septum formation and cell splitting, although the exact function of the protein has not been discovered (92). It has been speculated that SmdA may be interacting with Atl due to it being pulled down with SmdA in a pulldown assay and that the same phenotype of reduced cell wall splitting is seen in both SmdA-depleted cells and Atl mutants (92). One of the suggestions is that SmdA is involved in the transport or processing of Atl (92). As Atl is a significant contributor to the biofilm attachment stage in *S. aureus* both in methicillin-resistant and -susceptible strains, this is consistent with the decrease in biofilm formation observed in SmdA-depleted cells in this work (56). Additionally, the lower concentration of PIAs in the SmdA-depleted biofilm implies a link to the *ica*-operon. Although speculative, as Atl is involved in the first stages of biofilm formation, a possibility is that its activities stimulate a regulator of the *ica*-operon to advance the formation into the maturation stage.

The role of SmdA in other *S. aureus* strains was also explored, namely SH1000 and the MRSA strain JE2. Neither of these exhibited a decrease in biofilm formation from SmdA-depletion (**Figure 4.15**). SH1000 and MRSA strains, such as JE2, have been reported to utilize the PIA-independent biofilm formation pathway, which is in line with the obtained results. In the case

that SmdA and the *ica*-operon are linked, a decrease in biofilm formation due to SmdA-depletion should not be seen in strains utilizing the PIA-independent pathway. These results further support the role of SmdA in the PIA-dependent pathway (56, 60). In addition to investigating its essential role in cell division, SmdA should be explored in terms of its role in biofilm formation and its possible link to the *ica*-operon.

5.6 XdrA is a potential regulator of the attachment stage of biofilm formation

A CRISPRi library was screened in an attachment assay to reveal genes involved in the attachment stage of biofilm formation. The CRISPRi system allows for the depletion of genes upon induction with aTc. In the attachment assay, an induced and an uninduced CRISPRi library was incubated in four steps, allowing attachment to occur for a total of four hours. The sgRNA targets more abundant in the induced than the uninduced library may be involved in attachment, as cells depleted of these genes were more frequently found among the unattached cells. The assay revealed 34 sgRNA targets more abundant (log2 FC > 1) in the induced library after attachment (**Table A5**), but only 3 (*SAOUHSC_00957*, *SAOUHSC_02888* and *xdrA*) that were statistically significant ($p < 0.05$) (**Table 4.1**). Some genes already known to be involved in attachment, like *atl*, were not more abundant in the induced library after the assay.

SAOUHSC_00957 and *SAOUHSC_02888* encode hypothetical proteins, which from their amino acid sequence are predicted to be involved in manganese efflux, and phosphorylation and transport of sugar, respectively. The method of how these genes may be involved in attachment is unknown. Their predicted functions are not previously associated with attachment; thus, they may be false positives. The assay was conducted for a longer time than the other attachment experiments in this work, meaning differences in growth may have contributed to the results. An increased growth rate resulting from the depletion of these genes would explain their increased abundance. This does not exclude the possibility of them being involved in attachment, but further research is needed to answer this. Shortening the duration of the assay to only one hour may minimise any effects seen by different growth rates as a result of the depletion and should be considered for potential repetitions and similar experiments.

The third sgRNA target recognised as significantly more abundant after the assay, *xdrA*, is a transcription factor found to regulate the expression of several genes, such as *spa* and *cap*-genes, encoding the known virulence factor Staphylococcal protein A and capsule-producing proteins, respectively (140, 154). *Staphylococcus* protein A (SpA) is a surface protein involved

in host immune evasion and is essential for *S. aureus* biofilm formation in the PIA-independent pathway by promoting cell-to-cell interactions (155, 156). The PIA-independent pathway is more frequently seen in MRSA strains, and XdrA is thought to be involved in β-lactam resistance (56, 139). Furthermore, the ECM of an XdrA-knockout was reported to contain significantly less eDNA than the wildtype (142). Altogether, this suggests a major role of XdrA in regulating biofilm formation by both surface- and cell-to-cell attachment, especially so in MRSA strain biofilms. Further studies should be conducted to elucidate the function of XdrA both in biofilm formation and host-immune evasion. Although speculative, it could prove a potential treatment target for MRSA biofilm infections.

The assay did not recognise some already known attachment-related genes, such as *atl*, suggesting the accuracy of the method could be improved. A challenge in genome-wide screens for genes involved in attachment is the notion that some attachment factors, such as eDNA, serve the whole cell population instead of single cells. This means that cells incapable of attaching to the surface due to the gene depletion could be attached regardless because other cells produce the necessary adhesins. Potential measures that could reduce this effect include shortening the incubation time in each well, increasing the number of transfer-incubation steps, or adding a washing step between transfers to disperse any loosely bound cells. As mentioned, the total duration of the assay should be shortened to minimise the effects seen by different growth rates. The CRISPRi attachment assay could prove a useful tool in studying biofilm-formation by several species of bacteria if the issues mentioned above are solved.

6 Concluding remarks

The experiments in this work could not fully elucidate the role of 00671 in *S. aureus* biofilm formation. Preliminary results indicate it may be involved in the attachment stage. Future studies should seek to assess the lytic activity of 00671 in the attachment stage. A link between 00671 and the *ica*-operon was discovered, which may be due to PIA and eDNA interaction in the ECM, globally regulated by the WalRK system. However, the eDNA contribution of 00671 to the ECM was weak and requires further investigation. Altogether, the experiments exploring the role of 00671 suggest a weak or no effect on biofilm formation. However, it should be noted that 00671 and SsaA were found to be genetically negatively correlated in biofilms. Therefore, the lack of 00671-activity may have been compensated by increased SsaA-activity, thus erasing the effect of the 00671-knockout.

Interestingly, 00671 and SsaA were found to be genetically negatively correlated in both planktonic cells and biofilms. This correlation, and their similarity in structure, suggest a similar function of the two putative hydrolases. This is to our knowledge the first time such a correlation has been identified in *S. aureus*. Previous studies in *B. subtilis* link the WalRK accessory proteins YycI and YycH to the regulation of peptidoglycan hydrolases to maintain homeostasis in the cell. This hypothesis should be considered in further studies. As the correlation was present in planktonic cells in addition to biofilms, a role of the hydrolases in cell division should be investigated.

The novel cell morphology determinant SmdA was discovered to be involved in *S. aureus* biofilm formation. It has been suggested that SmdA interacts with Atl, possibly its export, consistent with biofilm-formation involvement. A link between SmdA and the *ica*-operon was discovered, indicating a role of the novel protein in the PIA-dependent pathway of biofilm-formation. This is supported by the lack of effect seen when depleting SmdA in SH1000 and JE2, strains associated with the PIA-independent pathway.

SAOUHSC_00957, SAOUHSC_02888, and *xdrA* were identified as important for attachment by the CRISPRi library screen. The two former encode hypothetical proteins, predicted to function in manganese- and sugar transport, respectively. Further experiments should be conducted to determine if they function in attachment or are false positives. XdrA has previously been reported to regulate cell-to-cell aggregation and eDNA release, and its role as a regulator of biofilm formation should be further investigated. The CRISPRi assay shows promise in terms of revealing attachment-related genes.

References

1. Etter D, Corti S, Spirig S, Cernela N, Stephan R, Johler S. 2020. *Staphylococcus aureus* Population Structure and Genomic Profiles in Asymptomatic Carriers in Switzerland. Frontiers in Microbiology 11:1289.
2. Ogston Alex. 1882. Micrococcus Poisoning. J Anat Physiol 16:526–567.
3. Ogston A. 1881. Report upon Micro-Organisms in Surgical Diseases. Br Med J 1:369.b2-375.
4. Miljković-Selimović B, Dinić M, Orlović J, Babić T. 2015. *Staphylococcus aureus*: Immunopathogenesis and Human Immunity. Acta Facultatis Medicae Naissensis 32:243–257.
5. Foster T. 1996. *Staphylococcus*, p. . *In* Baron, S (ed.), Medical Microbiology, 4th ed. University of Texas Medical Branch at Galveston, Galveston (TX).
6. 2013. Point prevalence survey of healthcare-associated infections and antimicrobial use in European acute care hospitals 2011-2012. European Centre for Disease Prevention and Control. https://www.ecdc.europa.eu/en/publications-data/point-prevalence-survey-healthcare-associated-infections-and-antimicrobial-use-0. Retrieved 18 November 2021.
7. Weiner-Lastinger LM, Abner S, Edwards JR, Kallen AJ, Karlsson M, Magill SS, Pollock D, See I, Soe MM, Walters MS, Dudeck MA. 2020. Antimicrobial-resistant pathogens associated with adult healthcare-associated infections: Summary of data reported to the National Healthcare Safety Network, 2015–2017. Infection Control & Hospital Epidemiology 41:1–18.
8. van Hal SJ, Jensen SO, Vaska VL, Espedido BA, Paterson DL, Gosbell IB. 2012. Predictors of Mortality in *Staphylococcus aureus* Bacteremia. Clin Microbiol Rev 25:362–386.
9. Kourtis AP. 2019. Vital Signs: Epidemiology and Recent Trends in Methicillin-Resistant and in Methicillin-Susceptible *Staphylococcus aureus* Bloodstream Infections — United States. MMWR Morb Mortal Wkly Rep 68.
10. Noskin GA, Rubin RJ, Schentag JJ, Kluytmans J, Hedblom EC, Jacobson C, Smulders M, Gemmen E, Bharmal M. 2007. National Trends in *Staphylococcus aureus* Infection Rates: Impact on Economic Burden and Mortality over a 6-Year Period (1998–2003). Clinical Infectious Diseases 45:1132–1140.
11. Joanne M. Willey, Lina M. Sherwood, Christopher J. Woolverton. 2017. Prescott's Microbiology, 10th Edition. McGraw-Hill Education, New York, USA.
12. Rammelkamp CH, Maxon T. 1942. Resistance of *Staphylococcus aureus* to the Action of Penicillin. Experimental Biology and Medicine 51:386–389.
13. Jevons MP. 1961. "Celbenin" - resistant Staphylococci. Br Med J 1:124–125.
14. Brakstad OG, A. Maeland J. 1997. Mechanisms of methicillin resistance in staphylococci. APMIS 105:264–276.
15. Hiramatsu K, Cui L, Kuroda M, Ito T. 2001. The emergence and evolution of methicillin-resistant *Staphylococcus aureus*. Trends in Microbiology 9:486–493.
16. McGuinness WA, Malachowa N, DeLeo FR. 2017. Vancomycin Resistance in *Staphylococcus aureus*. Yale J Biol Med 90:269–281.
17. Köck R, Becker K, Cookson B, Gemert-Pijnen JE van, Harbarth S, Kluytmans J, Mielke M, Peters G, Skov RL, Struelens MJ, Tacconelli E, Torné AN, Witte W, Friedrich AW. 2010. Methicillin-resistant *Staphylococcus aureus* (MRSA): burden of disease and control challenges in Europe. Eurosurveillance 15:19688.
18. Feng Y, Chen C-J, Su L-H, Hu S, Yu J, Chiu C-H. 2008. Evolution and pathogenesis of *Staphylococcus aureus*: lessons learned from genotyping and comparative genomics. FEMS Microbiology Reviews 32:23–37.
19. Chambers HF. 2001. The changing epidemiology of *Staphylococcus aureus*? Emerg Infect Dis 7:178–182.
20. Wertheim HF, Melles DC, Vos MC, Leeuwen W van, Belkum A van, Verbrugh HA, Nouwen JL. 2005. The role of nasal carriage in *Staphylococcus aureus* infections. The Lancet Infectious Diseases 5:751–762.
21. Sakr A, Brégeon F, Mège J-L, Rolain J-M, Blin O. 2018. *Staphylococcus aureus* Nasal Colonization: An Update on Mechanisms, Epidemiology, Risk Factors, and Subsequent Infections. Front Microbiol 9:2419.
22. Balasubramanian D, Harper L, Shopsin B, Torres VJ. 2017. *Staphylococcus aureus* pathogenesis in diverse host environments. Pathog Dis 75:ftx005.

23. Thomer L, Schneewind O, Missiakas D. 2016. Pathogenesis of *Staphylococcus aureus* Bloodstream Infections. Annu Rev Pathol 11:343–364.
24. Abraham L, Bamberger DM. 2020. *Staphylococcus aureus* Bacteremia: Contemporary Management. Mo Med 117:341–345.
25. Lister JL, Horswill AR. 2014. *Staphylococcus aureus* biofilms: recent developments in biofilm dispersal. Frontiers in Cellular and Infection Microbiology 4.
26. Tong SYC, Davis JS, Eichenberger E, Holland TL, Fowler VG. 2015. *Staphylococcus aureus* Infections: Epidemiology, Pathophysiology, Clinical Manifestations, and Management. Clin Microbiol Rev 28:603–661.
27. Kluytmans J, van Belkum A, Verbrugh H. 1997. Nasal carriage of *Staphylococcus aureus*: epidemiology, underlying mechanisms, and associated risks. Clin Microbiol Rev 10:505–520.
28. Cheung GYC, Bae JS, Otto M. Pathogenicity and virulence of *Staphylococcus aureus*. Virulence 12:547–569.
29. Lyon GJ, Novick RP. 2004. Peptide signaling in *Staphylococcus aureus* and other Gram-positive bacteria. Peptides 25:1389–1403.
30. Le KY, Otto M. 2015. Quorum-sensing regulation in staphylococci—an overview. Front Microbiol 6:1174.
31. Thompson TA, Brown PD. 2017. Association between the agr locus and the presence of virulence genes and pathogenesis in *Staphylococcus aureus* using a Caenorhabditis elegans model. International Journal of Infectious Diseases 54:72–76.
32. Peter Parham. 2015. The Immune System, 4th Edition. W. W. Norton & Company, New York, USA.
33. Soong G, Martin FJ, Chun J, Cohen TS, Ahn DS, Prince A. 2011. *Staphylococcus aureus* Protein A Mediates Invasion across Airway Epithelial Cells through Activation of RhoA GTPase Signaling and Proteolytic Activity. J Biol Chem 286:35891–35898.
34. Hermann I, Räth S, Ziesemer S, Volksdorf T, Dress RJ, Gutjahr M, Müller C, Beule AG, Hildebrandt J-P. 2015. *Staphylococcus aureus* Hemolysin A Disrupts Cell–Matrix Adhesions in Human Airway Epithelial Cells. Am J Respir Cell Mol Biol 52:14–24.
35. Foster TJ. 2019. The MSCRAMM Family of Cell-Wall-Anchored Surface Proteins of Gram-Positive Cocci. Trends in Microbiology 27:927–941.
36. Scherr T, Heim C, Morrison J, Kielian T. 2014. Hiding in Plain Sight: Interplay between Staphylococcal Biofilms and Host Immunity. Frontiers in Immunology 5.
37. Hanke ML, Heim CE, Angle A, Sanderson SD, Kielian T. 2013. Targeting Macrophage Activation for the Prevention and Treatment of *Staphylococcus aureu*s Biofilm Infections. The Journal of Immunology 190:2159–2168.
38. de la Fuente-Núñez C, Reffuveille F, Fernández L, Hancock RE. 2013. Bacterial biofilm development as a multicellular adaptation: antibiotic resistance and new therapeutic strategies. Current Opinion in Microbiology 16:580–589.
39. Savage VJ, Chopra I, O'Neill AJ. 2013. *Staphylococcus aureus* Biofilms Promote Horizontal Transfer of Antibiotic Resistance. Antimicrob Agents Chemother 57:1968–1970.
40. Kranjec C, Morales Angeles D, Torrissen Mårli M, Fernández L, García P, Kjos M, Diep DB. 2021. Staphylococcal Biofilms: Challenges and Novel Therapeutic Perspectives. Antibiotics (Basel) 10:131.
41. Petrova OE, Sauer K. 2012. Sticky Situations: Key Components That Control Bacterial Surface Attachment. J Bacteriol 194:2413–2425.
42. del Pozo JL, Patel R. 2007. The Challenge of Treating Biofilm-associated Bacterial Infections. Clinical Pharmacology & Therapeutics 82:204–209.
43. Wolcott R, Costerton JW, Raoult D, Cutler SJ. 2013. The polymicrobial nature of biofilm infection. Clinical Microbiology and Infection 19:107–112.
44. Heilmann C, Schweitzer O, Gerke C, Vanittanakom N, Mack D, Götz F. 1996. Molecular basis of intercellular adhesion in the biofilm-forming *Staphylococcus epidermidis*. Mol Microbiol 20:1083–1091.
45. Arciola CR, Campoccia D, Montanaro L. 2018. Implant infections: adhesion, biofilm formation and immune evasion. 7. Nat Rev Microbiol 16:397–409.
46. Moormeier DE, Bayles KW. 2017. *Staphylococcus aureus* Biofilm: A Complex Developmental Organism. Mol Microbiol 104:365–376.

47. Vega NM, Gore J. 2014. Collective Antibiotic Resistance: Mechanisms and Implications. Curr Opin Microbiol 21:28–34.
48. Waters EM, Rowe SE, O'Gara JP, Conlon BP. 2016. Convergence of *Staphylococcus aureus* Persister and Biofilm Research: Can Biofilms Be Defined as Communities of Adherent Persister Cells? PLOS Pathogens 12:e1006012.
49. Hirschhausen N, Schlesier T, Peters G, Heilmann C. 2012. Characterization of the modular design of the autolysin/adhesin Aaa from *Staphylococcus aureus*. PLoS One 7:e40353.
50. Houston P, Rowe SE, Pozzi C, Waters EM, O'Gara JP. 2011. Essential Role for the Major Autolysin in the Fibronectin-Binding Protein-Mediated *Staphylococcus aureus* Biofilm Phenotype. Infect Immun 79:1153–1165.
51. Activity of the major staphylococcal autolysin Atl - Biswas - 2006 - FEMS Microbiology Letters - Wiley Online Library. https://onlinelibrary.wiley.com/doi/full/10.1111/j.1574-6968.2006.00281.x. Retrieved 15 March 2022.
52. Liu Q, Wang X, Qin J, Cheng S, Yeo W-S, He L, Ma X, Liu X, Li M, Bae T. 2017. The ATP-Dependent Protease ClpP Inhibits Biofilm Formation by Regulating Agr and Cell Wall Hydrolase Sle1 in *Staphylococcus aureus*. Front Cell Infect Microbiol 7:181.
53. Gross M, Cramton SE, Götz F, Peschel A. 2001. Key Role of Teichoic Acid Net Charge in *Staphylococcus aureus* Colonization of Artificial Surfaces. Infect Immun 69:3423–3426.
54. Foster TJ, Geoghegan JA, Ganesh VK, Höök M. 2014. Adhesion, invasion and evasion: the many functions of the surface proteins of *Staphylococcus aureus*. Nat Rev Microbiol 12:49–62.
55. Nguyen HTT, Nguyen TH, Otto M. 2020. The staphylococcal exopolysaccharide PIA – Biosynthesis and role in biofilm formation, colonization, and infection. Comput Struct Biotechnol J 18:3324–3334.
56. Pozzi C, Waters EM, Rudkin JK, Schaeffer CR, Lohan AJ, Tong P, Loftus BJ, Pier GB, Fey PD, Massey RC, O'Gara JP. 2012. Methicillin Resistance Alters the Biofilm Phenotype and Attenuates Virulence in *Staphylococcus aureus* Device-Associated Infections. PLoS Pathog 8:e1002626.
57. Otto M. 2013. Staphylococcal Infections: Mechanisms of Biofilm Maturation and Detachment as Critical Determinants of Pathogenicity. Annu Rev Med 64:175–188.
58. Schilcher K, Horswill AR. 2020. Staphylococcal Biofilm Development: Structure, Regulation, and Treatment Strategies. Microbiol Mol Biol Rev 84:e00026-19.
59. Kiedrowski MR, Crosby HA, Hernandez FJ, Malone CL, McNamara JO, Horswill AR. 2014. *Staphylococcus aureus* Nuc2 Is a Functional, Surface-Attached Extracellular Nuclease. PLoS One 9:e95574.
60. Boles BR, Horswill AR. 2008. agr-Mediated Dispersal of *Staphylococcus aureus* Biofilms. PLoS Pathog 4:e1000052.
61. Beenken KE, Blevins JS, Smeltzer MS. 2003. Mutation of *sarA* in *Staphylococcus aureus* Limits Biofilm Formation. Infect Immun 71:4206–4211.
62. Zheng L, Yan M, Fan F, Ji Y. 2015. The Essential WalK Histidine Kinase and WalR Regulator Differentially Mediate Autolysis of *Staphylococcus aureus* RN4220. J Nat Sci 1:e111.
63. The biofilm matrix | Nature Reviews Microbiology. https://www.nature.com/articles/nrmicro2415. Retrieved 24 April 2022.
64. Whitchurch CB, Tolker-Nielsen T, Ragas PC, Mattick JS. 2002. Extracellular DNA Required for Bacterial Biofilm Formation. Science 295:1487–1487.
65. Mann EE, Rice KC, Boles BR, Endres JL, Ranjit D, Chandramohan L, Tsang LH, Smeltzer MS, Horswill AR, Bayles KW. 2009. Modulation of eDNA Release and Degradation Affects *Staphylococcus aureus* Biofilm Maturation. PLoS One 4:e5822.
66. Qin Z, Ou Y, Yang L, Zhu Y, Tolker-Nielsen T, Molin S, Qu D. 2007. Role of autolysin-mediated DNA release in biofilm formation of *Staphylococcus epidermidis*. Microbiology (Reading) 153:2083–2092.
67. Dengler V, Foulston L, DeFrancesco AS, Losick R. 2015. An Electrostatic Net Model for the Role of Extracellular DNA in Biofilm Formation by *Staphylococcus aureus*. J Bacteriol 197:3779–3787.
68. Mlynek KD, Bulock LL, Stone CJ, Curran LJ, Sadykov MR, Bayles KW, Brinsmade SR. 2020. Genetic and Biochemical Analysis of CodY-Mediated Cell Aggregation in *Staphylococcus aureus* Reveals an Interaction between Extracellular DNA and Polysaccharide in the Extracellular Matrix. J Bacteriol 202:e00593-19.

69. Beceiro A, Tomás M, Bou G. 2013. Antimicrobial Resistance and Virulence: a Successful or Deleterious Association in the Bacterial World? Clin Microbiol Rev 26:185–230.
70. Speziale P, Pietrocola G, Foster TJ, Geoghegan JA. 2014. Protein-based biofilm matrices in Staphylococci. Front Cell Infect Microbiol 4:171.
71. Geoghegan JA, Corrigan RM, Gruszka DT, Speziale P, O'Gara JP, Potts JR, Foster TJ. 2010. Role of Surface Protein SasG in Biofilm Formation by *Staphylococcus aureus*. J Bacteriol 192:5663–5673.
72. Caiazza NC, O'Toole GA. 2003. Alpha-Toxin Is Required for Biofilm Formation by *Staphylococcus aureus*. J Bacteriol 185:3214–3217.
73. O'Gara JP. 2007. ica and beyond: biofilm mechanisms and regulation in *Staphylococcus epidermidis* and *Staphylococcus aureus*. FEMS Microbiol Lett 270:179–188.
74. Chopra S, Harjai K, Chhibber S. 2015. Antibiotic susceptibility of *ica*-positive and *ica*-negative MRSA in different phases of biofilm growth. 1. J Antibiot 68:15–22.
75. Giesbrecht P, Kersten T, Maidhof H, Wecke J. 1998. Staphylococcal Cell Wall: Morphogenesis and Fatal Variations in the Presence of Penicillin. Microbiol Mol Biol Rev 62:1371–1414.
76. Sutton JAF, Carnell OT, Lafage L, Gray J, Biboy J, Gibson JF, Pollitt EJG, Tazoll SC, Turnbull W, Hajdamowicz NH, Salamaga B, Pidwill GR, Condliffe AM, Renshaw SA, Vollmer W, Foster SJ. 2021. *Staphylococcus aureus* cell wall structure and dynamics during host-pathogen interaction. PLOS Pathogens 17:e1009468.
77. Dmitriev BA, Toukach FV, Holst O, Rietschel ET, Ehlers S. 2004. Tertiary Structure of *Staphylococcus aureus* Cell Wall Murein. J Bacteriol 186:7141–7148.
78. Do T, Page JE, Walker S. 2020. Uncovering the activities, biological roles, and regulation of bacterial cell wall hydrolases and tailoring enzymes. J Biol Chem 295:3347–3361.
79. Bacterial peptidoglycan (murein) hydrolases | FEMS Microbiology Reviews | Oxford Academic. https://academic.oup.com/femsre/article/32/2/259/2683953. Retrieved 12 March 2021.
80. Dubrac S, Boneca IG, Poupel O, Msadek T. 2007. New Insights into the WalK/WalR (YycG/YycF) Essential Signal Transduction Pathway Reveal a Major Role in Controlling Cell Wall Metabolism and Biofilm Formation in *Staphylococcus aureus*. J Bacteriol 189:8257–8269.
81. Dubrac S, Msadek T. 2004. Identification of Genes Controlled by the Essential YycG/YycF Two-Component System of *Staphylococcus aureus*. Journal of Bacteriology 186:1175–1181.
82. Takada H, Yoshikawa H. 2018. Essentiality and function of WalK/WalR two-component system: the past, present, and future of research*. Bioscience, Biotechnology, and Biochemistry 82:741–751.
83. Delauné A, Dubrac S, Blanchet C, Poupel O, Mäder U, Hiron A, Leduc A, Fitting C, Nicolas P, Cavaillon J-M, Adib-Conquy M, Msadek T. 2012. The WalKR System Controls Major Staphylococcal Virulence Genes and Is Involved in Triggering the Host Inflammatory Response. Infect Immun 80:3438–3453.
84. Ranjit DK, Endres JL, Bayles KW. 2011. *Staphylococcus aureus* CidA and LrgA Proteins Exhibit Holin-Like Properties ▿. J Bacteriol 193:2468–2476.
85. Marita Torrissen Mårli. 2020. Using CRISPR interference to study novel biofilm-associated genes in *Staphylococcus aureus*. Master thesis, NMBU.
86. Buist G, Steen A, Kok J, Kuipers OP. 2008. LysM, a widely distributed protein motif for binding to (peptido)glycans. Molecular Microbiology 68:838–847.
87. Bateman A, Rawlings ND. 2003. The CHAP domain: a large family of amidases including GSP amidase and peptidoglycan hydrolases. Trends in Biochemical Sciences 28:234–237.
88. Osipovitch DC, Therrien S, Griswold KE. 2015. Discovery of novel *S. aureus* autolysins and molecular engineering to enhance bacteriolytic activity. Appl Microbiol Biotechnol 99:6315–6326.
89. Szweda P, Schielmann M, Kotlowski R, Gorczyca G, Zalewska M, Milewski S. 2012. Peptidoglycan hydrolases-potential weapons against *Staphylococcus aureus*. Appl Microbiol Biotechnol 96:1157–1174.
90. Dobihal GS, Brunet YR, Flores-Kim J, Rudner DZ. Homeostatic control of cell wall hydrolysis by the WalRK two-component signaling pathway in Bacillus subtilis. eLife 8:e52088.
91. Bose JL, Lehman MK, Fey PD, Bayles KW. 2012. Contribution of the *Staphylococcus aureus* Atl AM and GL Murein Hydrolase Activities in Cell Division, Autolysis, and Biofilm Formation. PLOS ONE 7:e42244.
92. Myrbråten I, Stamsås G, Chan H, Angeles D, Knutsen T, Salehian Z, Shapaval V, Straume D, Kjos M. 2021. SmdA is a novel cell morphology determinant in *Staphylococcus aureus*.

93. Canette A, Briandet R. 2014. MICROSCOPY | Confocal Laser Scanning Microscopy, p. 676–683. *In* Batt, CA, Tortorello, ML (eds.), Encyclopedia of Food Microbiology (Second Edition). Academic Press, Oxford.
94. Alberts B, Johnson A, Lewis J, Raff M, Roberts K, Walter P. 2002. Studying Gene Expression and Function. Molecular Biology of the Cell 4th edition.
95. Besharova O, Suchanek VM, Hartmann R, Drescher K, Sourjik V. 2016. Diversification of Gene Expression during Formation of Static Submerged Biofilms by *Escherichia coli*. Frontiers in Microbiology 7.
96. Misteli T, Spector DL. 1997. Applications of the green fluorescent protein in cell biology and biotechnology. Nat Biotechnol 15:961–964.
97. Malone CL, Boles BR, Lauderdale KJ, Thoendel M, Kavanaugh JS, Horswill AR. 2009. Fluorescent Reporters for *Staphylococcus aureus*. J Microbiol Methods 77:251–260.
98. James D. Watson, Tania A. Baker, Michael Levine, Alexander Gann, Richard Losick. 2014. Molecular biology of the gene7th Edition. Cold Spring Harbour Laboratory Press, USA.
99. Gleditzsch D, Pausch P, Müller-Esparza H, Özcan A, Guo X, Bange G, Randau L. 2018. PAM identification by CRISPR-Cas effector complexes: diversified mechanisms and structures. RNA Biol 16:504–517.
100. Jinek M, Chylinski K, Fonfara I, Hauer M, Doudna JA, Charpentier E. 2012. A programmable dual RNA-guided DNA endonuclease in adaptive bacterial immunity. Science 337:816–821.
101. Qi LS, Larson MH, Gilbert LA, Doudna JA, Weissman JS, Arkin AP, Lim WA. 2013. Repurposing CRISPR as an RNA-Guided Platform for Sequence-Specific Control of Gene Expression. Cell 152:1173–1183.
102. Liu X, Gallay C, Kjos M, Domenech A, Slager J, van Kessel SP, Knoops K, Sorg RA, Zhang J, Veening J. 2017. High-throughput CRISPRi phenotyping identifies new essential genes in *Streptococcus pneumoniae*. Mol Syst Biol 13:931.
103. Peters JM, Colavin A, Shi H, Czarny TL, Larson MH, Wong S, Hawkins JS, Lu CHS, Koo B-M, Marta E, Shiver AL, Whitehead EH, Weissman JS, Brown ED, Qi LS, Huang KC, Gross CA. 2016. A Comprehensive, CRISPR-based Functional Analysis of Essential Genes in Bacteria. Cell 165:1493–1506.
104. de Bakker V, Liu X, Bravo AM, Veening J-W. 2022. CRISPRi-seq for genome-wide fitness quantification in bacteria. Nat Protoc 17:252–281.
105. Stamsås GA, Myrbråten IS, Straume D, Salehian Z, Veening J-W, Håvarstein LS, Kjos M. 2018. CozEa and CozEb play overlapping and essential roles in controlling cell division in *Staphylococcus aureus*. Molecular Microbiology 109:615–632.
106. Sanjana NE. 2017. Genome-scale CRISPR pooled screens. Analytical Biochemistry 532:95–99.
107. Bastos M do C de F, Coutinho BG, Coelho MLV. 2010. Lysostaphin: A Staphylococcal Bacteriolysin with Potential Clinical Applications. Pharmaceuticals (Basel) 3:1139–1161.
108. Oliver WT, Wells JE. 2015. Lysozyme as an alternative to growth promoting antibiotics in swine production. Journal of Animal Science and Biotechnology 6:35.
109. Kaunitz JD. 2015. The Discovery of PCR: ProCuRement of Divine Power. Dig Dis Sci 60:2230–2231.
110. Lo YMD. 1998. Introduction to the Polymerase Chain Reaction, p. 3–10. *In* Clinical Applications of PCR. Humana Press, New Jersey.
111. R. Ramesh, A. Munshi, S. K. Panda. 1992. Polymerase Chain Reaction. The National Medical Journal of India Vol. 5, No. 3.
112. Heckman KL, Pease LR. 2007. Gene splicing and mutagenesis by PCR-driven overlap extension. 4. Nat Protoc 2:924–932.
113. Lee PY, Costumbrado J, Hsu C-Y, Kim YH. 2012. Agarose Gel Electrophoresis for the Separation of DNA Fragments. J Vis Exp 3923.
114. Restriction Enzymes | Learn Science at Scitable. http://www.nature.com/scitable/topicpage/restriction-enzymes-545. Retrieved 7 March 2022.
115. Monk IR, Tree JJ, Howden BP, Stinear TP, Foster TJ. 2015. Complete Bypass of Restriction Systems for Major *Staphylococcus aureus* Lineages. mBio 6:e00308-15.
116. Asif A, Mohsin H, Tanvir R, Rehman Y. 2017. Revisiting the Mechanisms Involved in Calcium Chloride Induced Bacterial Transformation. Frontiers in Microbiology 8.

117. Panja S, Aich P, Jana B, Basu T. 2008. Plasmid DNA Binds to the Core Oligosaccharide Domain of LPS Molecules of *E. coli* Cell Surface in the CaCl2-Mediated Transformation Process. Biomacromolecules 9:2501–2509.
118. Grosser MR, Richardson AR. 2016. Method for Preparation and Electroporation of *S. aureus* and *S. epidermidis*. Methods Mol Biol 1373:51–57.
119. de Jong NWM, van der Horst T, van Strijp JAG, Nijland R. 2017. Fluorescent reporters for markerless genomic integration in *Staphylococcus aureus*. Sci Rep 7:43889.
120. Bae T, Schneewind O. 2006. Allelic replacement in *Staphylococcus aureus* with inducible counter-selection. Plasmid 55:58–63.
121. Arnaud M, Chastanet A, Débarbouillé M. 2004. New Vector for Efficient Allelic Replacement in Naturally Nontransformable, Low-GC-Content, Gram-Positive Bacteria. Appl Environ Microbiol 70:6887–6891.
122. Sadava D, Hillis M., David, Heller H., Craig, Berenbaum R., May. 2014. Life: The Science of Biology, 10th ed. Sinauer, USA.
123. Horwitz JP, Chua J, Curby RJ, Tomson AJ, Da Rooge MA, Fisher BE, Mauricio J, Klundt I. 1964. Substrates for Cytochemical Demonstration of Enzyme Activity. I. Some Substituted 3-Indolyl-β-D-glycopyranosides1a. J Med Chem 7:574–575.
124. Liu J, Shen Z, Tang J, Huang Q, Jian Y, Liu Y, Wang Y, Ma X, Liu Q, He L, Li M. 2021. Extracellular DNA released by glycine-auxotrophic *Staphylococcus epidermidis* small colony variant facilitates catheter-related infections. 1. Commun Biol 4:1–14.
125. O'Neill E, Pozzi C, Houston P, Humphreys H, Robinson DA, Loughman A, Foster TJ, O'Gara JP. 2008. A Novel *Staphylococcus aureus* Biofilm Phenotype Mediated by the Fibronectin-Binding Proteins, FnBPA and FnBPB. J Bacteriol 190:3835–3850.
126. Chiba A, Sugimoto S, Sato F, Hori S, Mizunoe Y. 2015. A refined technique for extraction of extracellular matrices from bacterial biofilms and its applicability. Microb Biotechnol 8:392–403.
127. Lukasz Komsta. 2011. outliers: Tests for outliers. https://CRAN.R-project.org/package=outliers.
128. R Core Team. 2021. R: A language and environment for statistical computing. R Foundation for Statistical Computing, Vienna, Austria. https://www.R-project.org/.
129. Howell SH, Ow DW, Schneider M. 1989. Use of the firefly luciferase gene as a reporter of gene expression in plants, p. 359–369. *In* Gelvin, SB, Schilperoort, RA, Verma, DPS (eds.), Plant Molecular Biology Manual. Springer Netherlands, Dordrecht.
130. Deluca M, McElroy WD. 1978. [1] Purification and properties of firefly luciferase, p. 3–15. *In* Methods in Enzymology. Academic Press.
131. Zimmer M. 2002. Green Fluorescent Protein (GFP): Applications, Structure, and Related Photophysical Behavior. Chem Rev 102:759–782.
132. MicrobeJ, a tool for high throughput bacterial cell detection and quantitative analysis | Nature Microbiology. https://www.nature.com/articles/nmicrobiol201677. Retrieved 27 March 2022.
133. Schneider CA, Rasband WS, Eliceiri KW. 2012. NIH Image to ImageJ: 25 years of image analysis. 7. Nat Methods 9:671–675.
134. Mäder U, Nicolas P, Depke M, Pané-Farré J, Debarbouille M, van der Kooi-Pol MM, Guérin C, Dérozier S, Hiron A, Jarmer H, Leduc A, Michalik S, Reilman E, Schaffer M, Schmidt F, Bessières P, Noirot P, Hecker M, Msadek T, Völker U, van Dijl JM. 2016. *Staphylococcus aureus* Transcriptome Architecture: From Laboratory to Infection-Mimicking Conditions. PLoS Genet 12:e1005962.
135. CRISPRi-seq for genome-wide fitness quantification in bacteria | Nature Protocols. https://www.nature.com/articles/s41596-021-00639-6. Retrieved 10 May 2022.
136. Moderated estimation of fold change and dispersion for RNA-seq data with DESeq2 - PMC. https://www.ncbi.nlm.nih.gov/pmc/articles/PMC4302049/. Retrieved 10 May 2022.
137. Comprehensive identification of essential *Staphylococcus aureus* genes using Transposon-Mediated Differential Hybridisation (TMDH) - PMC. https://www.ncbi.nlm.nih.gov/pmc/articles/PMC2721850/. Retrieved 19 May 2022.
138. Paruthiyil S, Pinochet-Barros A, Huang X, Helmann JD. 2020. Bacillus subtilis TerC Family Proteins Help Prevent Manganese Intoxication. J Bacteriol 202:e00624-19.
139. Ender M, Berger-Bächi B, McCallum N. 2009. A novel DNA-binding protein modulating methicillin resistance in *Staphylococcus aureus*. BMC Microbiol 9:15.

140. Lei MG, Lee CY. 2018. Repression of Capsule Production by XdrA and CodY in *Staphylococcus aureus*. J Bacteriol 200:e00203-18.
141. Biofilm Formation by *Staphylococcus aureus* is Triggered by a Drop in the Levels of the Second Messenger cyclic-di-AMP | bioRxiv. https://www.biorxiv.org/content/10.1101/2020.01.31.929125v1.full. Retrieved 19 May 2022.
142. DeFrancesco AS, Masloboeva N, Syed AK, DeLoughery A, Bradshaw N, Li G-W, Gilmore MS, Walker S, Losick R. 2017. Genome-wide screen for genes involved in eDNA release during biofilm formation by *Staphylococcus aureus*. Proc Natl Acad Sci U S A 114:E5969–E5978.
143. Kragh KN, Alhede M, Kvich L, Bjarnsholt T. 2019. Into the well—A close look at the complex structures of a microtiter biofilm and the crystal violet assay. Biofilm 1:100006.
144. Amador CI, Stannius RO, Røder HL, Burmølle M. 2021. High-throughput screening alternative to crystal violet biofilm assay combining fluorescence quantification and imaging. Journal of Microbiological Methods 190:106343.
145. Campoccia D, Montanaro L, Ravaioli S, Pirini V, Cangini I, Arciola CR. 2011. Exopolysaccharide Production by *Staphylococcus Epidermidis* and its Relationship with Biofilm Extracellular DNA. Int J Artif Organs 34:832–839.
146. The peptidoglycan and biofilm matrix of *Staphylococcus epidermidis* undergo structural changes when exposed to human platelets. https://journals.plos.org/plosone/article?id=10.1371/journal.pone.0211132#sec002. Retrieved 30 April 2022.
147. Okshevsky M, Meyer RL. 2014. Evaluation of fluorescent stains for visualizing extracellular DNA in biofilms. Journal of Microbiological Methods 105:102–104.
148. Szurmant H, Mohan MA, Imus PM, Hoch JA. 2007. YycH and YycI Interact To Regulate the Essential YycFG Two-Component System in *Bacillus subtilis*. J Bacteriol 189:3280–3289.
149. Cameron DR, Jiang J-H, Kostoulias X, Foxwell DJ, Peleg AY. 2016. Vancomycin susceptibility in methicillin-resistant *Staphylococcus aureus* is mediated by YycHI activation of the WalRK essential two-component regulatory system. Sci Rep 6:30823.
150. Gajdiss M, Monk IR, Bertsche U, Kienemund J, Funk T, Dietrich A, Hort M, Sib E, Stinear TP, Bierbaum G. 2020. YycH and YycI Regulate Expression of *Staphylococcus aureus* Autolysins by Activation of WalRK Phosphorylation. Microorganisms 8:870.
151. Poupel O, Moyat M, Groizeleau J, Antunes LCS, Gribaldo S, Msadek T, Dubrac S. 2016. Transcriptional Analysis and Subcellular Protein Localization Reveal Specific Features of the Essential WalKR System in *Staphylococcus aureus*. PLoS One 11:e0151449.
152. Pinho MG, Kjos M, Veening J-W. 2013. How to get (a)round: mechanisms controlling growth and division of coccoid bacteria. 9. Nat Rev Microbiol 11:601–614.
153. Clarke LA, Rebelo CS, Gonçalves J, Boavida MG, Jordan P. 2001. PCR amplification introduces errors into mononucleotide and dinucleotide repeat sequences. Mol Pathol 54:351–353.
154. McCallum N, Hinds J, Ender M, Berger-Bächi B, Stutzmann Meier P. 2010. Transcriptional Profiling of XdrA, a New Regulator of *spa* Transcription in *Staphylococcus aureus*. J Bacteriol 192:5151–5164.
155. Merino N, Toledo-Arana A, Vergara-Irigaray M, Valle J, Solano C, Calvo E, Lopez JA, Foster TJ, Penadés JR, Lasa I. 2009. Protein A-Mediated Multicellular Behavior in *Staphylococcus aureus*. J Bacteriol 191:832–843.
156. Votintseva AA, Fung R, Miller RR, Knox K, Godwin H, Wyllie DH, Bowden R, Crook DW, Walker AS. 2014. Prevalence of *Staphylococcus aureus* protein A (*spa*) mutants in the community and hospitals in Oxfordshire. BMC Microbiol 14:63.
157. Atilano ML, Pereira PM, Vaz F, Catalão MJ, Reed P, Grilo IR, Sobral RG, Ligoxygakis P, Pinho MG, Filipe SR. 2014. Bacterial autolysins trim cell surface peptidoglycan to prevent detection by the *Drosophila* innate immune system. eLife 3:e02277.

Appendix

A1. List and description of strains used in this work.

Strain	Genotype and characteristics[1]	Source or reference
***S. aureus* NCTC8325-4**		
DMA014	Δ*icaA*	Lab collection
DMA064	MM149 pLOW lacA m(*gfp*)	Lab collection
DMA087	pDMA032 (pLOW p00671_*luc_gfp*)	Lab collection
DMA089	pDMA038(pLOW_pssaA_*luc_gfp*)	Lab collection
DMA094	MM149 pDMA038 (pLOW_p*ssaA_luc_gfp*)	Lab collection
MM149	Δ00671::Spc	Lab collection
MM154	MM149 pLOW-00671, *eryR*	Lab collection
MM74	pLOW-*dCas9* pVL2336-sgRNA(*icaA*)	Lab collection
RM2	DMA089 pRN10	This work
RM3	DMA094 pRN10	This work
RM4	DMA087 pRN10	This work
IM311	pLOW-dCas9 + pCG248-sgRNA(*smdA*)	Lab collection
IM307	pLOW-dCas9_extra_lacO + pVL2336-sgRNA(*luc*)	Lab collection
RM5	s*arA P1-mKate*	This work
RM8	*sarA P1-mKate* pDMA032 (pLOW_p00671_*luc_gfp*)	This work
RM9	MM149 *sarA P1-mKate*	This work
RM10	*sarA P1-mKate* pDMA038 (pLOW_p*ssaA_luc_gfp*)	This work
RM11	MM149 *sarA P1-mKate* pDMA038 (pLOW_p*ssaA_luc_gfp*)	This work
RM12	*sarA P1-mKate* pDMA044 (pLOW_p*ssaA_cfp*)	
RM13	pDMA044 (pCG248_p*ssaA_cfp*)	This work
RM14	MM149 pDMA044 (pCG248__p*ssaA_cfp*)	This work
RM15	pDMA032 (pLOW p00671_*luc_gfp*) + pDMA044 (pCG248_p*ssaA_cfp*)	This work
Δatl	Δ*atl*	Atilano et al. (2014) (157)
***S. aureus* SH1000**		
IM269	pLOW-*dCas9* + pCG248-sgRNA(*smdA*)	Lab collection
IM284	pLOW-*dCas9* + pCG248-sgRNA(*luc*)	Lab collection
MM41	pVL2336-sgRNA(*icaA*)	
***S. aureus* JE2**		
MK1947	pLOW-*dCas9_aad9* + pcg248 (*smdA*)	Lab collection
MDB44	pLOW-*dCas9_aad9* + pCG248-sgRNA(*luc*)	Lab collection
***E. coli* IM08B**		
RM1	pRN10	This work
RM6	pDMA045 (pMAD_Δ*ssaA*, *tetR*)	This work
RM7	pDMA044 (pCG248_p*ssaA_cfp*)	This work

1 tetR; tetracycline resistance gene

A2. Map of constructed plasmids pDMA045 (A) and pDMA044 (B) with primers and restriction sites

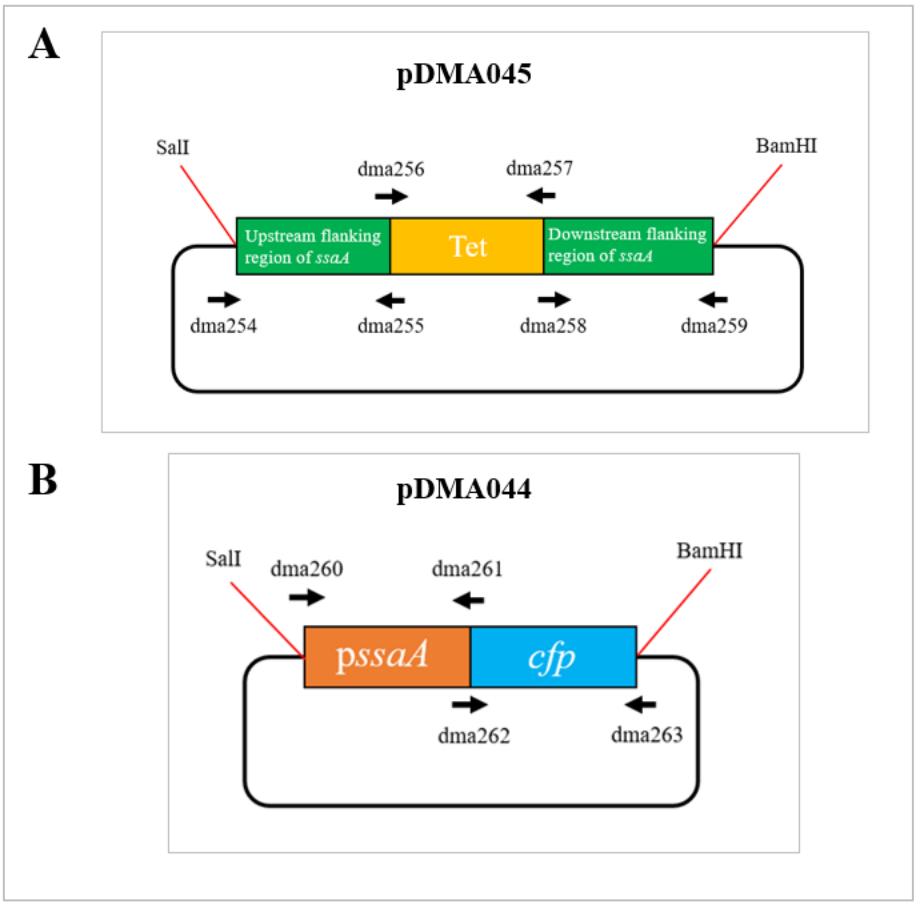

A3. Statistical test results of 00671- and SsaA-expression and -correlation

Table A3.1. Wildtype 00671-expression **(**WT p00671), one-way ANOVA

ANOVA table	SS	DF	MS	F (DFn, DFd)	P value
Treatment (between columns)	6212061907	2	3106030953	F (2, 897) = 70,34	P<0,0001
Residual (within columns)	39610250657	897	44158585		
Total	45822312564	899			

Table A3.2 Wildtype 00671-expression (WT p00671), Post hoc Tukey

Tukey's multiple comparisons test	Mean Diff,	95,00% CI of diff,	Below threshold?	Summary	Adjusted P Value
Exponential vs. Transtitional	-2752	-4026 to -1479	Yes	****	<0,0001
Exponential vs. Exponential	-6414	-7688 to -5140	Yes	****	<0,0001
Transtitional vs. Exponential	-3662	-4935 to -2388	Yes	****	<0,0001

Table A3.3. Wildtype SsaA-expression (WT pssaA), one-way ANOVA

ANOVA table	SS	DF	MS	F (DFn, DFd)	P value
Treatment (between columns)	3662817029	2	1831408514	F (2, 897) = 109,3	P<0,0001
Residual (within columns)	15030340079	897	16756232		
Total	18693157108	899			

Table A3.4. Wildtype SsaA-expression (WT pssaA), Post hoc Tukey

Tukey's multiple comparisons test	Mean Diff,	95,00% CI of diff,	Below threshold?	Summary	Adjusted P Value
Exponential vs. Transtitional	2917	2132 to 3702	Yes	****	<0,0001
Exponential vs. Stationary	4913	4128 to 5697	Yes	****	<0,0001
Transtitional vs. Stationary	1996	1211 to 2780	Yes	****	<0,0001

Table A3.5. Δ00671 SsaA-expression (Δ00671 pssaA), one-way ANOVA

ANOVA table	SS	DF	MS	F (DFn, DFd)	P value
Treatment (between columns)	1559038062	2	779519031	F (2, 897) = 12,24	P<0,0001
Residual (within columns)	57145147303	897	63706965		
Total	58704185364	899			

Table A3.6. Δ00671 SsaA-expression (Δ00671 pssaA), Post-hoc, Tukey

Tukey's multiple comparisons test	Mean Diff,	95,00% CI of diff,	Below threshold?	Summary	Adjusted P Value
Exponential vs. Transtitional	354,9	-1175 to 1885	No	ns	0,8493
Exponential vs. Stationary	2952	1423 to 4482	Yes	****	<0,0001
Transtitional vs. Stationary	2598	1068 to 4128	Yes	***	0,0002

A4. RNA-sequencing results of downregulation of α-hemolysin (Hla) in Δ00671

Table A4. Downregulation of α-hemolysin in Δ00671 (Danae Morales Angeles, unpublished). Change in expression is stated in log2 fold change compared with the wildtype strain.

Name	Differential expression log2 ratio	Locus tag
α-hemolysin CDS	-3.05	*SAOUHSC_01121*

A5. sgRNA-targets revealed as more abundant, but not significantly so, after the CRISPRi attachment assay

Table A5. List of sgRNA targets with a log2 fold change of more than 1 after attachment, but with a p-value above 0.05.

Gene name	Log2 Fold Change	p-value	Locus tag
murA2	2.374952254	0.411579412	*SAOUHSC_02365*
SAOUHSC_02367	1.925718448	0.305465095	*SAOUHSC_02367*
uvrC	1.874649742	0.75235367	*SAOUHSC_01102*
glpT	1.429134189	0.147906983	*SAOUHSC_00317*
fmtA	1.423576039	0.231717487	*SAOUHSC_00998*
SAOUHSC_02355	1.38214501	0.493146981	*SAOUHSC_02355*
SAOUHSC_00663	1.274692271	0.532824095	*SAOUHSC_00663*
icaA	1.270887944	0.167493438	*SAOUHSC_03002*
asp3	1.250375309	0.076369766	*SAOUHSC_02986*
SAOUHSC_02083	1.243876167	0.475019859	*SAOUHSC_02083*
SAOUHSC_02783	1.212050705	0.401972189	*SAOUHSC_02783*
SAOUHSC_02817	1.203705106	0.624013744	*SAOUHSC_02817*
SAOUHSC_A01079	1.197234417	0.514834652	*SAOUHSC_A01079*
agrB	1.190516186	0.561313361	*SAOUHSC_02261*
SAOUHSC_A02635	1.15811924	0.771662334	*SAOUHSC_A02635*
SAOUHSC_01152	1.136856011	0.660176359	*SAOUHSC_01152*
SAOUHSC_01863	1.129086473	0.872548862	*SAOUHSC_01863*
SAOUHSC_00711	1.122672042	0.598473013	*SAOUHSC_00711*
sigH	1.118367724	0.379025396	*SAOUHSC_00515*
nifZ	1.114944973	0.625241942	*SAOUHSC_01825*
NA	1.095062809	0.754429652	*SAOUHSC_01669*
SAOUHSC_01289	1.089705551	0.847914296	*SAOUHSC_01289*
SAOUHSC_01325	1.07982554	0.77420148	*SAOUHSC_01325*
sgtB	1.06929593	0.763520374	*SAOUHSC_02012*
SAOUHSC_02338	1.068718474	0.862246784	*SAOUHSC_02338*
phnD	1.051290807	0.794381722	*SAOUHSC_00105*
SAOUHSC_00088	1.040399547	0.941352131	*SAOUHSC_00088*
SAOUHSC_01761	1.036975254	0.870282468	*SAOUHSC_01761*
ctsR	1.032194834	0.923431563	*SAOUHSC_00502*
queG	1.007007269	0.962160273	*SAOUHSC_01989*

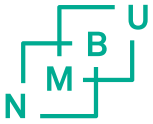

Norges miljø- og biovitenskapelige universitet
Noregs miljø- og biovitskapelege universitet
Norwegian University of Life Sciences

Postboks 5003
NO-1432 Ås
Norway